Particle Detectors

Summer Student Lectures 2008

Werner Riegler, CERN, werner.riegler@cern.ch

- **History of Instrumentation ↔ History of Particle Physics**
- **The 'Real' World of Particles**
- **Interaction of Particles with Matter**
- **Tracking with Gas and Solid State Detectors**
- **Calorimetry, Particle ID, Detector Systems**

Detectors based on Ionization

Gas detectors:

- Wire Chambers
- Drift Chambers
- Time Projection Chambers
- Transport of Electrons and Ions in Gases

→ Solid State Detectors

- Transport of Electrons and Holes in Solids
- Si- Detectors
- Diamond Detectors

Solid State Detectors

Gas Detectors

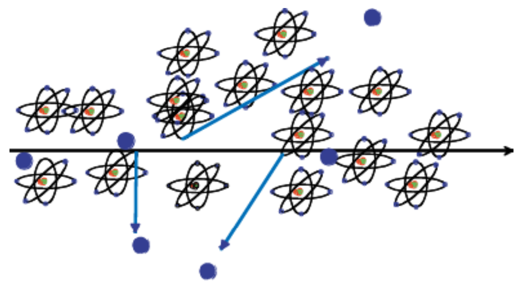

In gaseous detectors, a charged particle is liberating electrons from the atoms, which are freely bouncing between the gas atoms.

An applied electric field makes the electrons and ions move, which induces signals on the metal readout electrodes.

For individual gas atoms, the electron energy levels are discrete.

Solid State Detectors

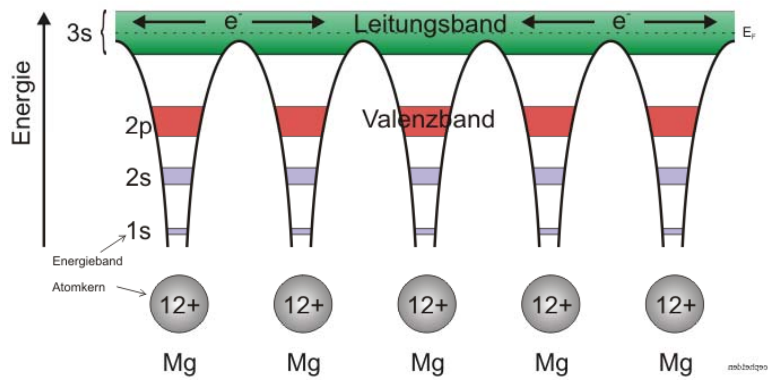

In solids (crystals), the electron energy levels are in 'bands'.

Inner shell electrons, in the lower energy bands, are closely bound to the individual atoms and always stay with 'their' atoms.

In a crystal there are however energy bands that are still bound states of the crystal, but they belong to the entire crystal. Electrons in this bands and the holes in the lower band can freely move around the crystal, if an electric field is applied.

Solid State Detectors

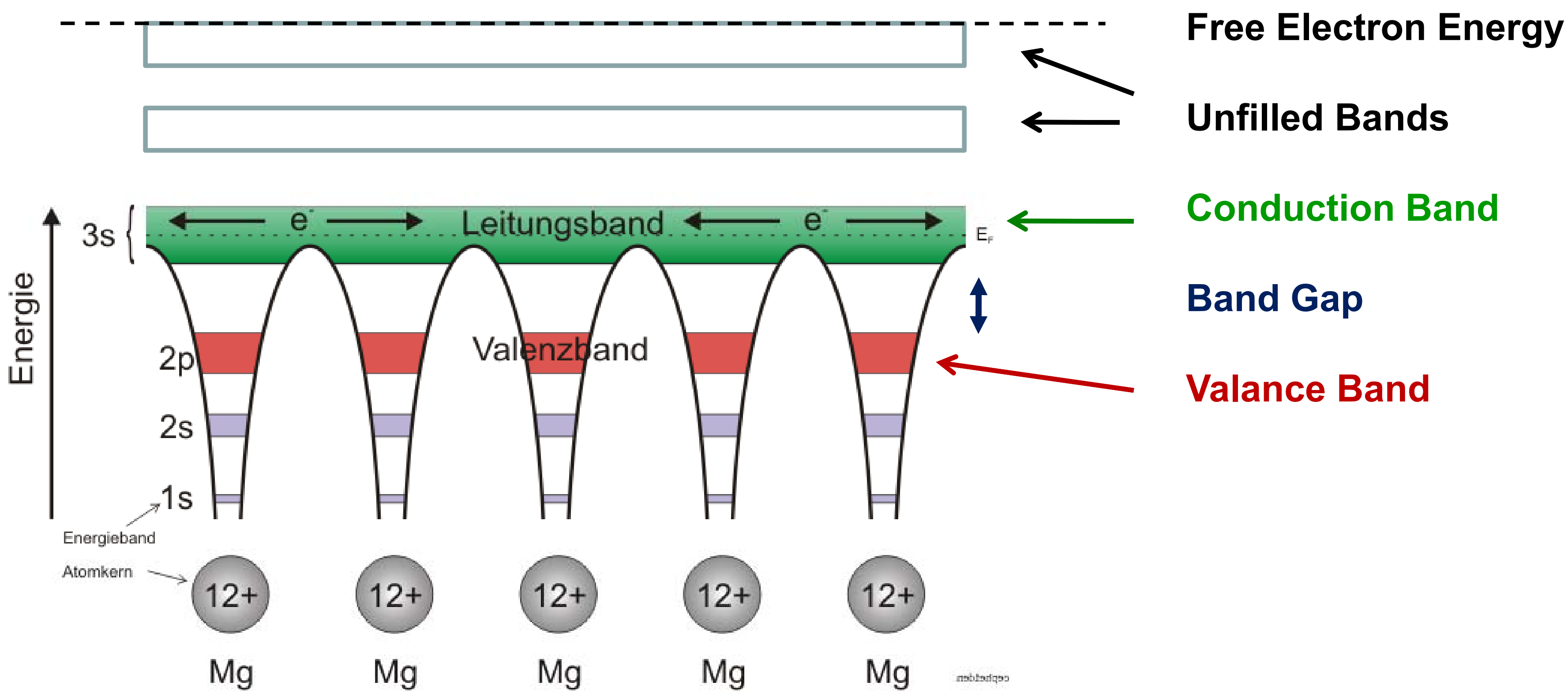

Solid State Detectors

Conductor, Insulator, Semiconductor

In case the conduction band is filled the crystal is a conductor.

In case the conduction band is empty and 'far away' from the valence band, the crystal is an insulator.

In case the conduction band is empty but the distance to the valence band is small, the crystal is a semiconductor.

Band Gap, e-h pair Energy

The energy gap between the last filled band – the valence band – and the conduction band is called band gap E_g.

The band gap of Diamond/Silicon/Germanium is 5.5, 1.12, 0.66 eV.

The average energy to produce an electron/hole pair for Diamond/Silicon/Germanium is 13, 3.6, 2.9eV.

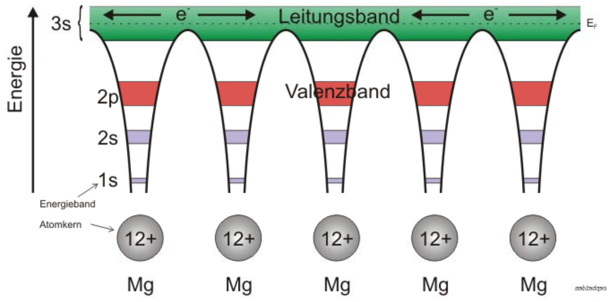

Temperature, Charged Particle Detection

In case an electron in the valence band gains energy by some process, it can be excited into the conduction band and a hole in the valence band is left behind.

Such a process can be the passage of a charged particle, but also thermal excitation → probability is proportional Exp($-E_g/kT$).

The number of electrons in the conduction band is therefore increasing with temperature i.e. the conductivity of a semiconductor increases with temperature.

Solid State Detectors

Electron, Hole Movement:

It is possible to treat electrons in the conduction band and holes in the valence band similar to free particles, but with an effective mass different from elementary electrons not embedded in the lattice.

This mass is furthermore dependent on other parameters such as the direction of movement with respect to the crystal axis. All this follows from the QM treatment of the crystal (solid state physics).

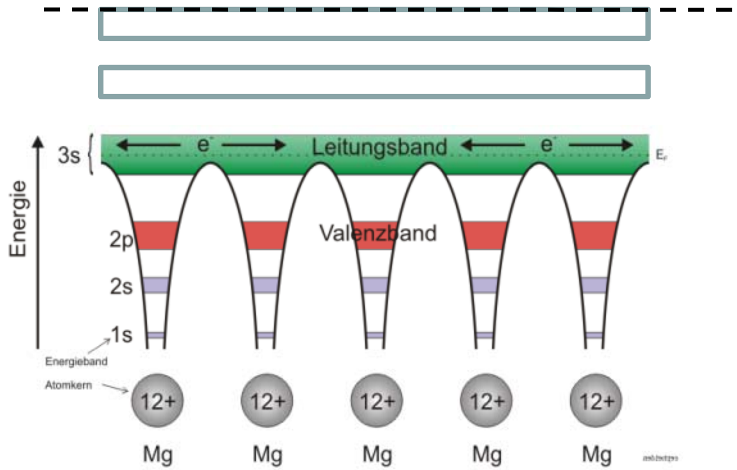

Cooling:

If we want to use a semiconductor as a detector for charged particles, the number of charge carriers in the conduction band due to thermal excitation must be smaller than the number of charge carriers in the conduction band produced by the passage of a charged particle.

Diamond (E_g=5.5eV) can be used for particle detection at room temperature,
Silicon (E_g=1.12 eV) and Germanium (E_g=0.66eV) must be cooled, or the free charge carriers must be eliminated by other tricks → doping → see later.

Solid State Detectors

Primary 'ionization':

The average energy to produce an electron/hole pair is:
Diamond (13eV), Silicon (3.6eV), Germanium (2.9eV)

Comparing to gas detectors, the density of a solid is about a factor 1000 larger than that of a gas and the energy to produce and electron/hole pair e.g. for Si is a factor 7 smaller than the energy to produce an electron-ion pair in Argon.

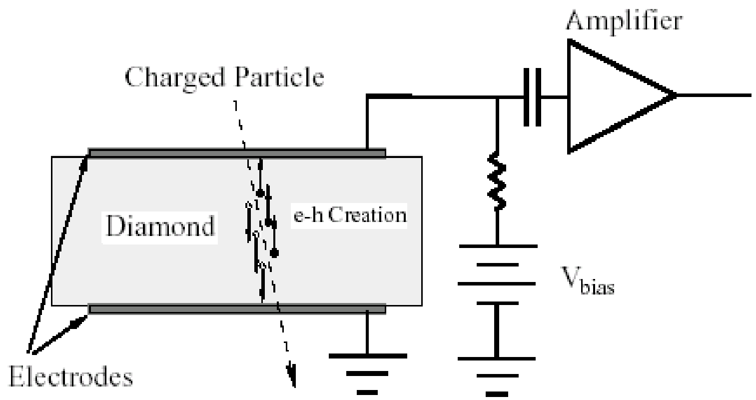

Diamond → A solid state ionization chamber

Solid State vs. Gas Detector:

The number of primary charges in a Si detector is therefore about 10^4 times larger than the one in gas → while gas detectors need internal charge amplification, solid state detectors don't need internal amplification.

While in gaseous detectors, the velocity of electrons and ions differs by a factor 1000, the velocity of electrons and holes in many semiconductor detectors is quite similar → very short signals.

Why do solid state detectors exist only since around 1980 while gas detectors are used since 1906 ?

Diamond Detector

Typical thickness – a few 100μm.
<1000 charge carriers/cm^3 at room temperature due to large band gap.

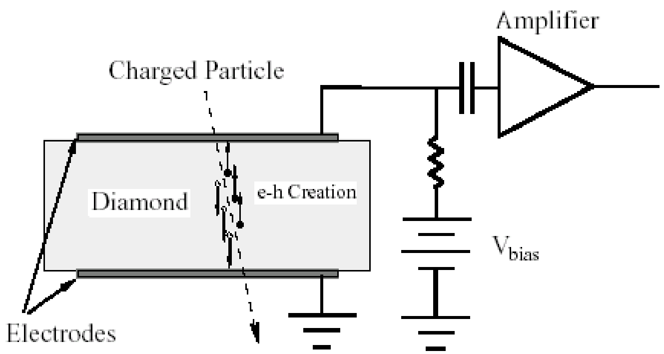

Velocity:
μ_e=1800 cm^2/Vs, μ_h=1600 cm^2/Vs
Velocity = μE, 10kV/cm → v=180 μm/ns → Very fast signals of only a few ns length !

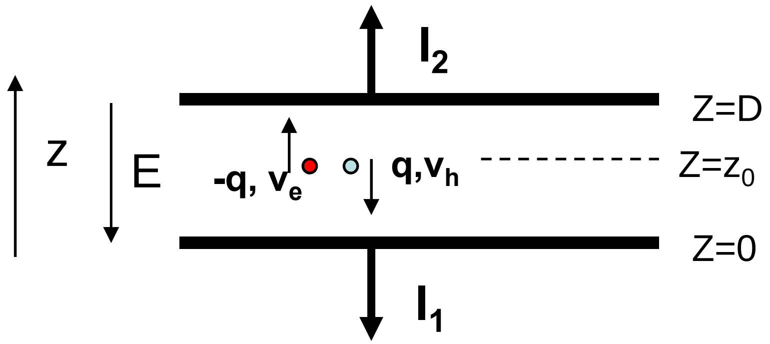

Diamond Detector

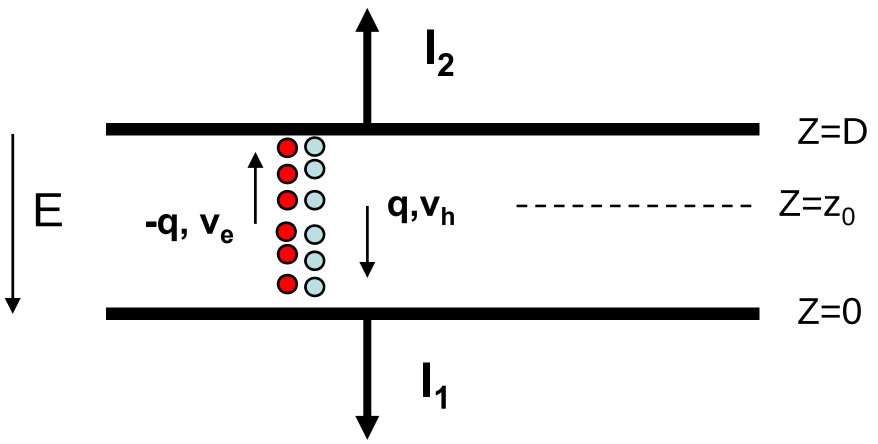

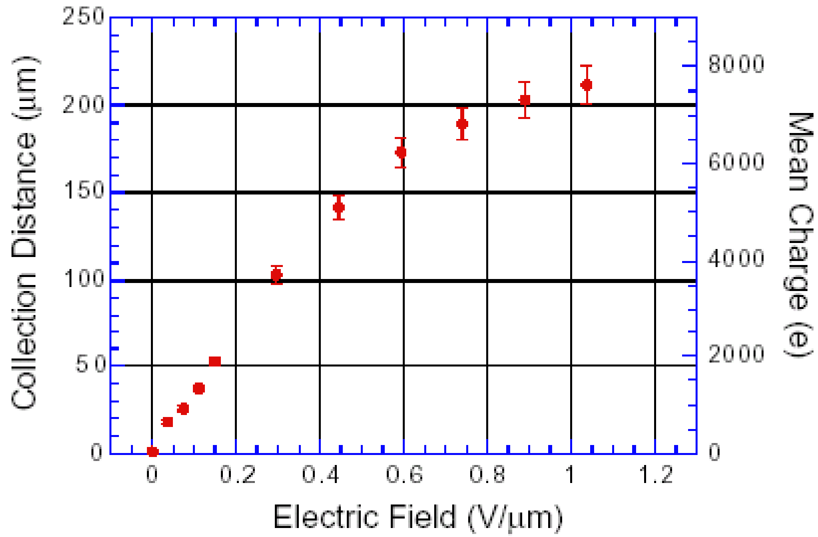

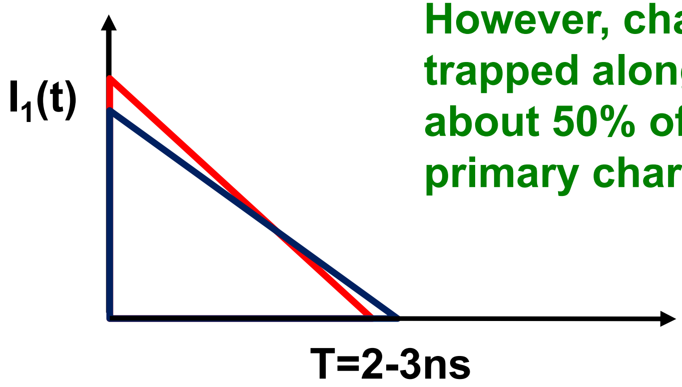

However, charges are trapped along the track, only about 50% of *produced* primary charge is *induced* →

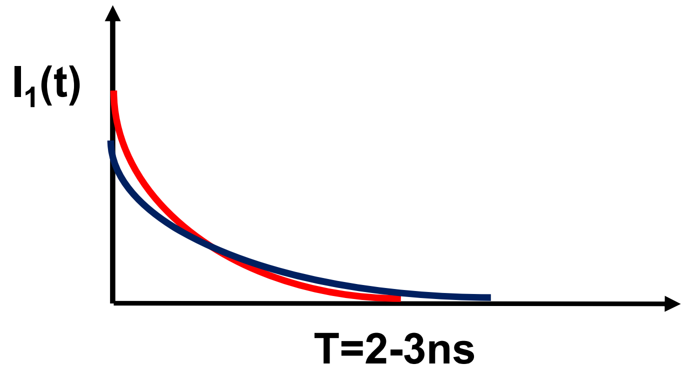

Silicon Detector

Velocity:

μ_e=1450 cm^2/Vs, μ_h=505 cm^2/Vs, 3.63eV per e-h pair.

~11000 e/h pairs in 100µm of silicon.

However: Free charge carriers in Si:

T=300 K: e,h = 1.45 x 10^{10} / cm^3 but only 33000 e/h pairs in 300µm produced by a high energy particle.

Why can we use Si as a solid state detector ???

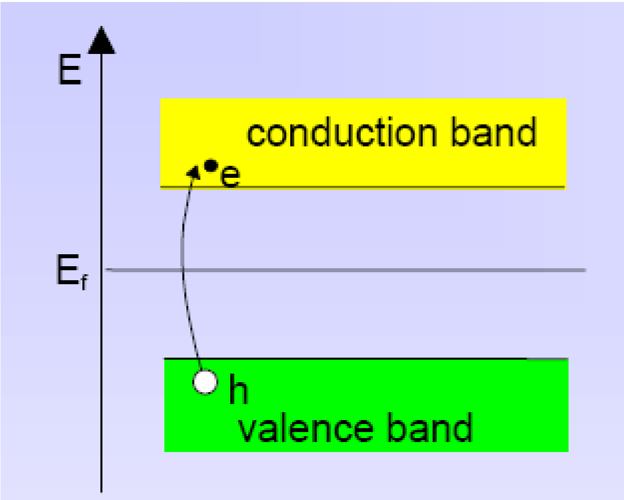

Doping of Silicon

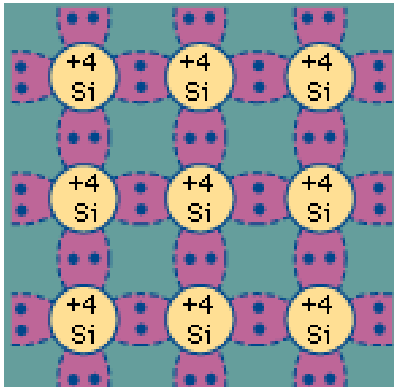

doping

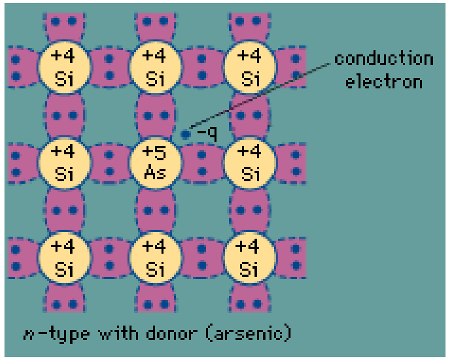

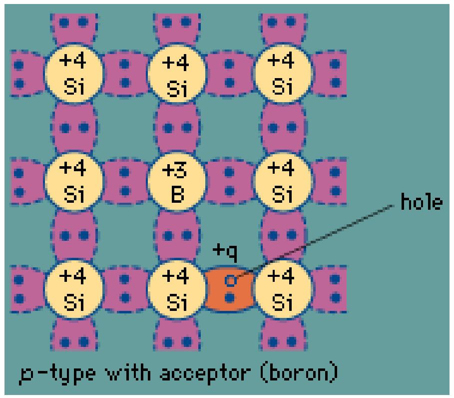

In a silicon crystal at a given temperature the number of electrons in the conduction band is equal to the number of holes in the valence band.

Doping Silicon with Arsen (+5) it becomes and n-type conductor (more electrons than holes).

Doping Silicon with Boron (+3) it becomes a p-type conductor (more holes than electrons).

Bringing p and n in contact makes a diode.

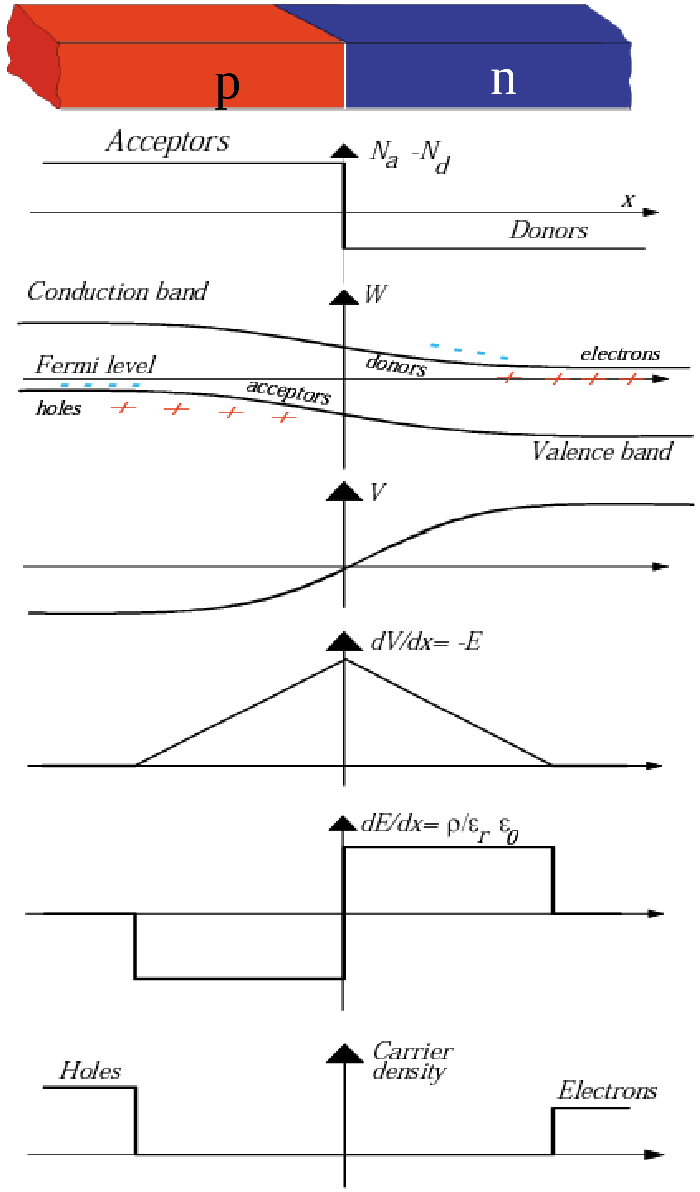

Si-Diode used as a Particle Detector !

At the p-n junction the charges are depleted and a zone free of charge carriers is established.

By applying a voltage, the depletion zone can be extended to the entire diode → highly insulating layer.

An ionizing particle produces free charge carriers in the diode, which drift in the electric field and induce an electrical signal on the metal electrodes.

As silicon is the most commonly used material in the electronics industry, it has one big advantage with respect to other materials, namely highly developed technology.

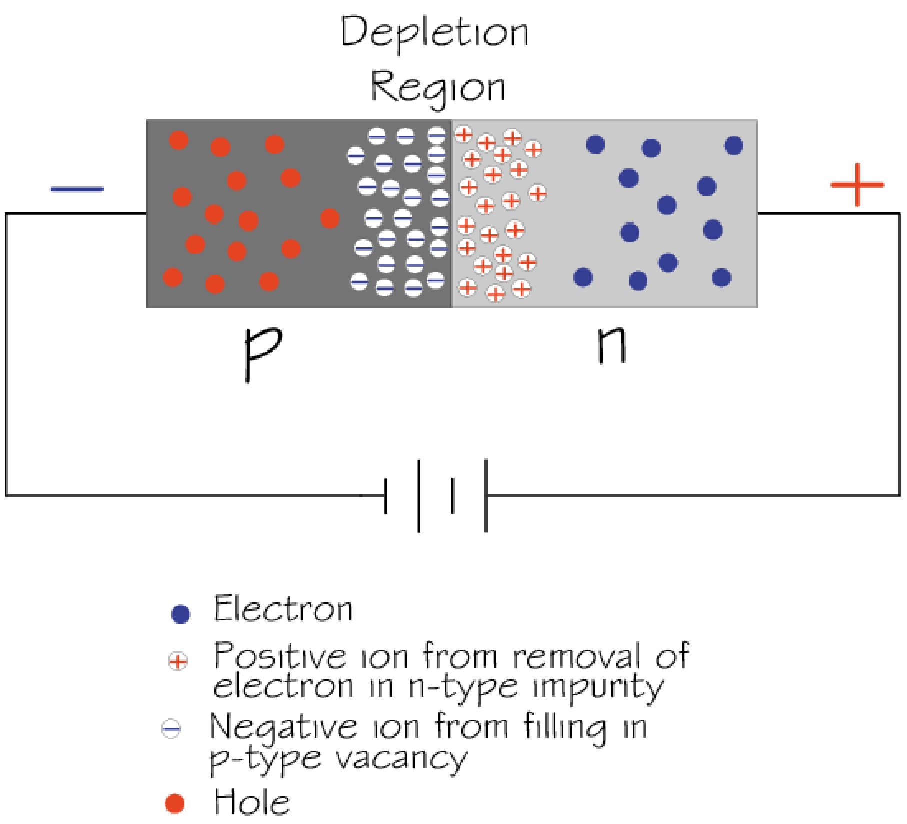

Under-Depleted Silicon Detector

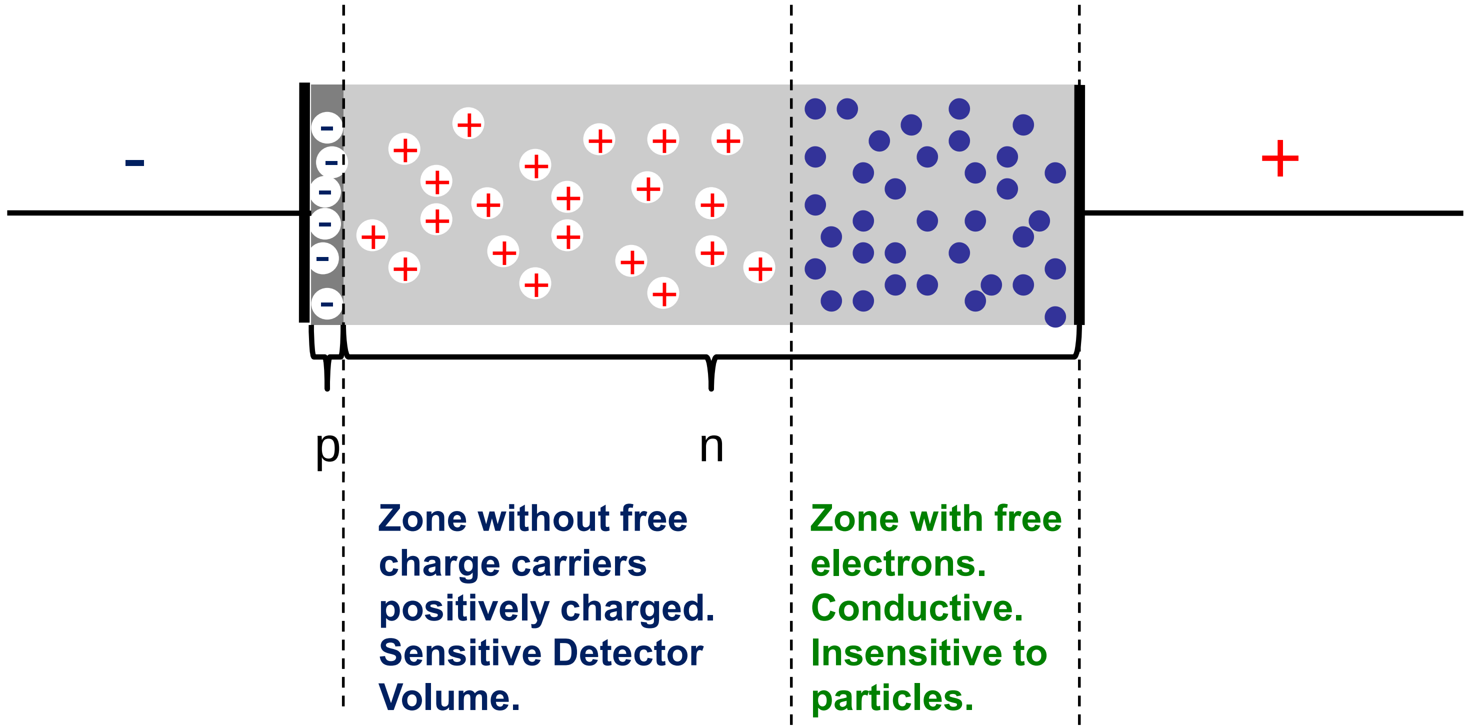

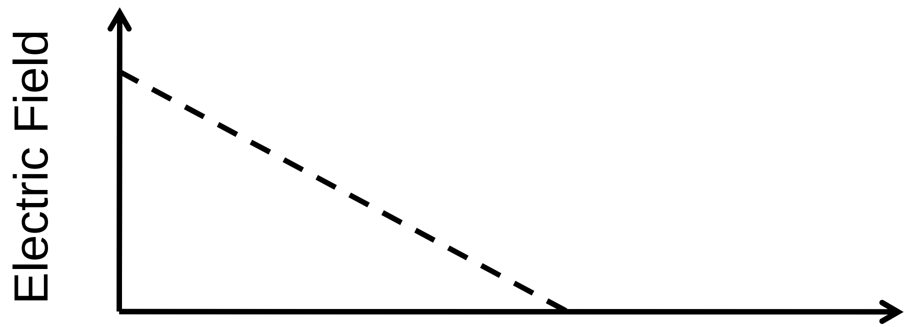

Fully-Depleted Silicon Detector

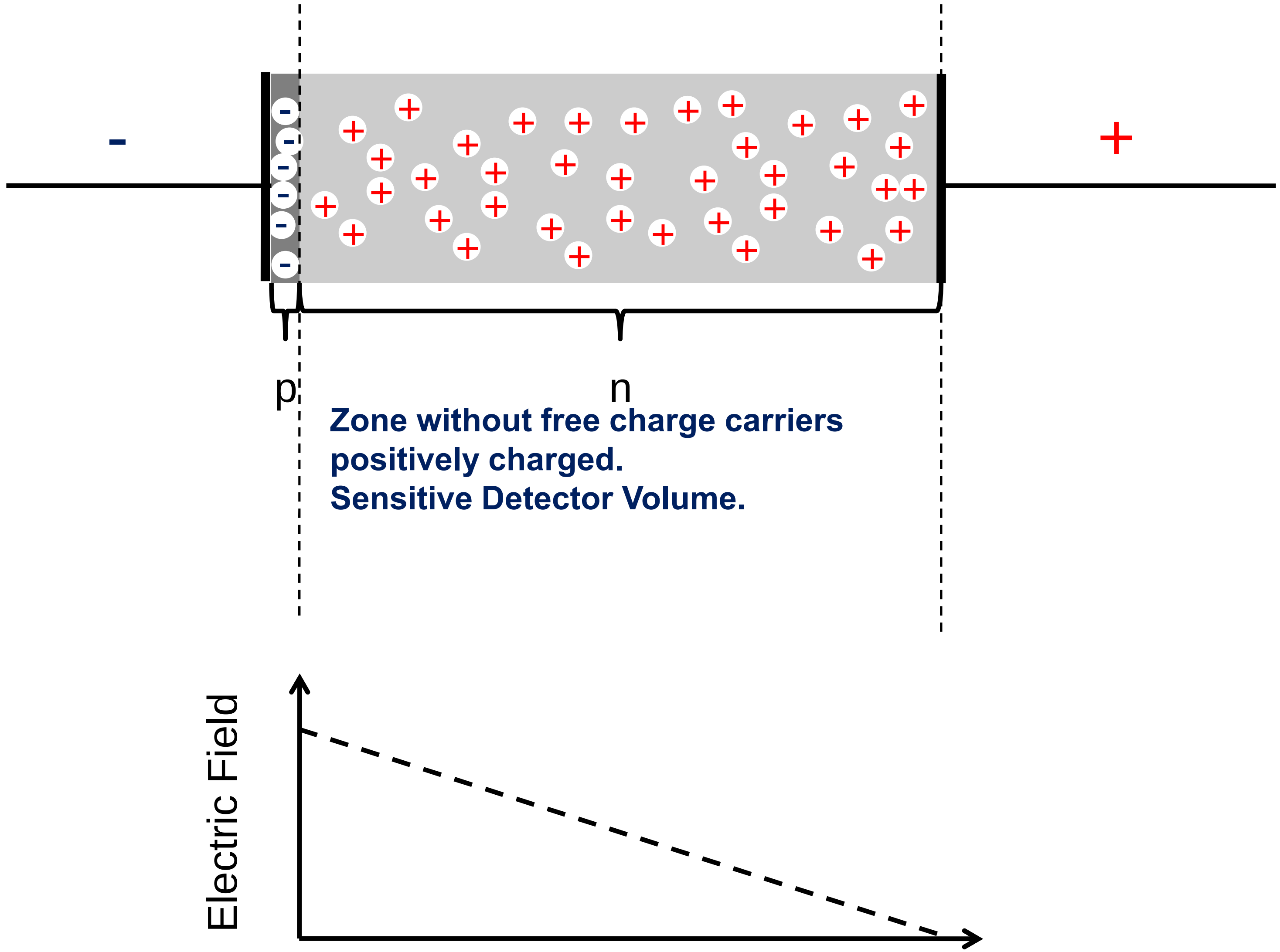

Over-Depleted Silicon Detector

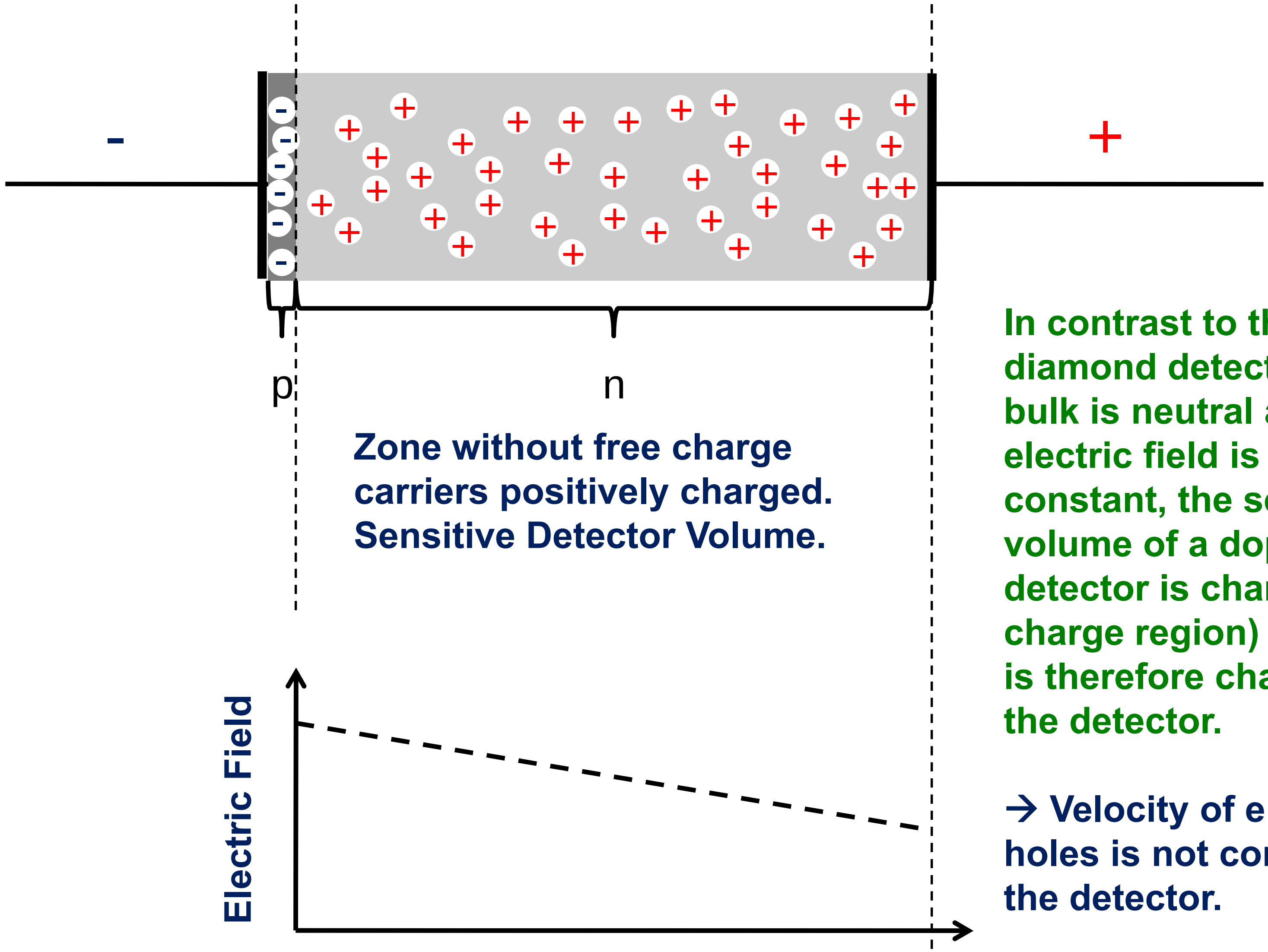

In contrast to the (un-doped) diamond detector where the bulk is neutral and the electric field is therefore constant, the sensitive volume of a doped silicon detector is charged (space charge region) and the field is therefore changing along the detector.

→ Velocity of electrons and holes is not constant along the detector.

Silicon Detector

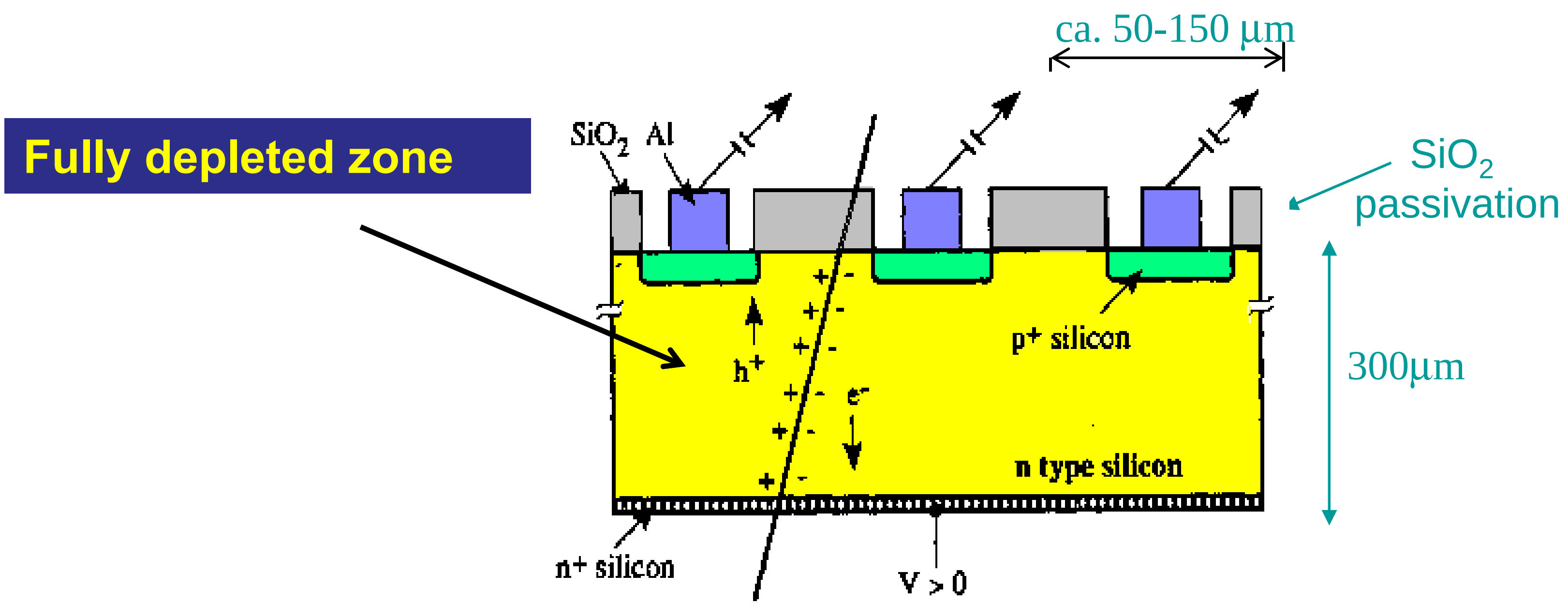

N (e-h) = 11 000/100µm

Position Resolution down to ~ 5µm !

Silicon Detector

Every electrode is connected to an amplifier →
Highly integrated readout electronics.

Two dimensional readout is possible.

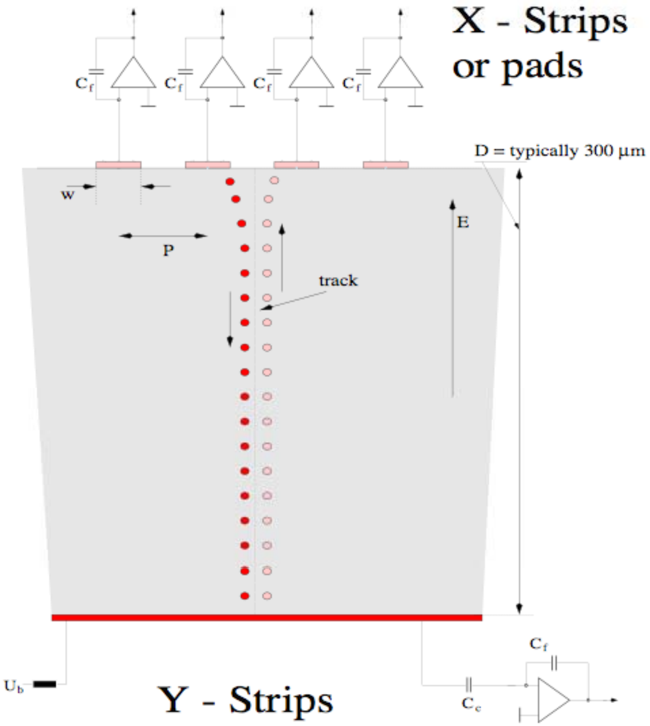

CMS Outer Barrel Module

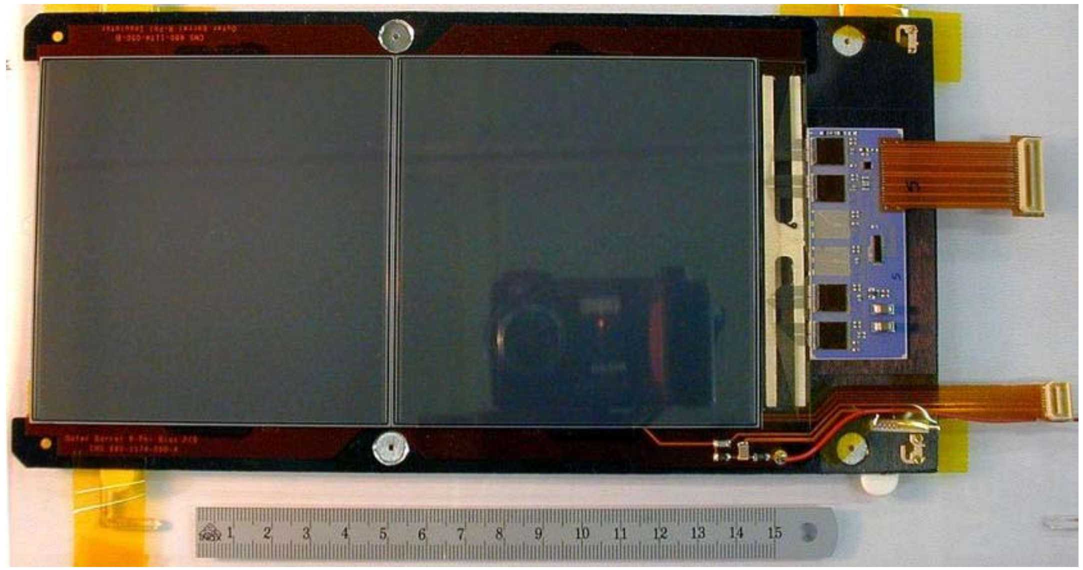

Large Silicon Systems

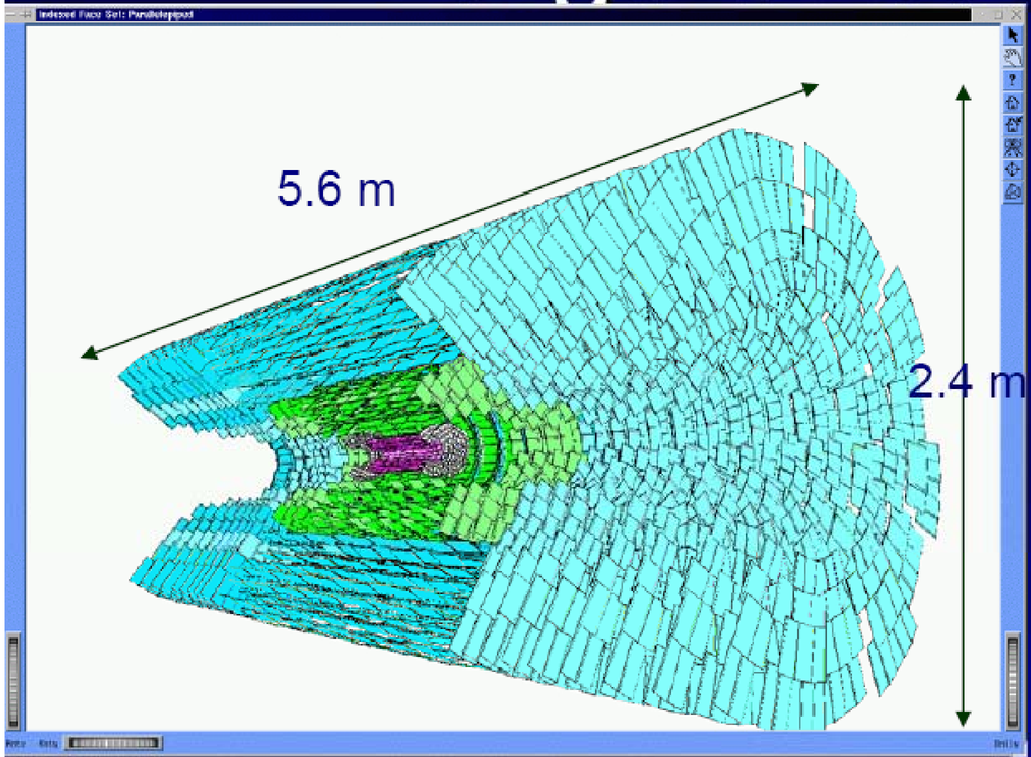

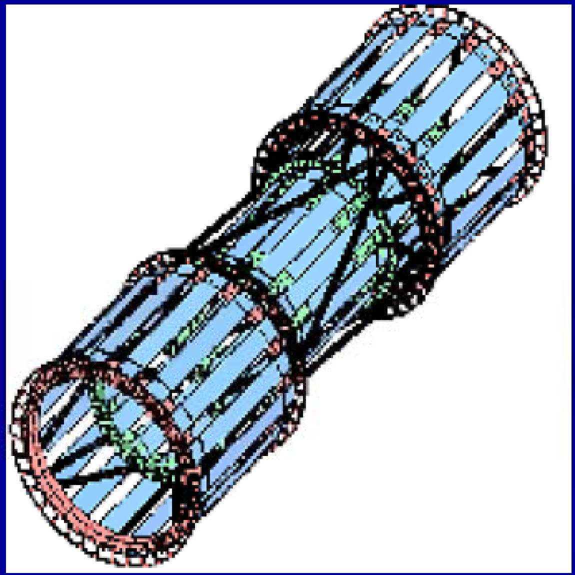

CMS tracker (~2007)

12000 modules

~ 445 m^2 silicon area

~ 24,328 silicon wafers

~ 60 M readout channels

CDF SVX IIa (2001-)

~ 11m^2 silicon area

~ 750 000 readout channels

CMS Tracker

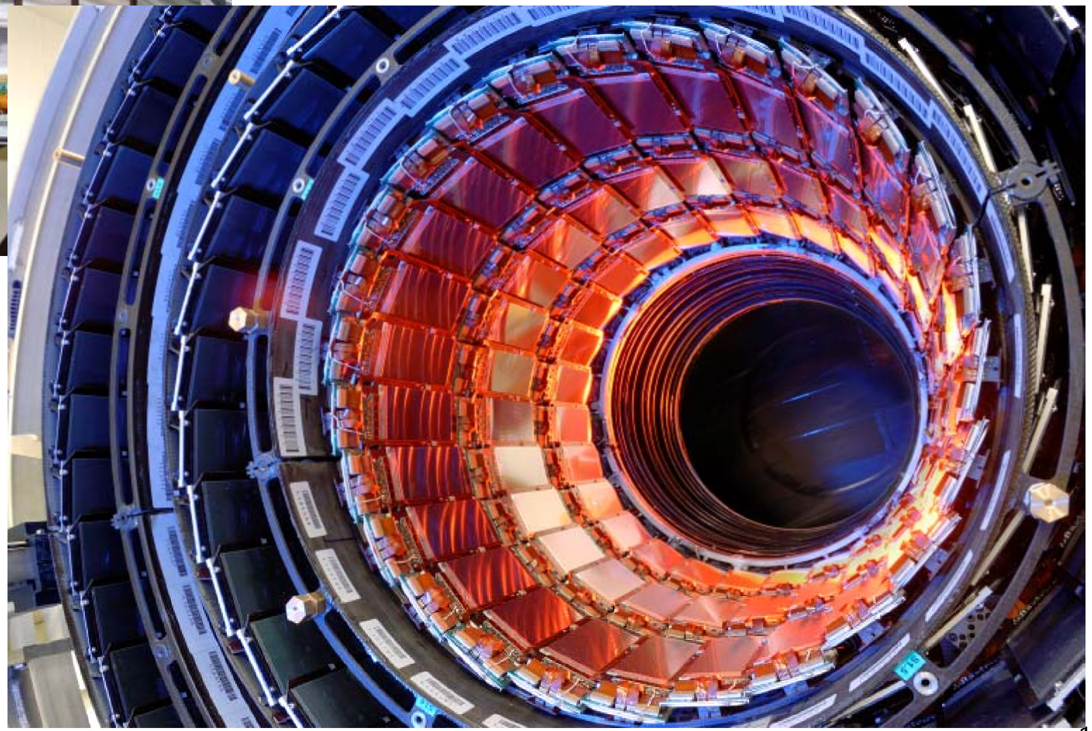

Silicon Drift Detector (like gas TPC !)

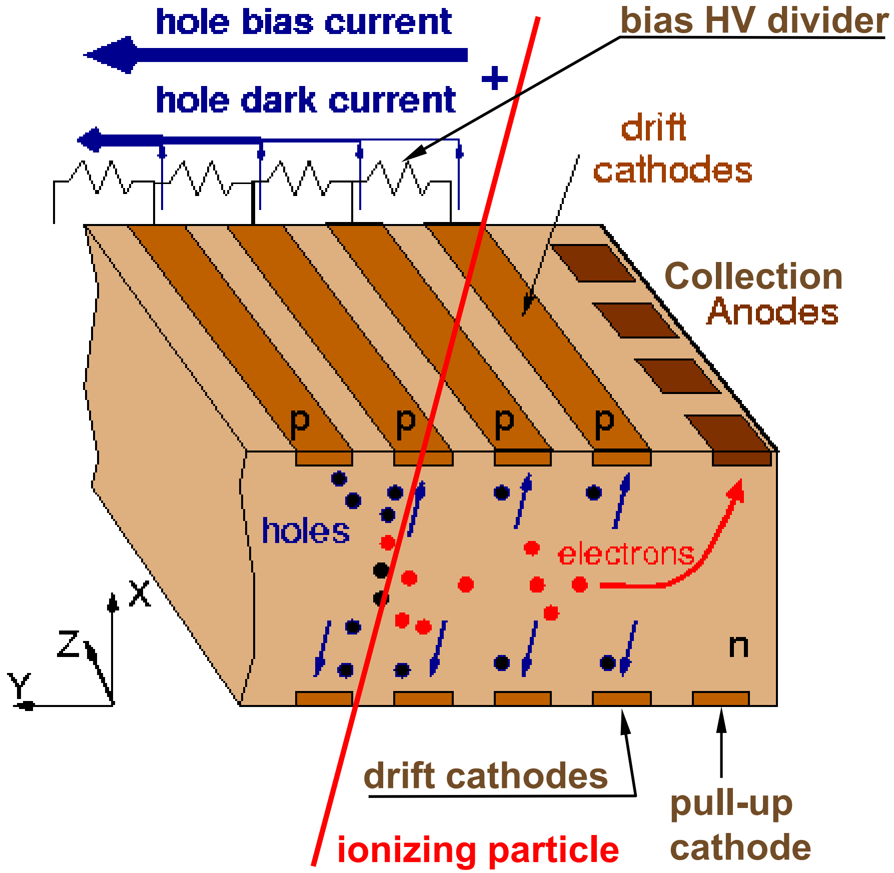

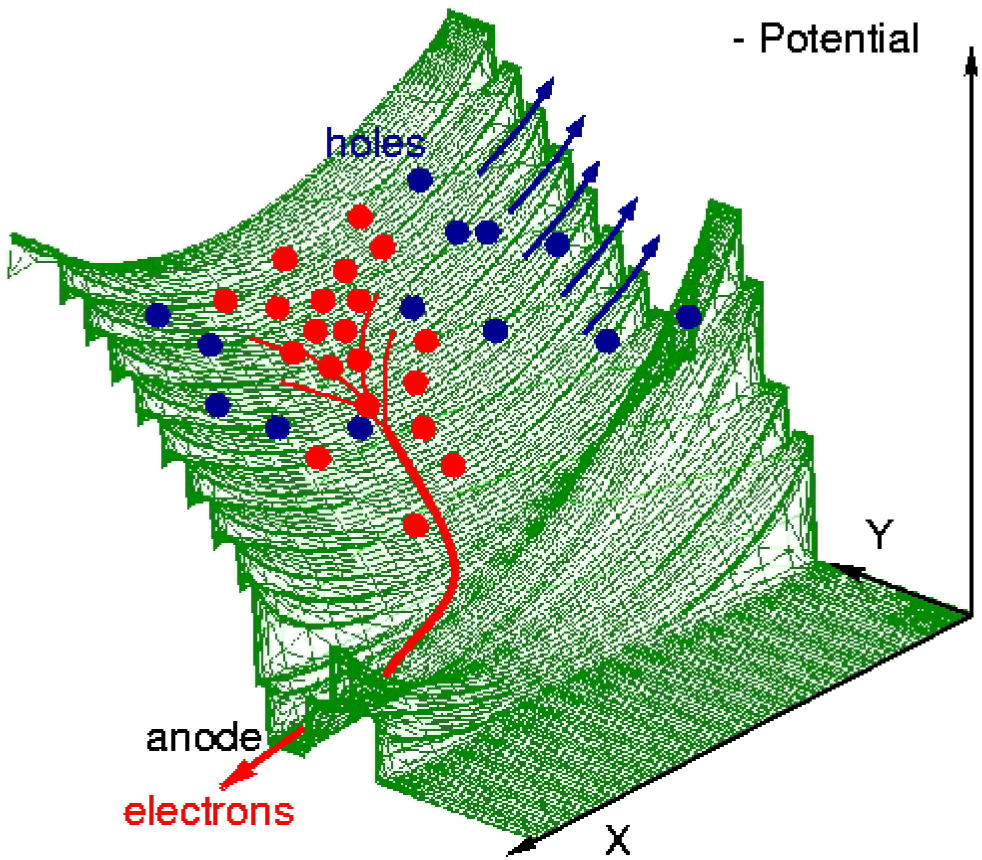

Silicon Drift Detector (like gas TPC !)

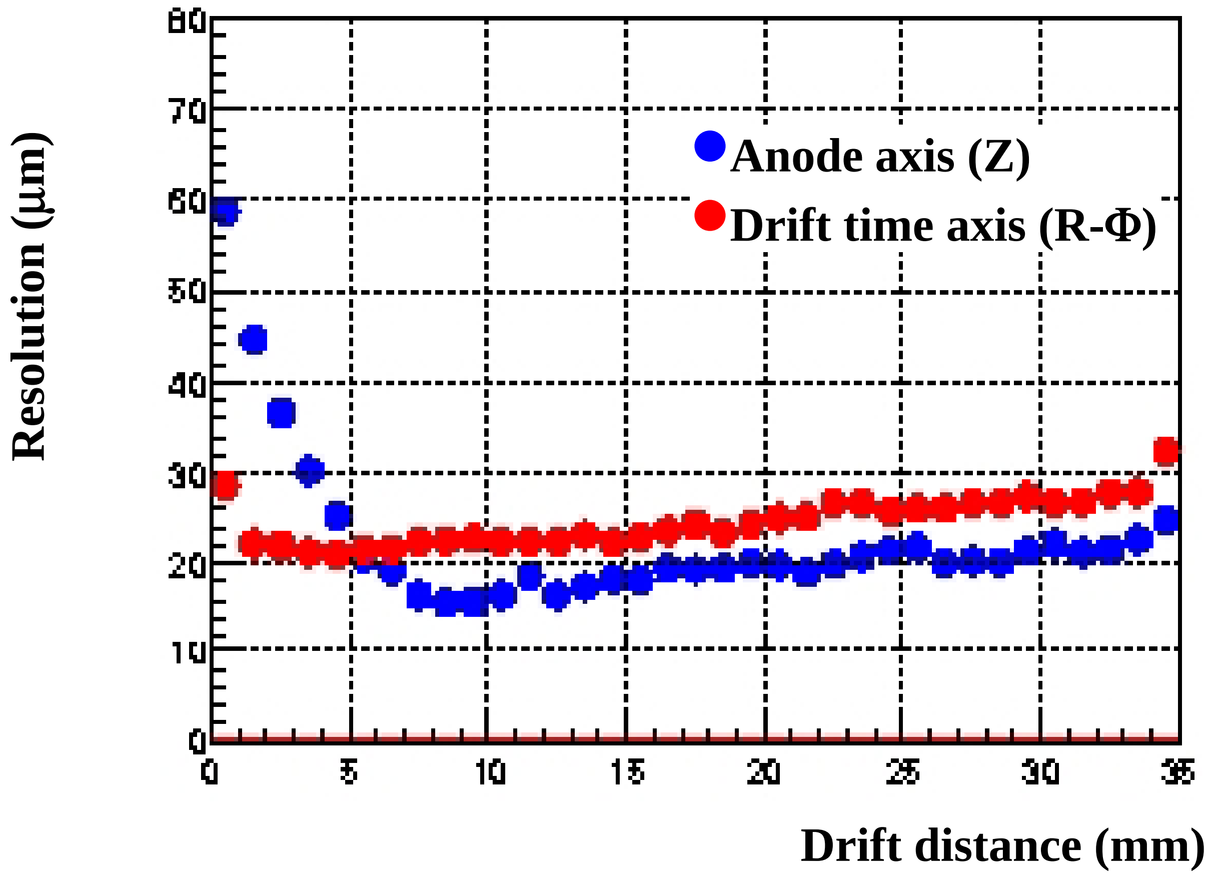

Pixel-Detectors

Problem:
2-dimensional readout of strip detectors results in ‘Ghost Tracks’ at high particle multiplicities i.e. many particles at the same time.

Solution:
Si detectors with 2 dimensional ‘chessboard’ readout. Typical size 50 x 200 µm.

Problem:
Coupling of readout electronics to the detector

Solution:
Bump bonding

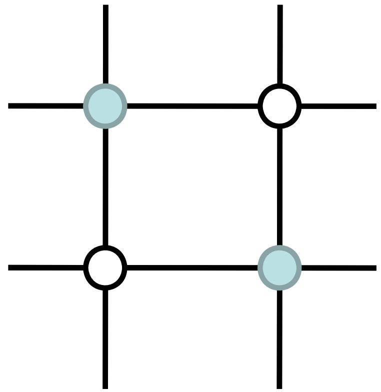

Bump Bonding of each Pixel Sensor to the Readout Electronics

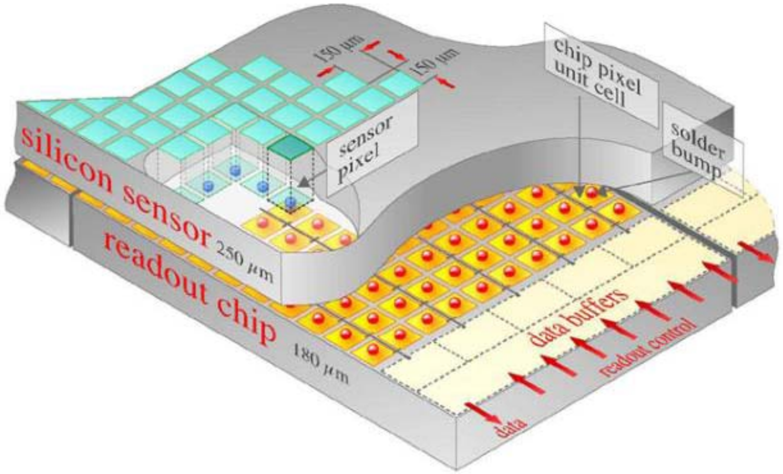

ATLAS: 1.4x10^8 pixels

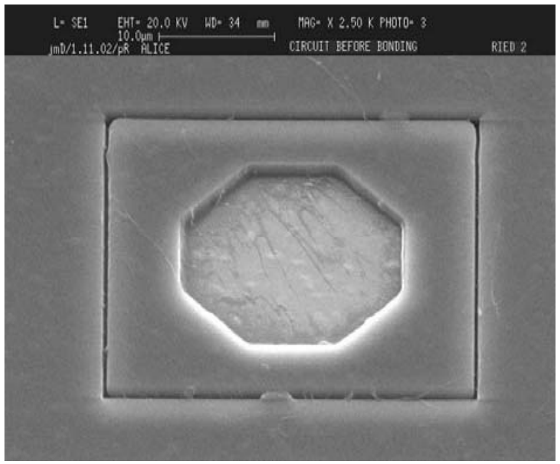

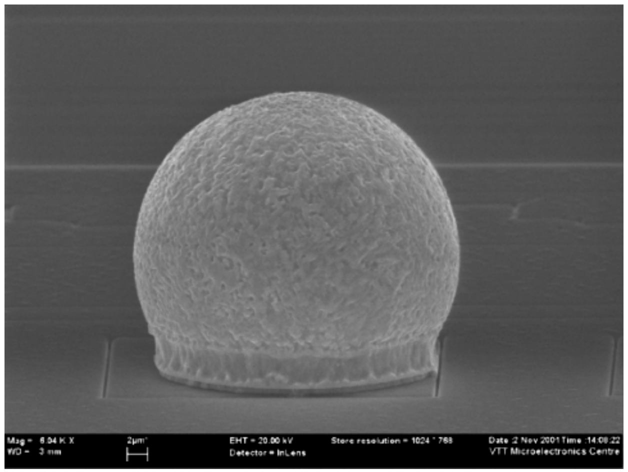

Radiation Effects ‘Aging’

Increase in leakage current

Increase in depletion voltage

Decrease in charge collection efficiency due to under-depletion and charge trapping.

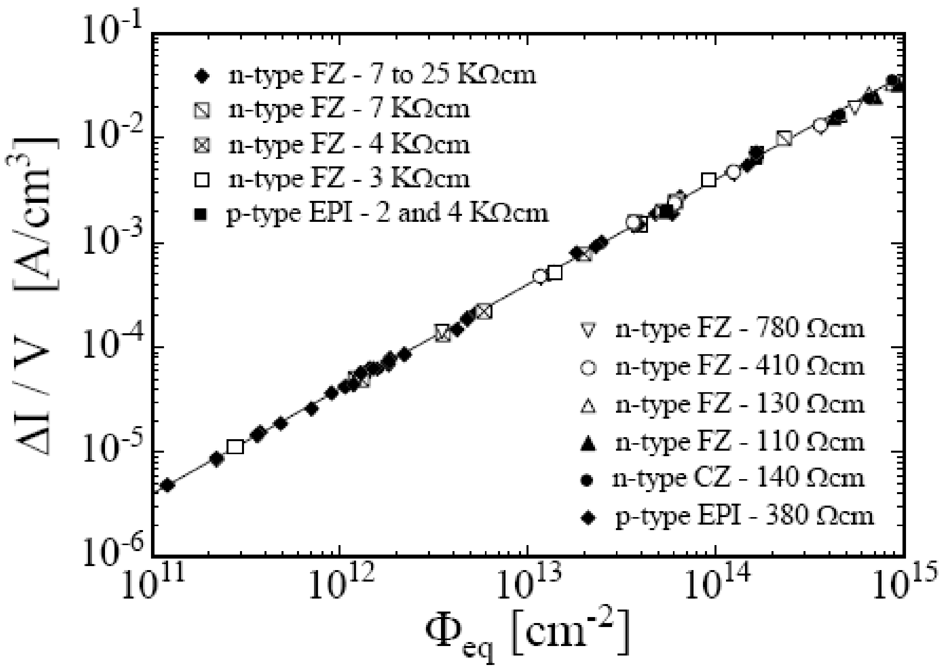

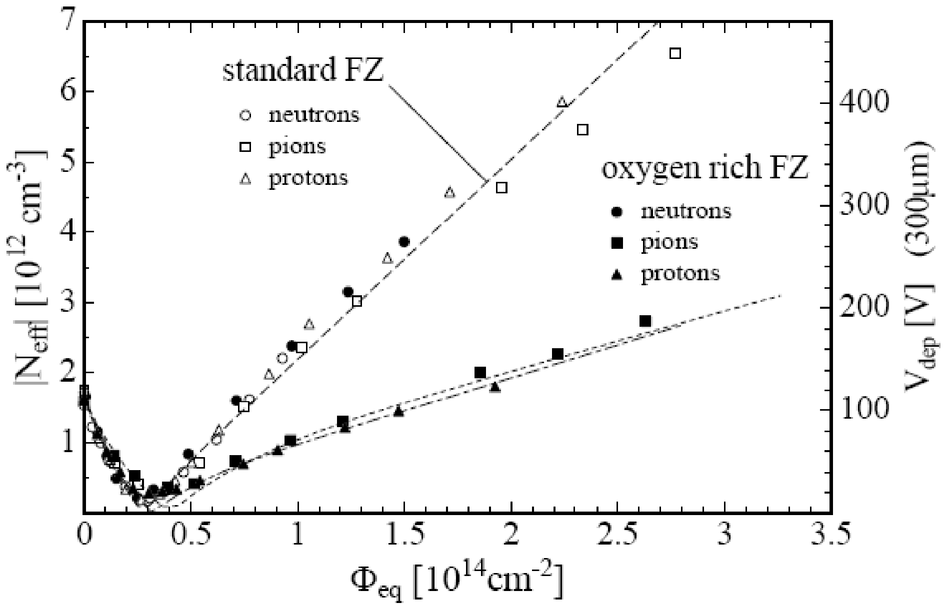

Obvious Goal: Monolithic Solid State Detectors
→Sensor and Readout Electronics as integral unit

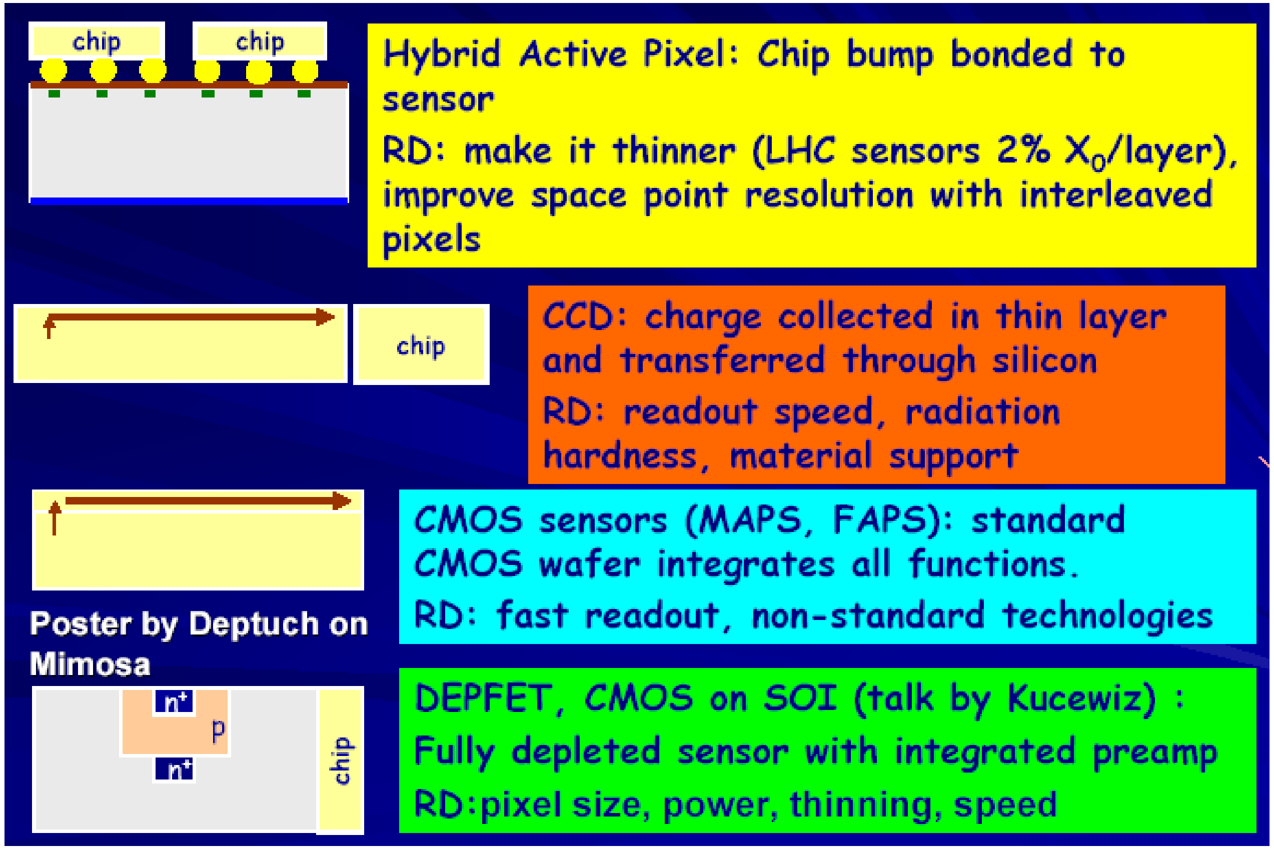

Large variety of monolithic pixel Detectors are explored, Currently mostly adapted to low collision rates of Linear Colliders.

Summary on Solid State Detectors

Solid state detectors provide very high precision tracking in particle physics experiments (down to 5um) for vertex measurement but also for momentum spectroscopy over large areas (CMS).

Technology is improving rapidly due to rapid Silicon development for electronics industry.

Typical numbers where detectors start to strongly degrade are 10^{14}-10^{15} hadron/cm^2.

Diamond, engineered Silicon and novel geometries provide higher radiation resistance.

Clearly, monolithic solid state detectors are the ultimate goal. Current developments along these lines are useful for low rate applications.

Bremsstrahlung

A charged particle of mass M and charge $q=Z_1e$ is deflected by a nucleus of charge Ze (which is partially 'shielded' by the electrons). During this deflection the charge is 'accelerated' and it therefore radiates → Bremsstrahlung.

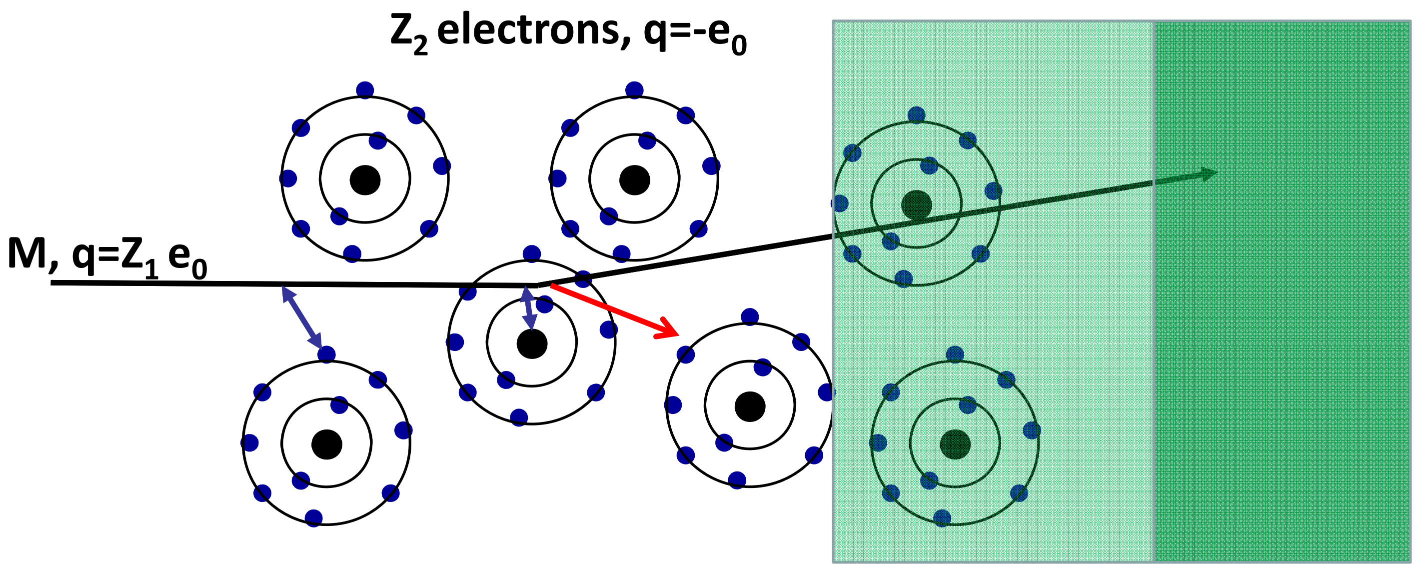

Bremsstrahlung, QM

2.6 Bremsstrahlung Q.M.

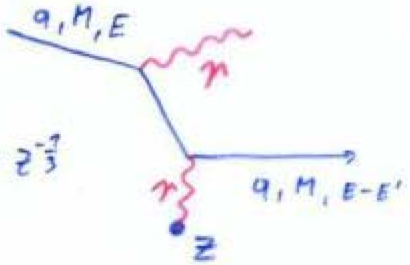

$q = Z_1 e, \quad E + Mc^2 \gg 137\, Mc^2\, Z^{-\frac{1}{3}}$

→ Highly Relativistic:

$$\frac{d\sigma(E,E')}{dE'} = 4\alpha Z^2 Z_1^4 \left(\frac{1}{4\pi\varepsilon_0}\frac{e^2}{Mc^2}\right)^2 \frac{1}{E'} F(E,E')$$

$$F(E,E') = \left[1 + \left(1 - \frac{E'}{E+Mc^2}\right)^2 - \frac{2}{3}\left(1 - \frac{E'}{E+Mc^2}\right)\right] \ln 183 Z^{-\frac{1}{3}} + \frac{1}{9}\left(1 - \frac{E'}{E+Mc^2}\right)$$

$$\frac{dE}{dx} = -\frac{N_A \rho}{A}\int_0^E E' \frac{d\sigma}{dE'} dE' \approx 4\alpha Z^2 Z_1^4 \left(\frac{1}{4\pi\varepsilon_0}\frac{e^2}{Mc^2}\right)^2 E\left[\ln 183 Z^{-\frac{1}{3}} + \frac{1}{18}\right]$$

$$\frac{dE}{dx} = -\frac{N_A \rho}{A} 4\alpha Z^2 Z_1^4 \left(\frac{1}{4\pi\varepsilon_0}\frac{e^2}{Mc^2}\right)^2 E \ln\left(183 Z^{-\frac{1}{3}}\right)$$

$$E(x) = E_0 e^{-\frac{x}{X_0}} \qquad X_0 = \frac{A}{4\alpha N_A \rho Z^2 \left(\frac{1}{4\pi\varepsilon_0}\frac{e^2}{Mc^2}\right)^2 \ln 183 Z^{-\frac{1}{3}}}$$

X_0 ... Radiation length

Proportional to Z^2/A of the Material.

Proportional to Z_1^4 of the incoming particle.

Proportional to ρ of the material.

Proportional $1/M^2$ of the incoming particle.

Proportional to the Energy of the Incoming particle →

$E(x)=\mathrm{Exp}(-x/X_0)$ – 'Radiation Length'

$X_0 \propto M^2 A / (\rho\, Z_1^4\, Z^2)$

X_0: Distance where the Energy E_0 of the incoming particle decreases $E_0 \mathrm{Exp}(-1)=0.37 E_0$.

Critical Energy

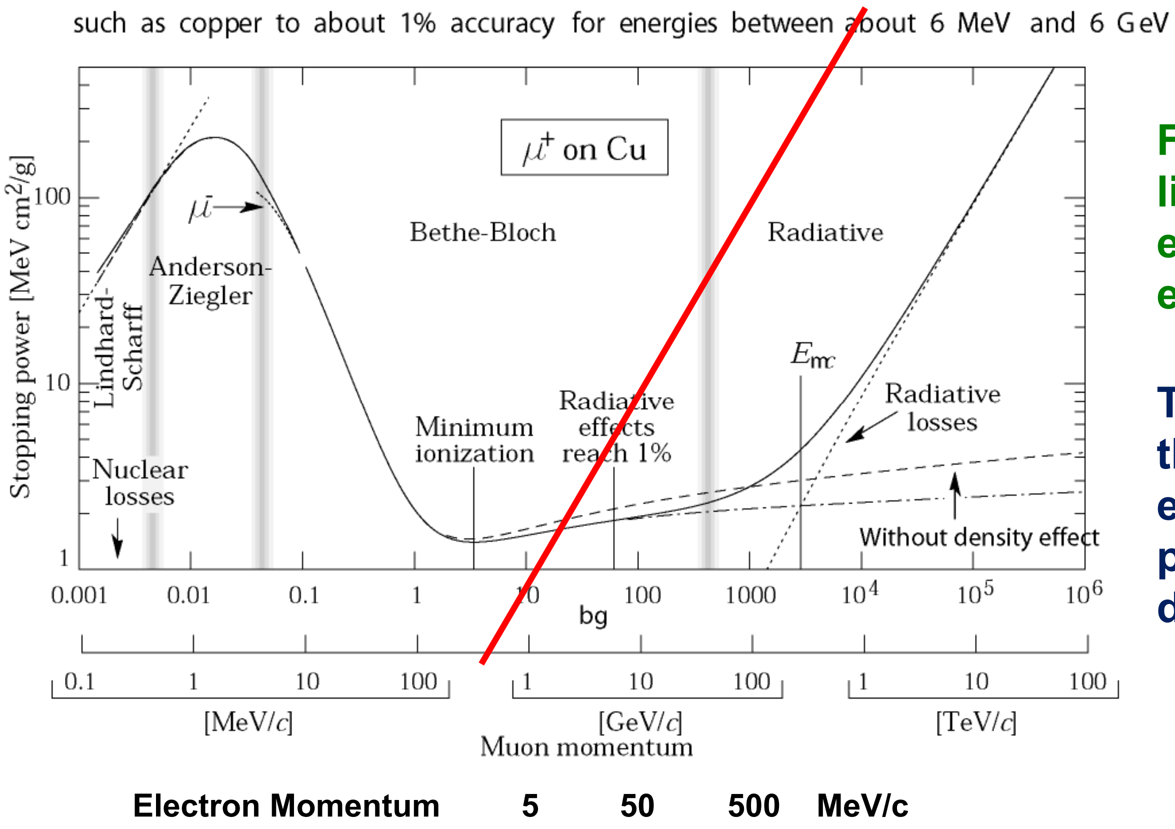

For the muon, the second lightest particle after the electron, the critical energy is at 400GeV.

The EM Bremsstrahlung is therefore only relevant for electrons at energies of past and present detectors.

Critical Energy: If dE/dx (Ionization) = dE/dx (Bremsstrahlung)

Myon in Copper: p ≈ 400GeV
Electron in Copper: p ≈ 20MeV

Pair Production, QM

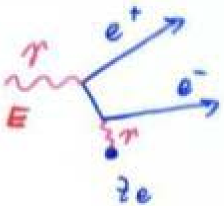

$\gamma + \text{Nucl.} \rightarrow e^+ + e^- + \text{Nucl}$

The Diagram is very similar to Bremsstrahlung

$e^- + \text{Nucl} \rightarrow \gamma + e^- + \text{Nucl}$

'Crossing Symmetry: bring particle to the other side and make it the antiparticle' → 'same' crossection ...

$$\frac{d\sigma(E,E')}{dE'} = 4\alpha Z^2 r_e^2 \frac{1}{E} \cdot G(E,E') \qquad E \gg 137 m_e c^2 Z^{-\frac{1}{3}}$$

$$G(E,E') = \left[\left(\left(\frac{E'+m_ec^2}{E}\right)^2 + \left(1-\frac{E'+m_ec^2}{E}\right)^2 + \frac{2}{3}\frac{E'+m_ec^2}{E}\left(1-\frac{E'+m_ec^2}{E}\right)\right)\ln Z^{-\frac{1}{3}} - \frac{1}{9}\frac{E'+m_ec^2}{E}\left(1-\frac{E'+m_ec^2}{E}\right)\right]$$

$$\sigma = \int_0^{E-2m_ec^2} \frac{d\sigma}{dE'}dE' = 4\alpha Z^2 r_e^2 \cdot \frac{7}{9} \ln 183 Z^{-\frac{1}{3}}$$

$$P(x) = \frac{1}{\lambda} e^{-\frac{x}{\lambda}} \qquad \lambda = \frac{A}{\rho N_A \sigma} = \frac{9}{7} X_0$$

↳ Probability that Photon converts to $e^+ e^-$ after a distance x.

For $E\gamma \gg m_ec^2 = 0.5$MeV : $\lambda = 9/7 X_0$

Average distance a high energy photon has to travel before it converts into an $e^+ e^-$ pair is equal to 9/7 of the distance that a high energy electron has to travel before reducing it's energy from E_0 to E_0*Exp(-1) by photon radiation.

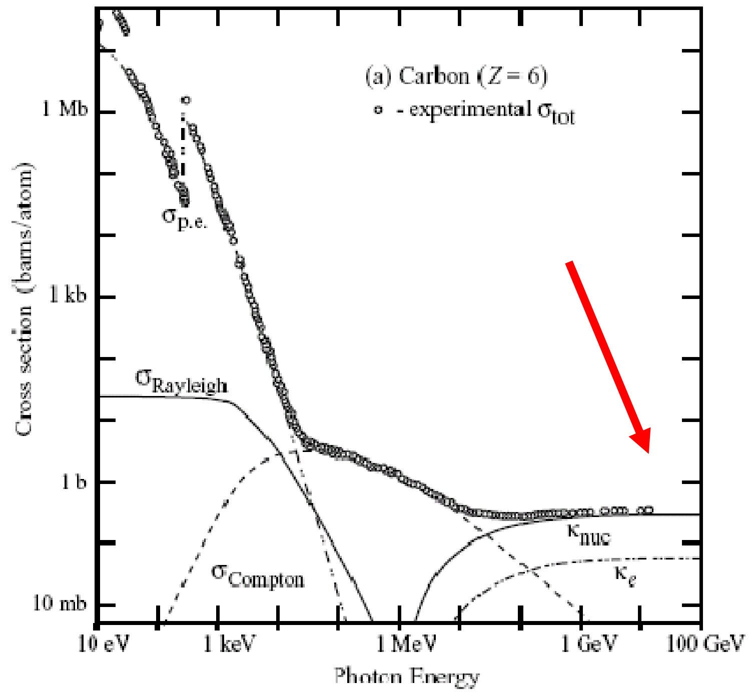

Bremsstrahlung + Pair Production → EM Shower

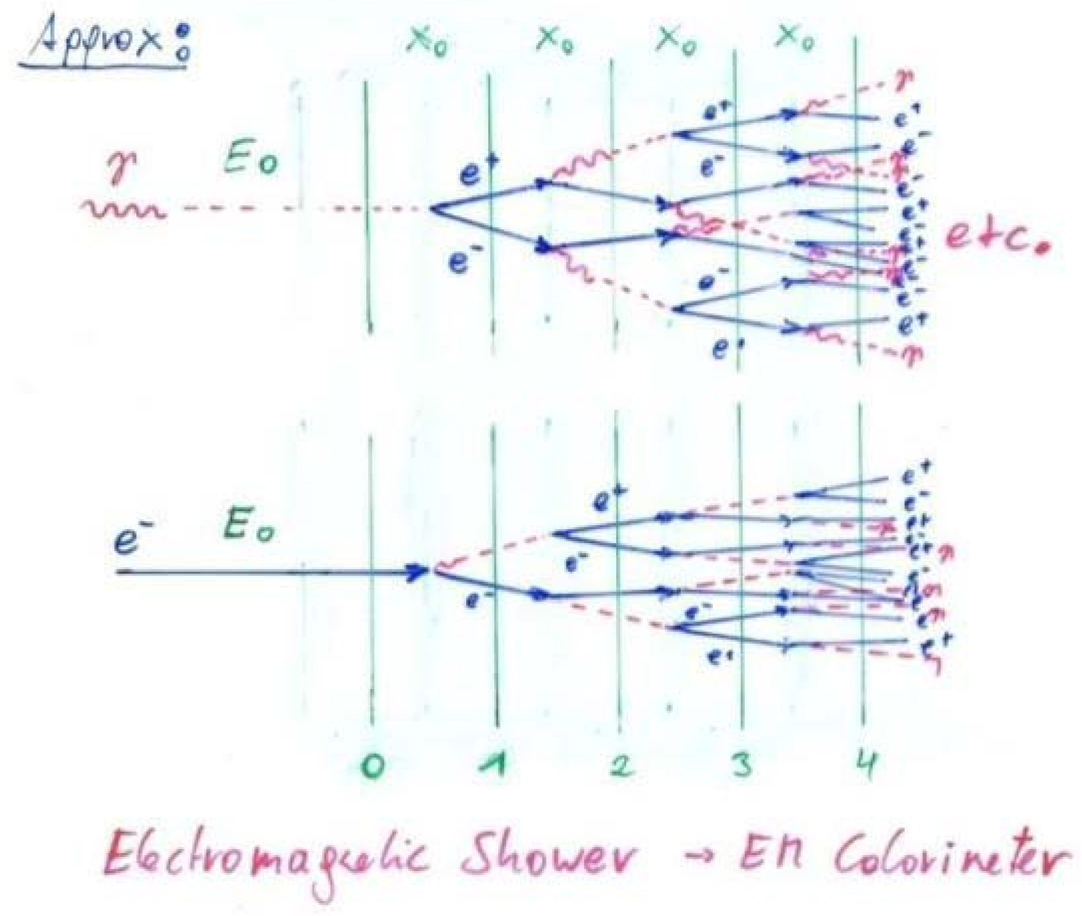

Electro-Magnetic Shower of High Energy Electrons and Photons

$N(n) = 2^n$ ..... Number of particles $(e^\pm, \gamma)$ after $n X_0$

$E(n) = \frac{E_0}{2^n}$ .... Average Energy of particles after $n X_0$

Shower stops if $E(n) = E_{critical}$

$\rightarrow n_{max} = \frac{1}{\ln 2} \ln \frac{E_0}{E_c}$ $\rightarrow$ Shower length rises with $\ln E_0$

Number of $e^\pm$ track segments (of length X_0) after $n X_0$:

$$N_{tr}(n) = 2^n$$

Total $e^\pm$ track length (after $n_{max} X_0$)

$$L = \sum_{n=0}^{n_{max}} 2^n X_0 = \left(2\frac{E_0}{E_c} - 1\right) X_0 \sim 2\frac{E_0}{E_c} X_0 = c_1 \cdot E_0$$

Total (charged) track length is proportional to the Energy of the Particle.

$\rightarrow$ Calorimeter Principle

Calorimetry: Energy Measurement by total Absorption of Particles

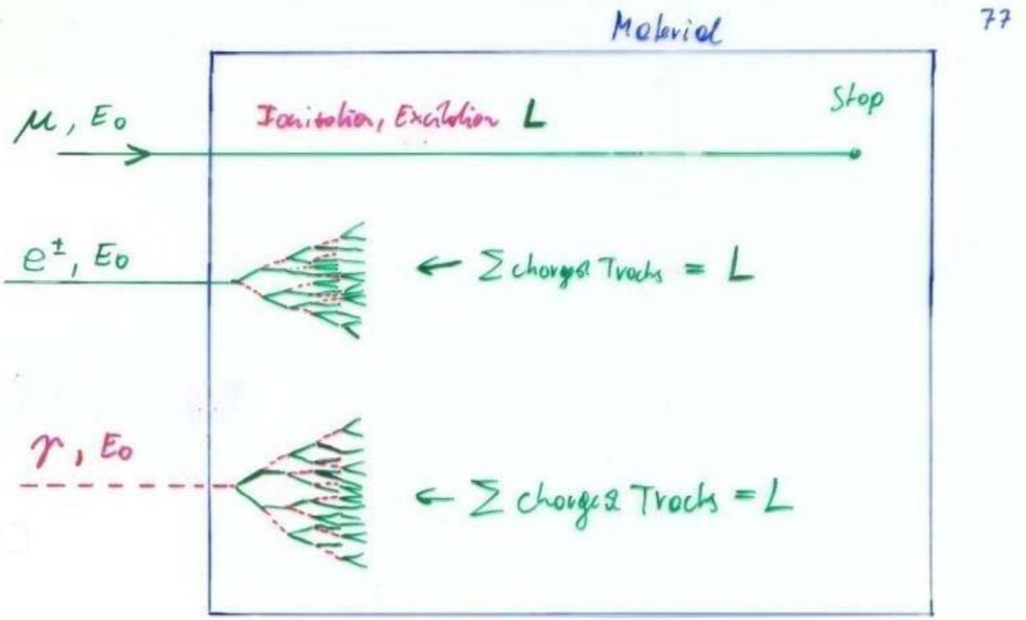

The $e^\pm$ in the Calorimeter ionize and excite the Material

Ionization: e^-, I^+ pairs in the Material

Excitation: Photons in the Material

Measuring the total Number of e^-, I^+ pairs or the total Number of Photons gives the particle Energy.

If N is the total Number of e^+, I^+ pairs or photons, or $N = c_1 E_0$:

$\Delta N = \sqrt{N}$ (Poisson Statistics)

$$\frac{\Delta E}{E} = \frac{\Delta N}{N} = \frac{1}{\sqrt{N}} = \frac{a}{\sqrt{E}} \rightarrow \text{Resolution}$$

Only Electrons and High Energy Photons show EM cascades at current GeV-TeV level Energies.

Strongly interacting particles like Pions, Kaons, produce hardonic showers in a similar fashion to the EM cascade →Hadronic calorimetry

Calorimetry: Energy Measurement by total Absorption of Particles

The Measurement is destructive. The particle can not be subject to further study.

Energy Measurement by

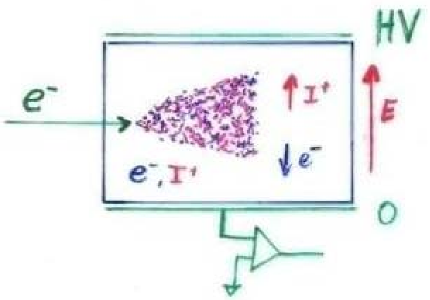

Collecting the produced Charge

Liquid Nobel Gases (Nobel Liquids)

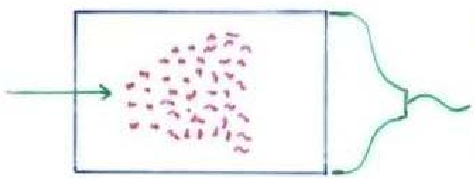

Measuring the Photons produced by the collision of the $e^\pm$ with Atom Electrons of the Material.

Scintillating Crystals, Plastic Scintillators

Total Amount of e^-, I^+ pairs or Photons is proportional to the total track length is proportional to the particle Energy.

Calorimetry

Calorimeters are blocks of instrumented material in which particles to be measured are fully absorbed and their energy transformed into a measurable quantity.

The interaction of the incident particle with the detector (through electro-magnetic or strong processes) produces a shower of secondary particles with progressively degraded energy.

The energy deposited by the charged particles of the shower in the active part of the calorimeter, which can be detected in the form of charge or light, serves as a measurement of the energy of the incident particle.

C.W. Fabjan and F. Gianotti, Rev. Mod. Phys., Vol. 75, N0. 4, October 2003

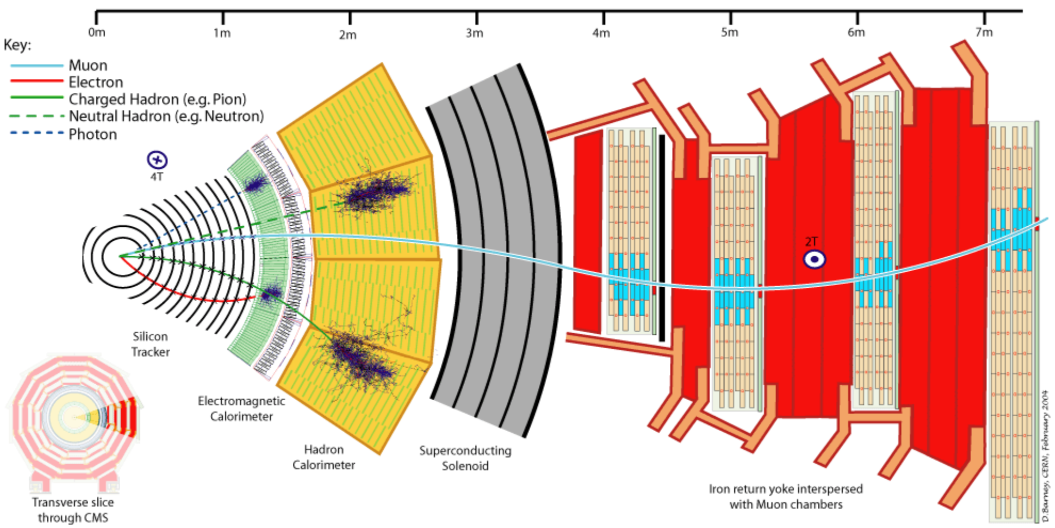

Calorimetry

Calorimeters can be classified into:

Electromagnetic Calorimeters,
to measure electrons and photons through their EM interactions.

Hadron Calorimeters,
Used to measure hadrons through their strong and EM interactions.

The construction can be classified into:

Homogeneous Calorimeters,
that are built of only one type of material that performs both tasks, energy degradation and signal generation.

Sampling Calorimeters,
that consist of alternating layers of an absorber, a dense material used to degrade the energy of the incident particle, and an active medium that provides the detectable signal.

C.W. Fabjan and F. Gianotti, Rev. Mod. Phys., Vol. 75, N0. 4, October 2003

Calorimetry

Calorimeters are attractive in our field for various reasons:

In contrast with magnet spectrometers, in which the momentum resolution deteriorates linearly with the particle momentum, on most cases the calorimeter energy resolution improves as 1/Sqrt(E), where E is the energy of the incident particle. Therefore calorimeters are very well suited for high-energy physics experiments.

In contrast to magnet spectrometers, calorimeters are sensitive to all types of particles, charged and neutral. They can even provide indirect detection of neutrinos and their energy through a measurement of the event missing energy.

Calorimeters are commonly used for trigger purposes since they can provide since they can provide fast signals that are easy to process and interpret.

They are space and therefore cost effective. Because the shower length increases only logarithmically with energy, the detector thickness needs to increase only logarithmically with the energy of the particles. In contrast for a fixed momentum resolution, the bending power BL^2 of a magnetic spectrometer must increase linearly with the particle momentum.

C.W. Fabjan and F. Gianotti, Rev. Mod. Phys., Vol. 75, N0. 4, October 2003

EM Calorimetry

Approximate longitudinal shower development

$N(n) = 2^n$ ..... Number of particles ($e^\pm, \gamma$) after $n X_0$

$E(n) = \frac{E_0}{2^n}$ .... Average Energy of particles after $n X_0$

Shower stops if $E(n) = E_{critical}$

$\rightarrow n_{max} = \frac{1}{\ln 2} \ln \frac{E_0}{E_c}$ $\rightarrow$ Shower length rises with $\ln E_0$

Radiation Length X_0 and Moliere Radius are two key parameters for choice of calorimeter materials

Approximate transverse shower development

The transverse Shower Dimension is mainly related to the Multiple scattering of the low Energy Electrons.

$$\theta_0 \sim \frac{21\,[\mathrm{MeV}]}{\beta p [\frac{\mathrm{MeV}}{c}]} z_1 \cdot \sqrt{\frac{x}{X_0}}$$

Electrons E_c , $E \sim p \cdot c$

$$\theta_0 \sim \frac{21\,[\mathrm{MeV}]}{\beta E_c [\mathrm{MeV}]} \cdot z_1 \cdot \sqrt{\frac{x}{X_0}} \qquad z_1 = 1, \beta \sim 1$$

$$E_c \sim \frac{610}{Z + 1.24}\ \mathrm{MeV} \sim \frac{610}{Z}\ \mathrm{MeV}$$

$$\theta_0 = 0.0344 \cdot Z \cdot \sqrt{\frac{x}{X_0}}$$

Moliere Radius ρ_M = Lateral Shower Radius after $1 X_0$:

$$\underline{\rho_M \approx 0.0344 \cdot Z \cdot X_0}$$

95% of Energy are in a Cylinder of $2\rho_M$ Radius.

Crystals for Homogeneous EM Calorimetry

In crystals the light emission is related to the crystal structure of the material. Incident charged particles create electron-hole pairs and photons are emitted when electrons return to the valence band.

The incident electron or photon is completely absorbed and the produced amount of light, which is reflected through the transparent crystal, is measured by photomultipliers or solid state photon detectors.

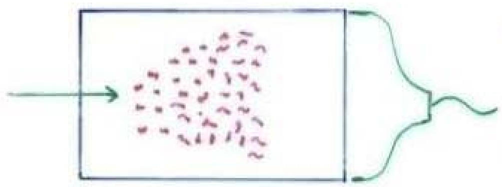

Measuring the Photons produced by the collision of the $e^\pm$ with Atom Electrons of the material.

Crystals for Homogeneous EM Calorimetry

	NaI(Tl)	CsI(Tl)	CsI	BGO	$PbWO_4$
Density (g/cm^3)	3.67	4.53	4.53	7.13	8.28
X_0 (cm)	2.59	1.85	1.85	1.12	0.89
R_M (cm)	4.5	3.8	3.8	2.4	2.2
Decay time (ns)	250	1000	10	300	5
slow component			36		15
Emission peak (nm)	410	565	305	410	440
slow component			480		
Light yield γ/MeV	4×10^4	5×10^4	4×10^4	8×10^3	1.5×10^2
Photoelectron yield (relative to NaI)	1	0.4	0.1	0.15	0.01
Rad. hardness (Gy)	1	10	10^3	1	10^5

Barbar@PEPII, 10ms interaction rate, good light yield, good S/N	KTeV@Tevatron, High rate, Good resolution	L3@LEP, 25us bunch crossing, Low radiation dose	CMS@LHC, 25ns bunch crossing, high radiation dose

Crystals for Homogeneous EM Calorimetry

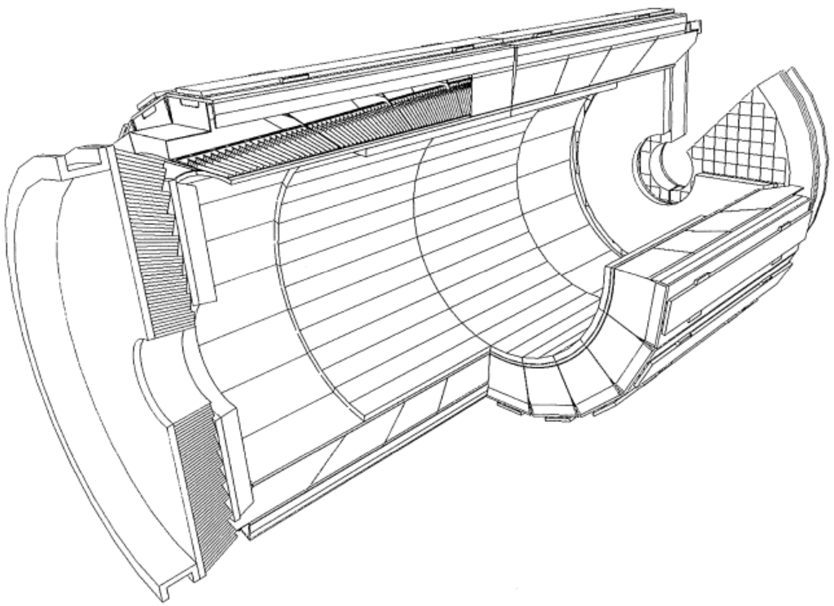

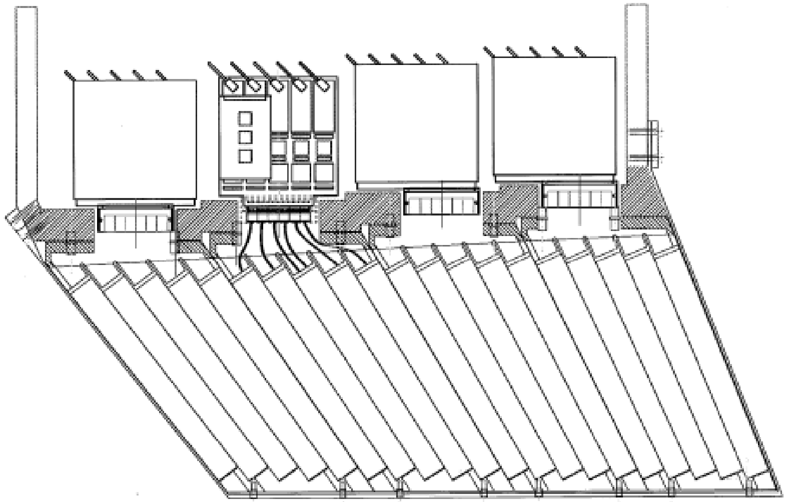

Fig. 2. Longitudinal drawing of module 2, showing the structure and the front-end electronics layout.

Noble Liquids for Homogeneous EM Calorimetry

	Ar	Kr	Xe
Z	18	36	58
A	40	84	131
X_0 (cm)	14	4.7	2.8
R_M (cm)	7.2	4.7	4.2
Density (g/cm^3)	1.4	2.5	3.0
Ionization energy (eV/pair)	23.3	20.5	15.6
Critical energy ϵ (MeV)	41.7	21.5	14.5
Drift velocity at saturation (mm/μs)	10	5	3

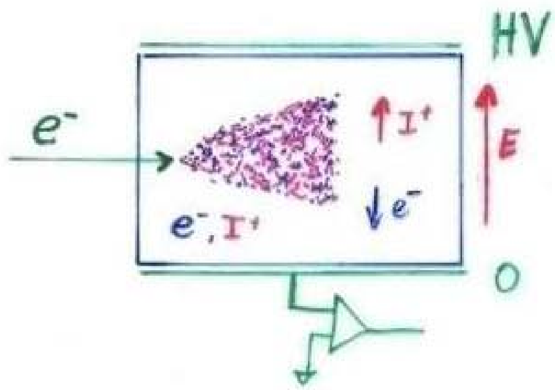

When a charge particle traverses these materials, about half the lost energy is converted into ionization and half into scintillation.

The best energy resolution would obviously be obtained by collecting both the charge and light signal. This is however rarely done because of the technical difficulties to extract light and charge in the same instrument.

Krypton is preferred in homogeneous detectors due to small radiation length and therefore compact detectors. Liquid Argon is frequently used due to low cost and high purity in sampling calorimeters (see later).

Noble Liquids for Homogeneous EM Calorimetry

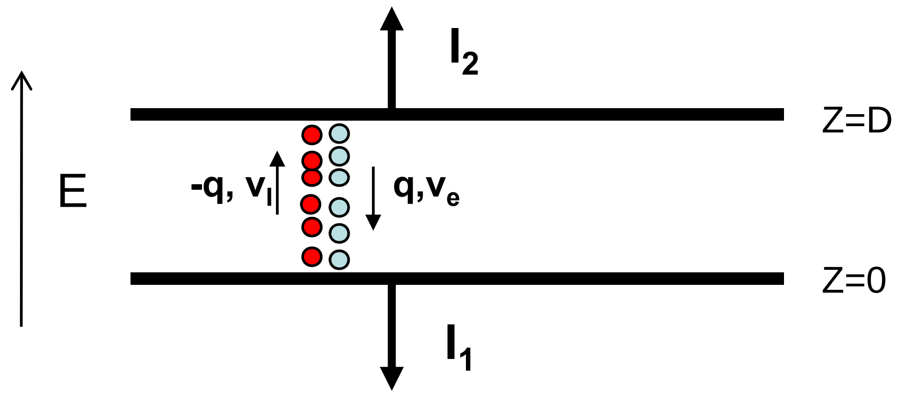

E.g. Liquid Argon, 5mm/ μs at 1kV/cm, 5mm gap → 1 μs for all electrons to reach the electrode.

The ion velocity is 10^3 to 10^5 times smaller → doesn't contribute to the signal for electronics of μs integration time.

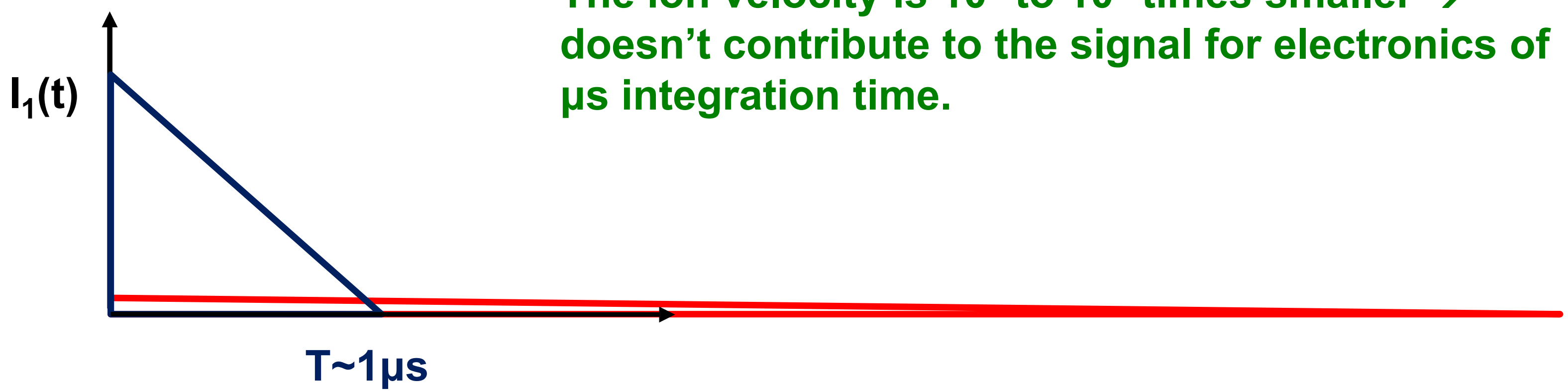

Homogeneous EM Calorimeters, Examples

NA48 Liquid Krypton
2cmx2cm cells
X_0 = 4.7cm
125cm length ($27X_0$)
ρ = 5.5cm

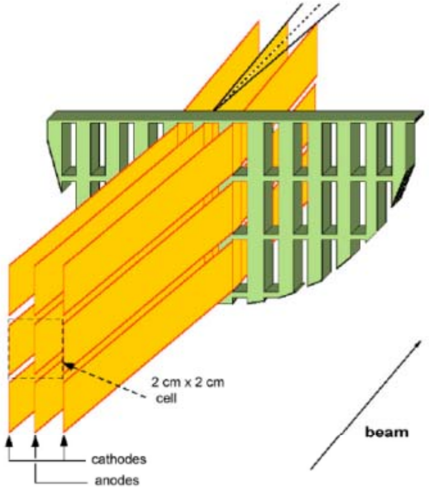

KTeV CsI
5cmx5cm and
X_0 = 1.85cm
2.5cmx2.5cm crystals
50cm length ($27X_0$)
ρ = 3.5cm

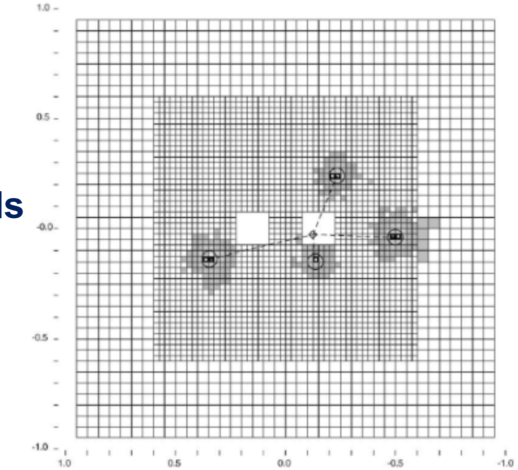

Fig. 1. Schematic of the KTeV CsI Calorimeter showing the cluster energy profiles due to four photons.

NA48 Experiment at CERN and KTeV Experiment at Fermilab, both built for measurement of direct CP violation. Homogenous calorimeters with Liquid Krypton (NA48) and CsI (KTeV). Excellent and very similar resolution.

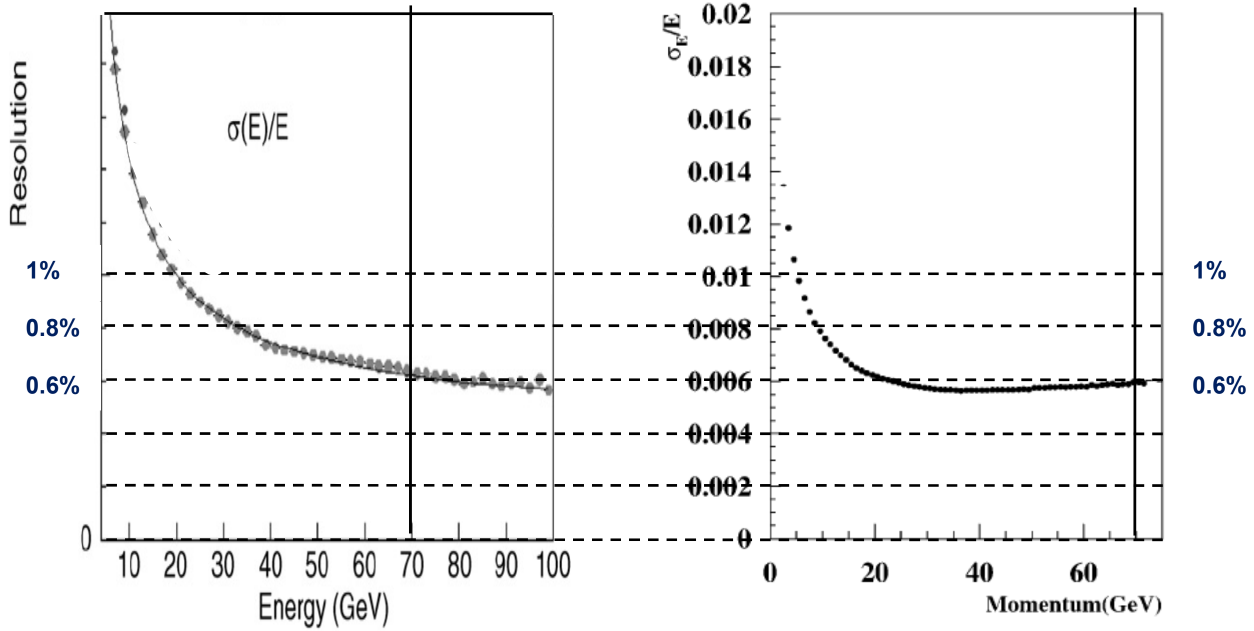

Sampling Calorimeters

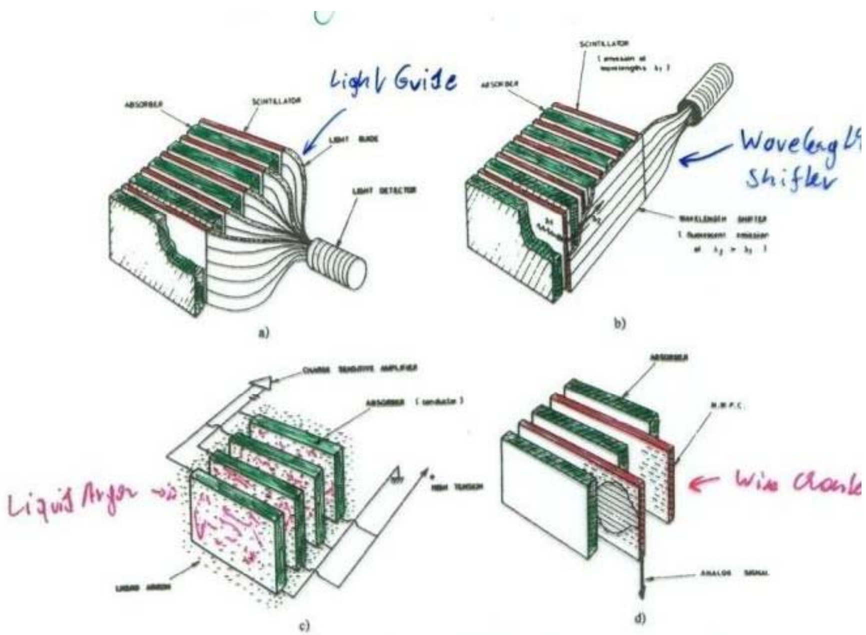

Alternation of "passive" absorber plates and "active" readout sections

Advantage:
- optimum choice of Absorber Material
- optimum choice of Signal Readout
- Compact and cheap Construction

"passive": Pb, Fe ....

"active": Scintillator (Signal -> Photons)

Noble Liquid, e.g. Ar (Signal -> e^-, I^+)

Wire Chambers (Signal -> e^-, I^+)

Energy resolution of sampling calorimeters is in general worse than that of homogeneous calorimeters, owing to the sampling fluctuations – the fluctuation of ratio of energy deposited in the active and passive material.

The resolution is typically in the range 5-20%/Sqrt[E(GeV)] for EM calorimeters. On the other hand they are relatively easy to segment longitudinally and laterally and therefore they usually offer better space resolution and particle identification than homogeneous calorimeters.

The active medium can be scintillators (organic), solid state detectors, gas detectors or liquids.

Sampling Fraction = Energy deposited in Active/Energy deposited in passive material.

Hadronic Calorimetry

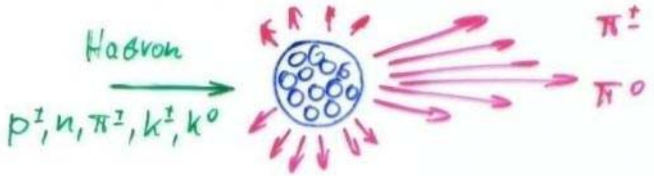

Strong Interaction

Approximate Energy Distribution

~50%	~20%	~30%
π^+, π^- $\pi^0 \to \gamma\gamma$	Nuclear Excitation	Slow Nucleons
$\pi^+\pi^-$ $\pi^+\pi^-, \pi^0 \to \gamma\gamma$	5-30 MeV	
Hadron kaskade	p, n, γ	

$\pi^0 \to \gamma\gamma \to$ Electromagnetic Component

In Hadronic Cascades the Longitudinal Shower is given by the Absorption Length λ_a $I \sim e^{-\frac{x}{\lambda_a}}$

In typical Detector Materials λ_a is much larger than X_0

$$\lambda \sim \frac{1}{\rho} \cdot 35\, A^{\frac{1}{3}}$$

	ρ	X_0	λ
Fe	7.87	1.76 cm	~17 cm
Pb	11.35	0.56 cm	~17 cm

Energy Resolution:

- A large Fraction of the Energy 'disappears' into
  - Binding Energy of emitted Nucleons
  - $\pi \to \mu + \nu$ which are not absorbed
- π^0's Decaying into $\gamma\gamma$ start an EM Cascade ($\tau \sim 10^{-16}$ s)

— Energy Resolution is worse than for EM Calorimeters

Hadron Calorimeters are Large because ● is large

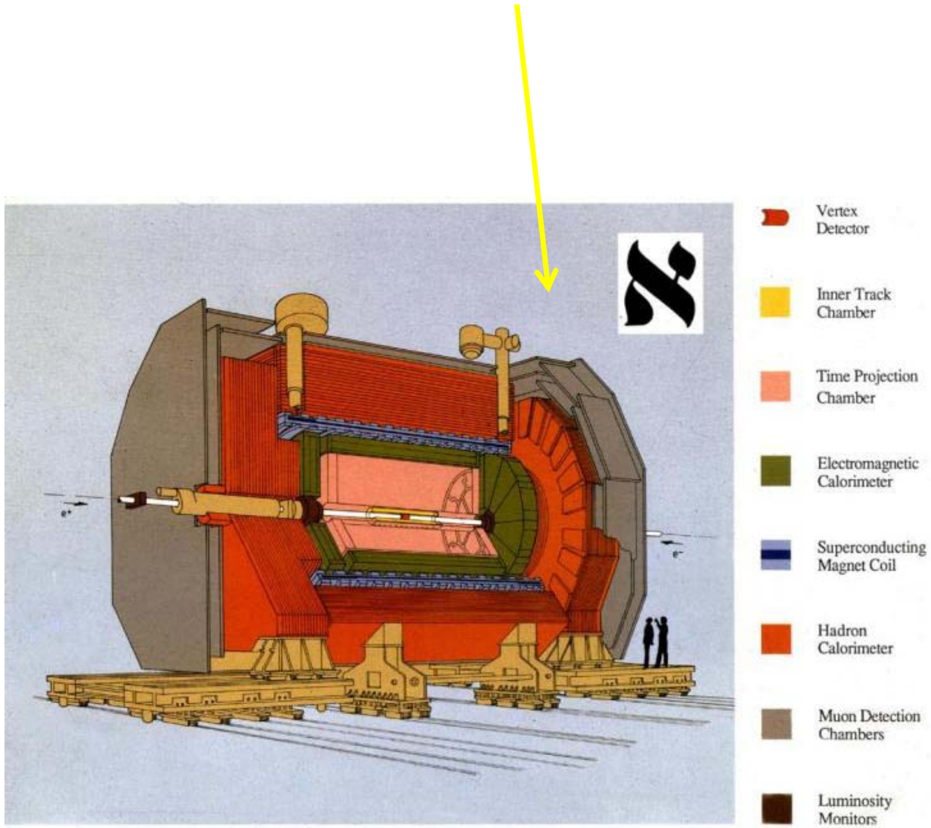

Fig. 1 - The ALEPH Detector

Hadron Calorimeters are large and heavy because the hadronic interaction length ●, the 'strong interaction equivalent' to the EM radiation length X_0, is large (5-10 times larger than X_0)

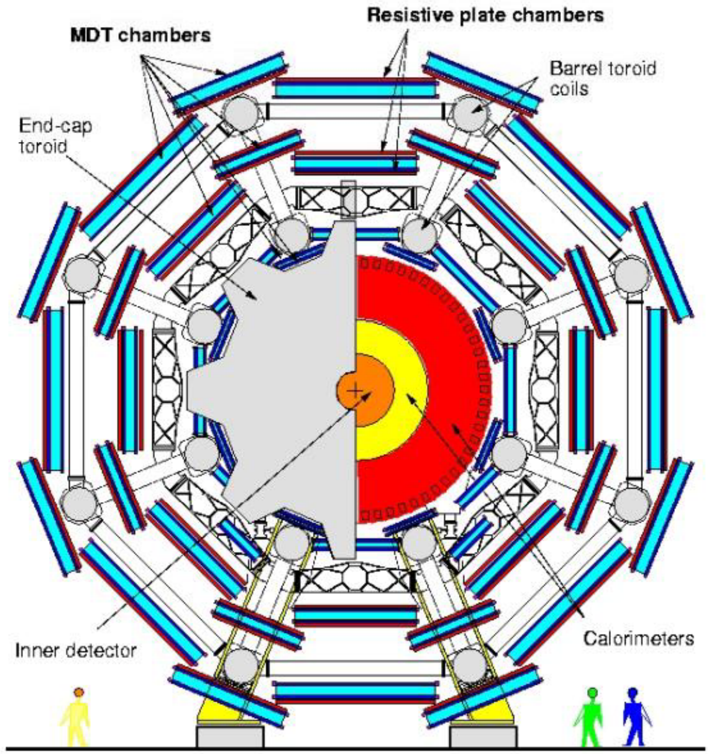

Hadron Calorimeters

By analogy with EM showers, the energy degradation of hadrons proceeds through an increasing number of (mostly) strong interactions with the calorimeter material.

However the complexity of the hadronic and nuclear processes produces a multitude of effects that determine the functioning and the performance of practical instruments, and make hadronic calorimeters more complicated instruments to optimize.

By analogy with EM showers, the energy degradation of hadrons proceeds through an increasing number of (mostly) strong interactions with the calorimeter material.

The hadronic interaction produces two classes of effects:

First, energetic secondary hadrons are produced with a mean free path of ● between interactions. Their momenta are typically a fair fraction of the primary hadron momentum i.e. at the GeV scale.

Second, in hadronic collisions with the material nuclei, a significant part of the primary energy is consumed in nuclear processes such as excitation, nucleon evaporation, spallation etc., resulting in particles with characteristic nuclear energies on the MeV scale.

C.W. Fabjan and F. Gianotti, Rev. Mod. Phys., Vol. 75, N0. 4, October 2003

Because part of the energy is therefore ‘invisible’, the resolution of hadron calorimeters is typically worse than in EM calorimeters 20-100%/Sqrt[E(GeV)] .

Particle ID

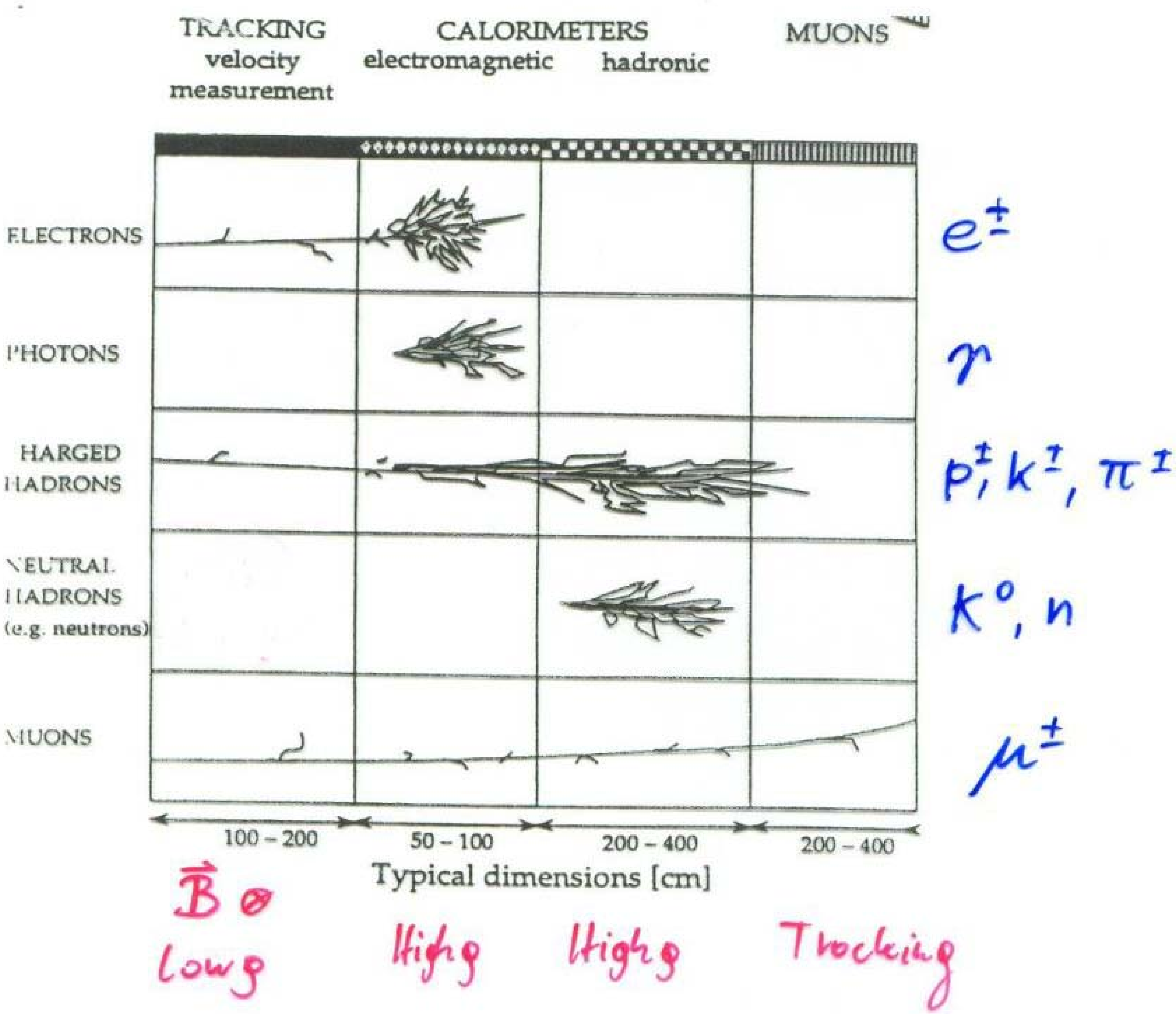

TRACKING
velocity
measurement
CALORIMETERS
electromagnetic
hadronic
MUONS
ELECTRONS
PHOTONS
HARGED
HADRONS
NEUTRAL
HADRONS
(e.g. neutrons)
MUONS
$e^\pm$
γ
$p^\pm, k^\pm, \pi^\pm$
K^0, n
$\mu^\pm$
100 – 200
50 – 100
200 – 400
200 – 400
Typical dimensions [cm]
$\vec{B}$ ⊗
Low g
High g
High g
Tracking

Detector Systems, Selected Experiments

ALICE:	**Heavy Ion Experiment at CERN**
Donut:	**Neutrino Experiment at Fermilab**
CNGS:	**Long Baseline Neutrino Experiment CERN/Gran Sasso**
Amanda:	**Neutrino Experiment at the Southpole**
AMS:	**Particle Physics Experiment in Space**

ALICE

A heavy Ion Experiment at the LHC

ALICE

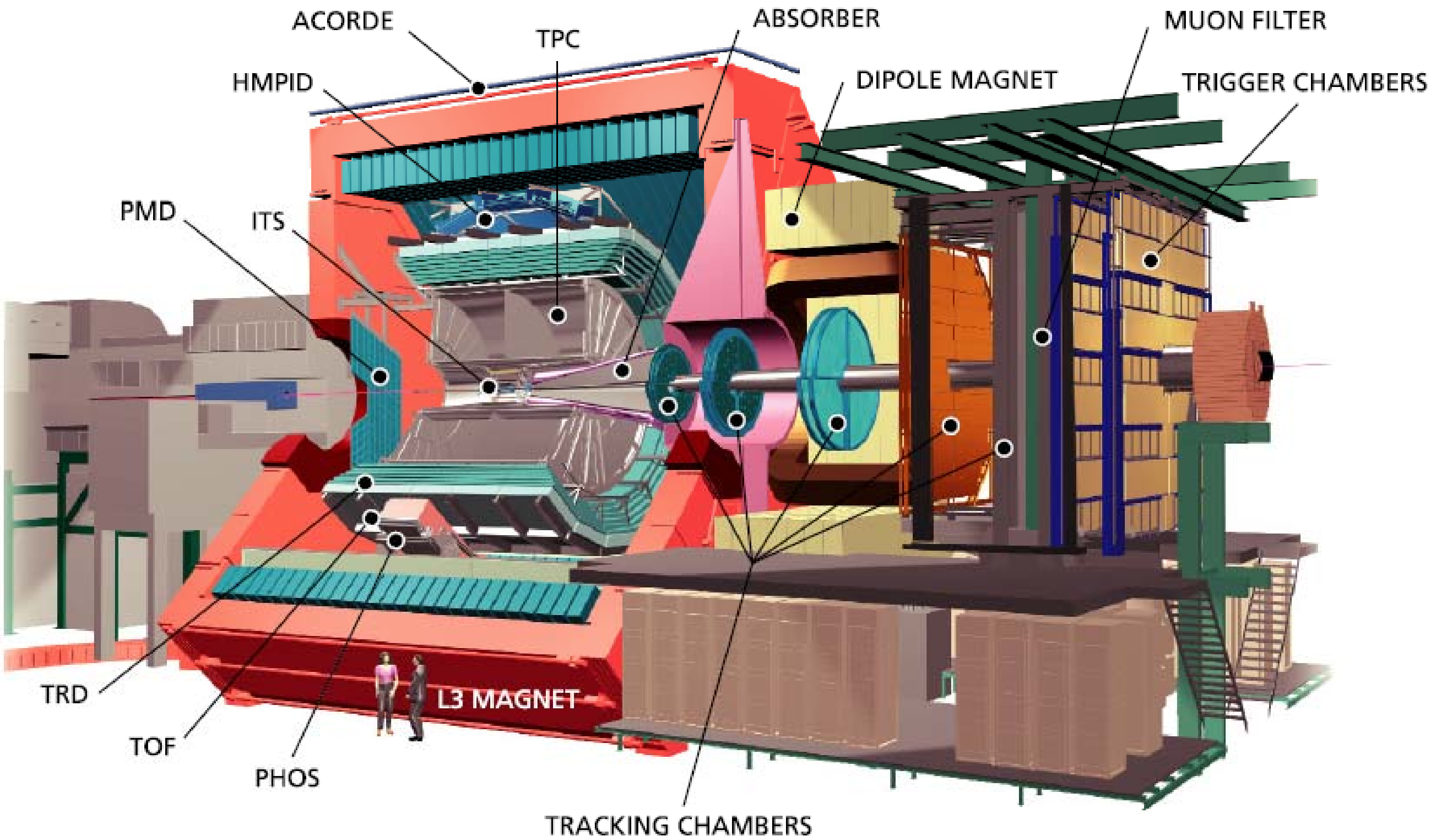
ACORDE
TPC
ABSORBER
MUON FILTER
HMPID
DIPOLE MAGNET
TRIGGER CHAMBERS
PMD
ITS
TRD
TOF
PHOS
L3 MAGNET
TRACKING CHAMBERS

ALICE Particle ID

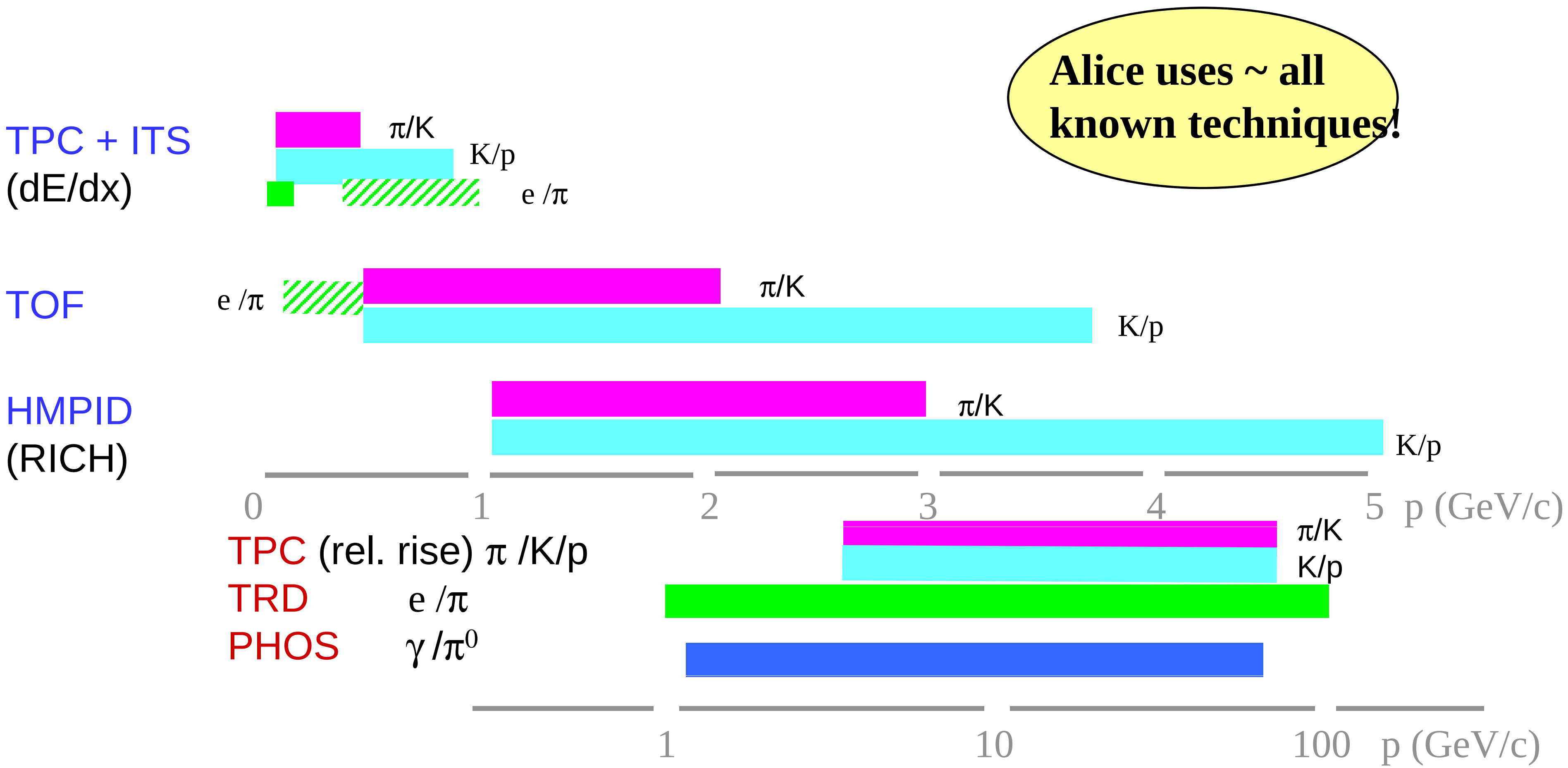

ALICE TPC

LHC: dN_{ch}/dy = 2000 - 4000

ALICE 'worst case' scenario:

dN_{ch}/dy = 8000

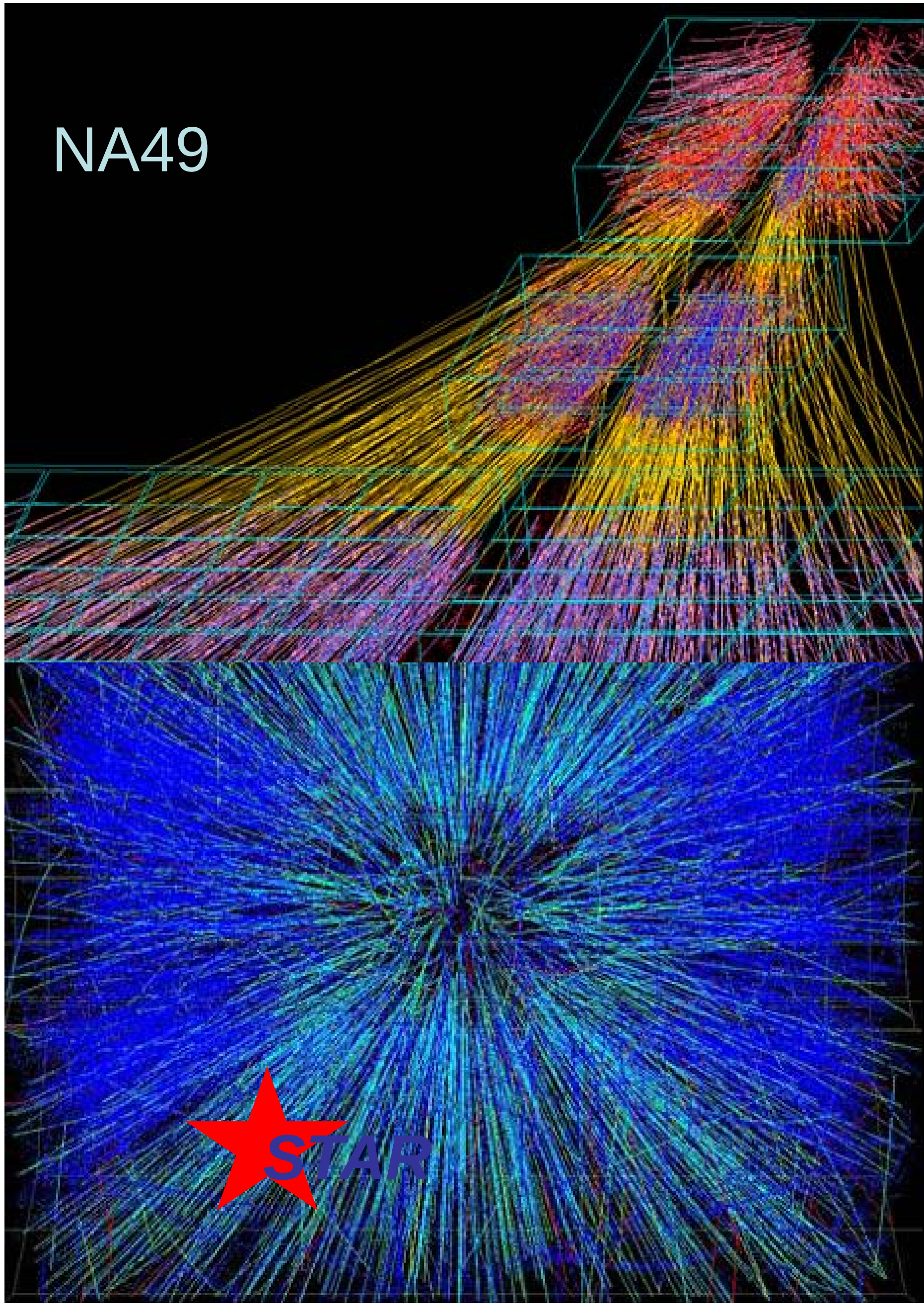

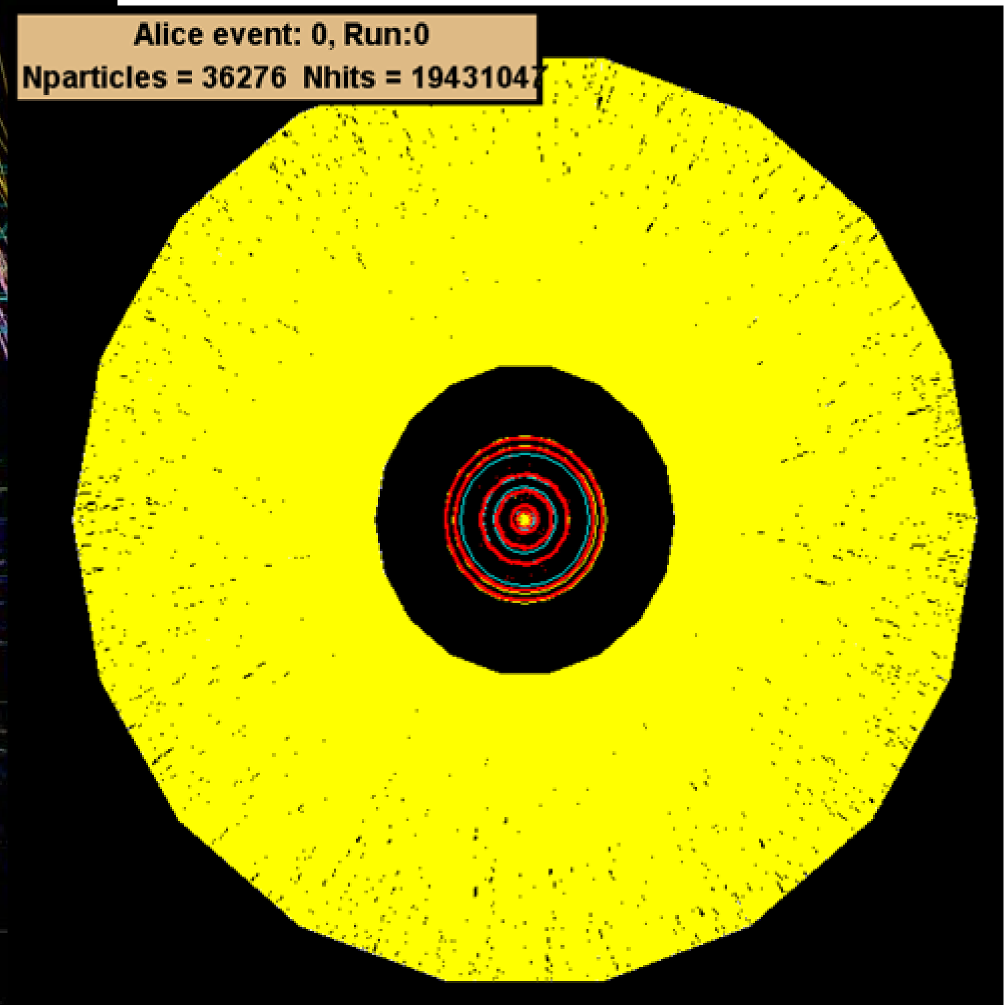

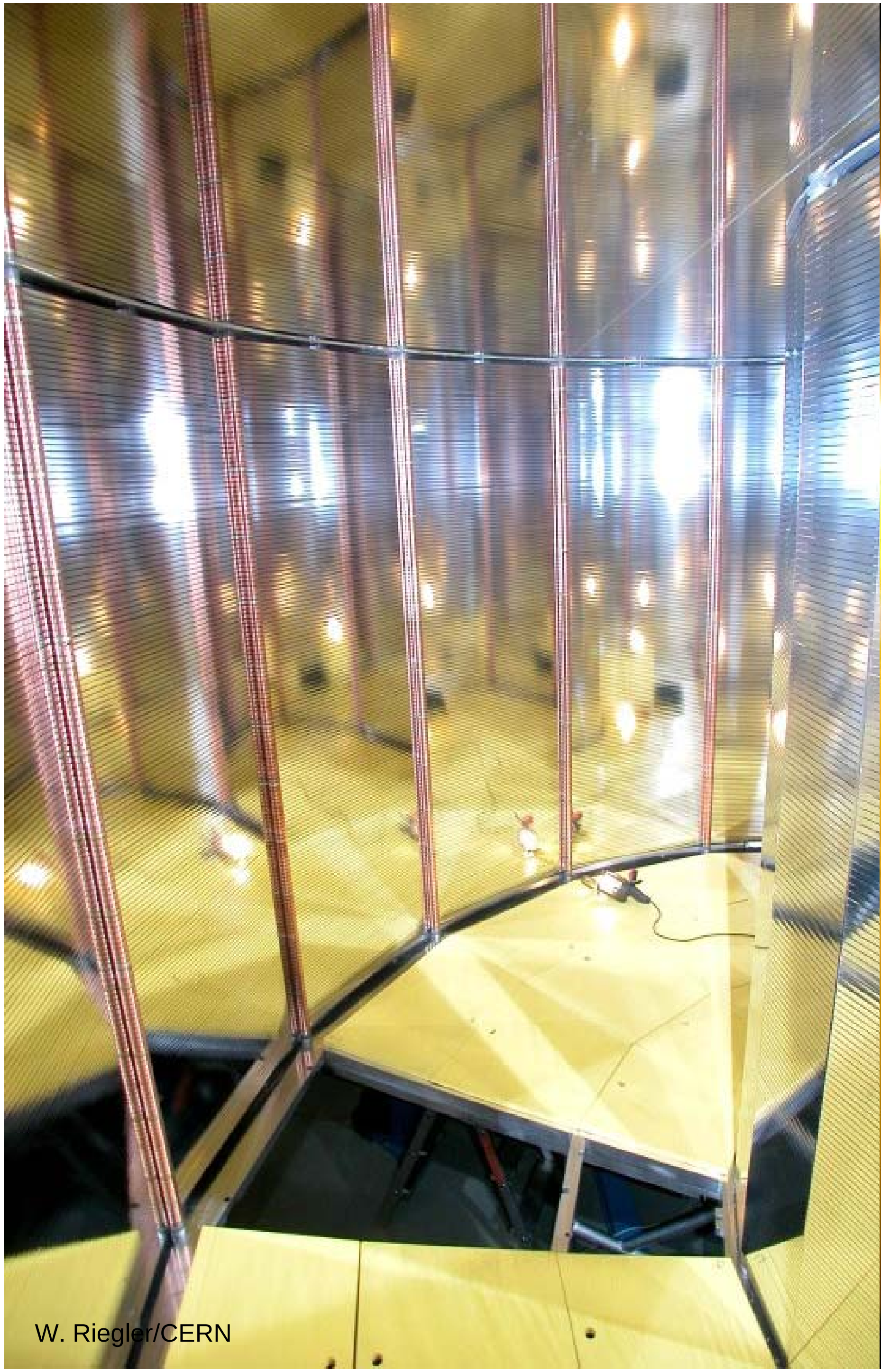
W. Riegler/CERN

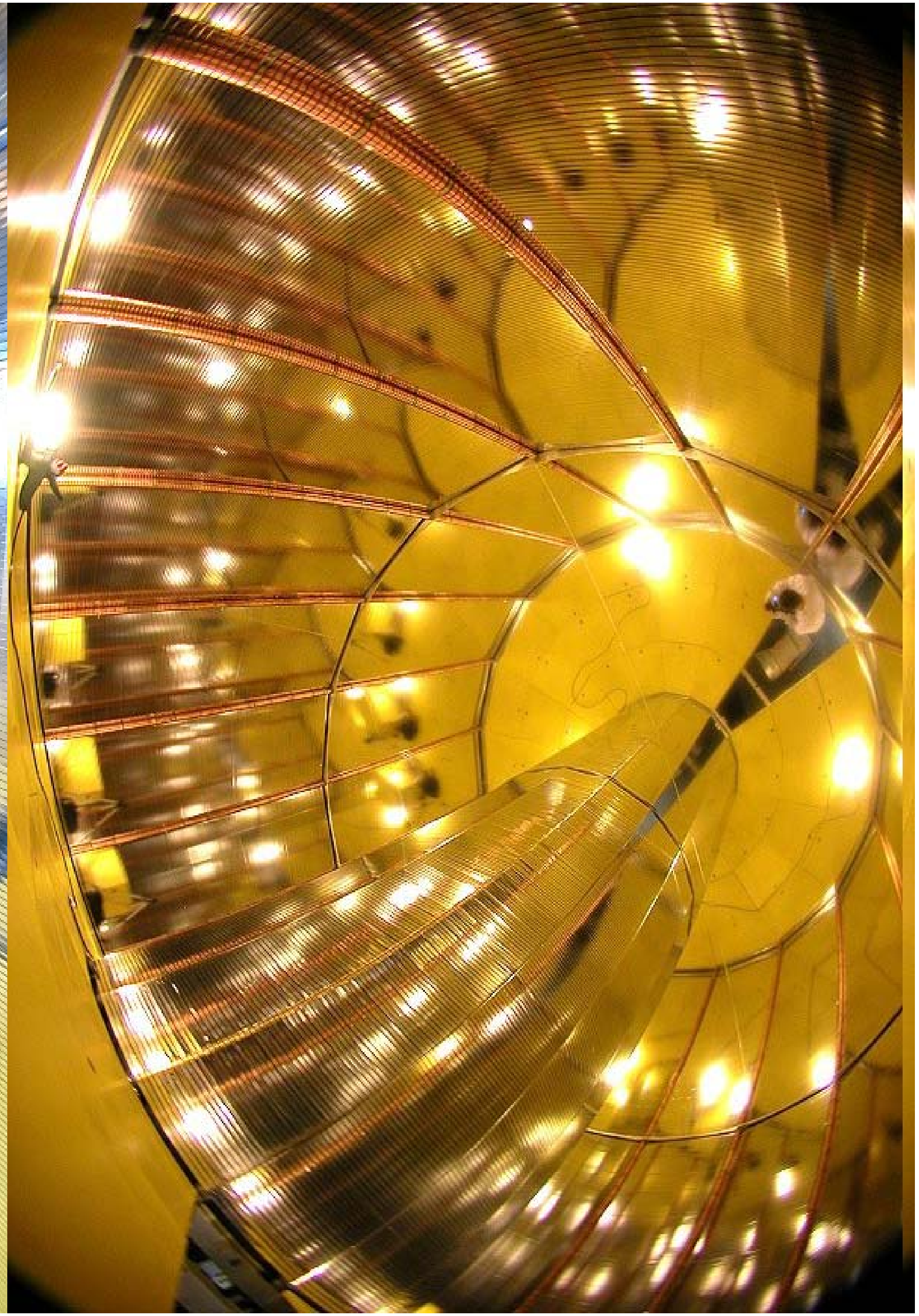

AMANDA

Antarctic **M**uon **A**nd **N**eutrino **D**etector **A**rray

AMANDA

South Pole

AMANDA

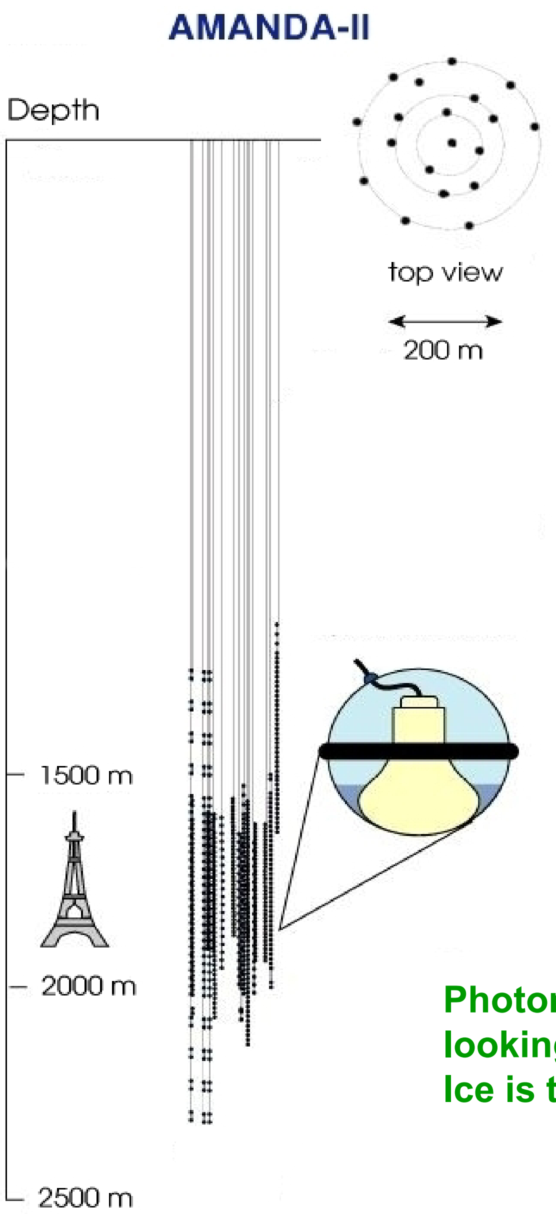

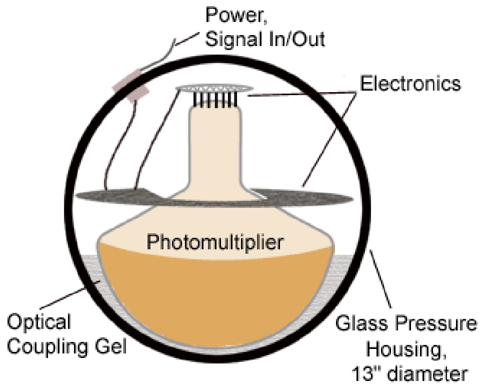

Photomultipliers in the Ice, looking downwards.
Ice is the detecting medium.

AMANDA

Look for upwards going Muons from Neutrino Interactions.
Cherekov Light propagating through the ice.

→ Find neutrino point sources in the universe !

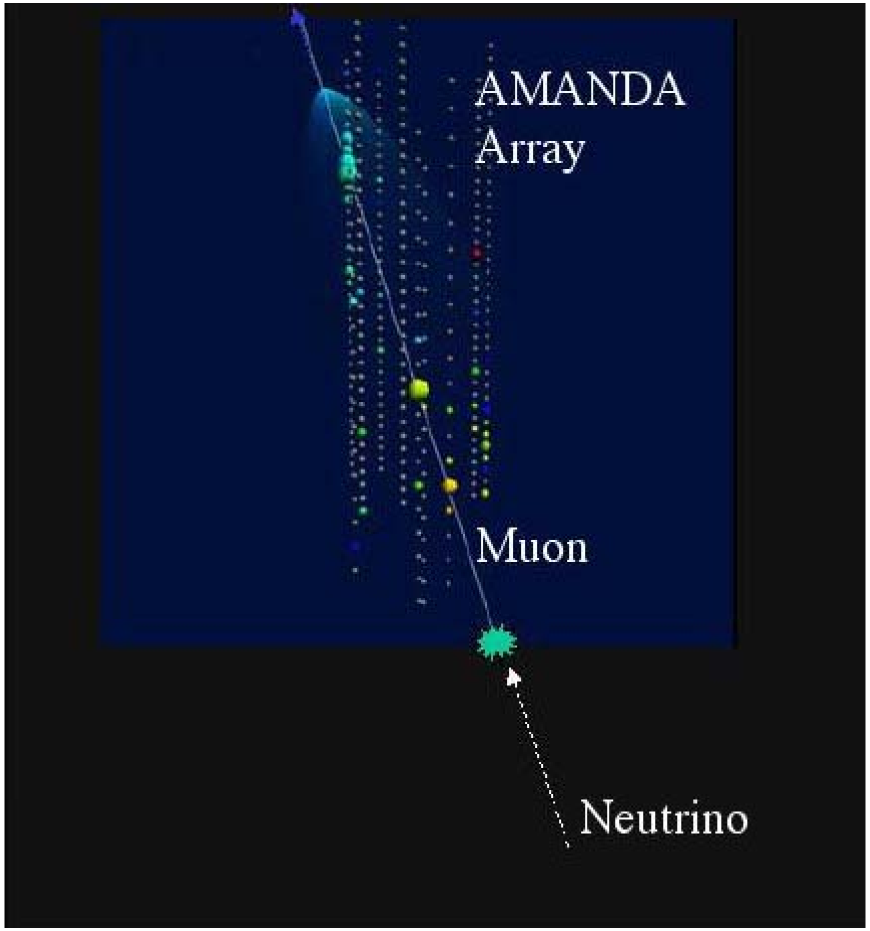

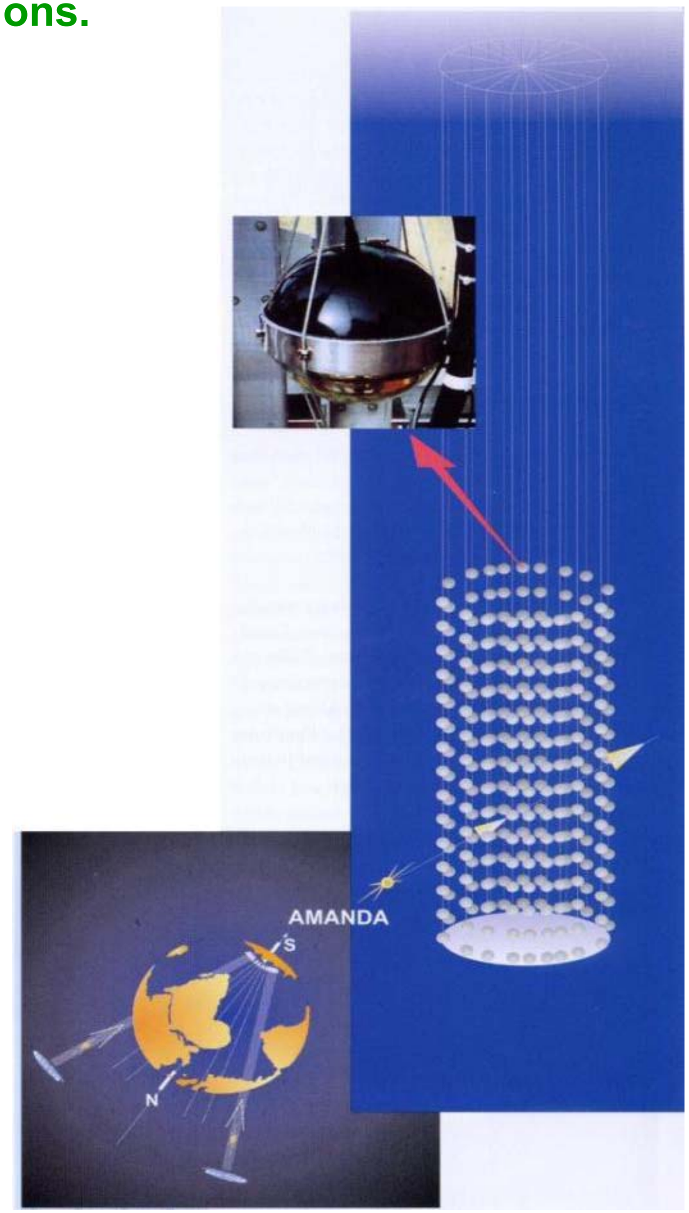

AMANDA

Event Display

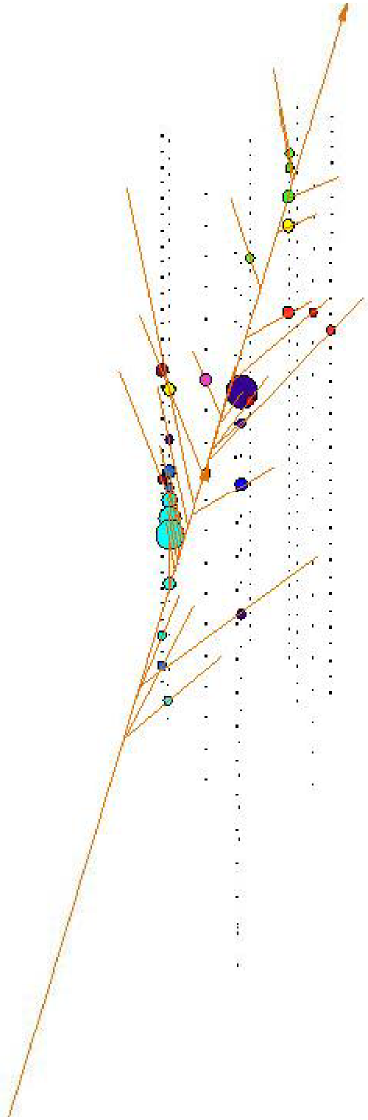

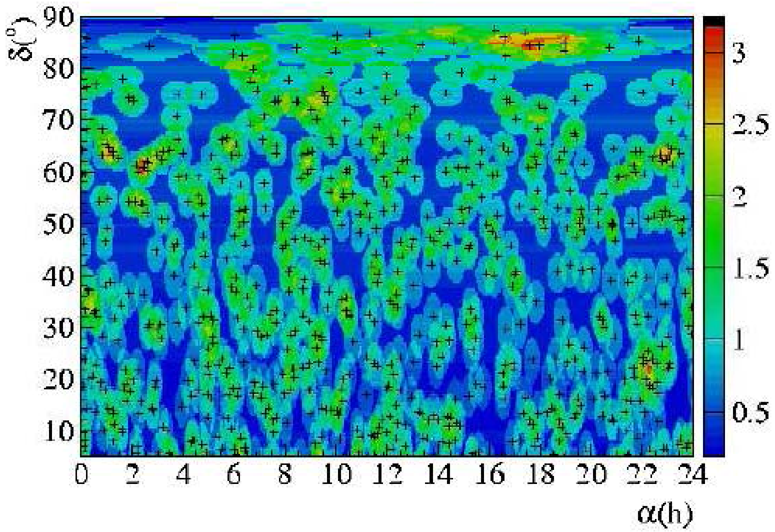

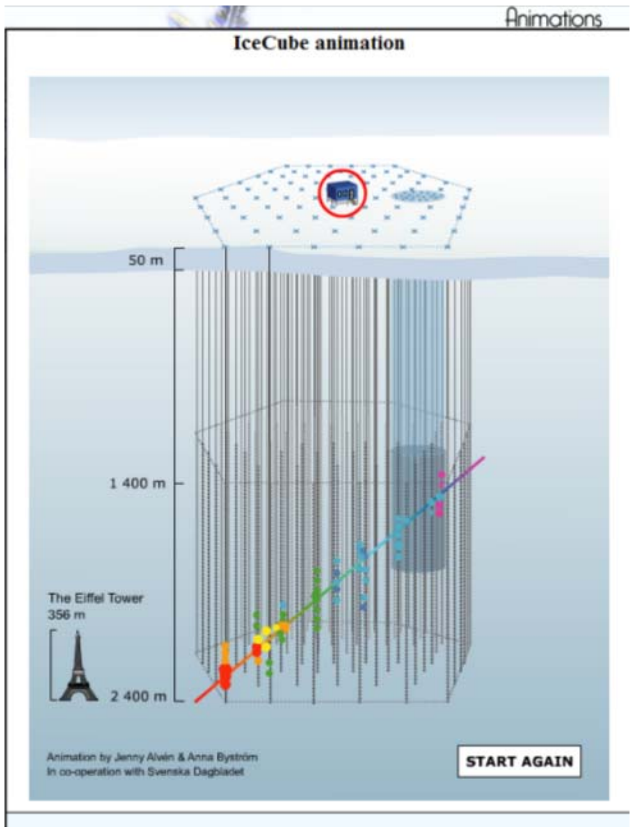

Up to now: No significant point sources but just neutrinos from cosmic ray interactions in the atmosphere were found .

→ Ice Cube for more statistics !

DONUT

Detector for Observation of Tau Neutrino.

DONUT

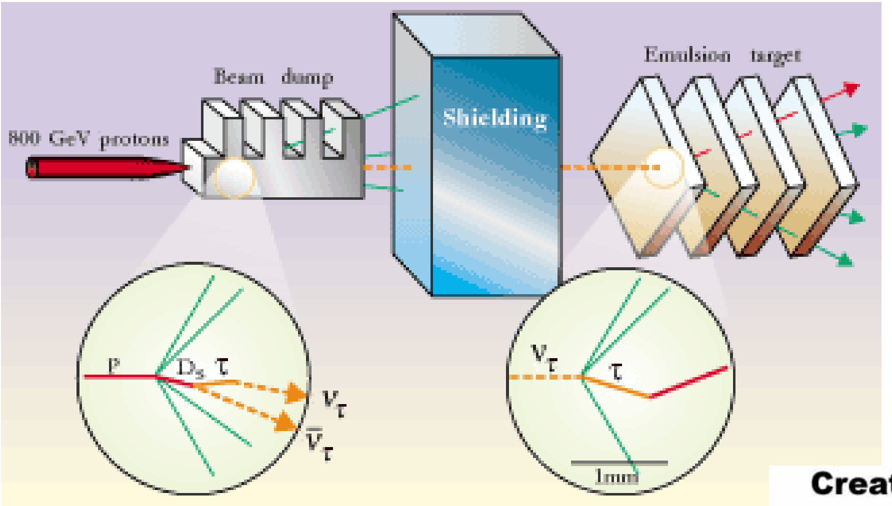
Beam dump
800 GeV protons
Shielding
Emulsion target
p
D_s
τ
ν_τ
$\bar{\nu}_\tau$
ν_τ
τ
1mm

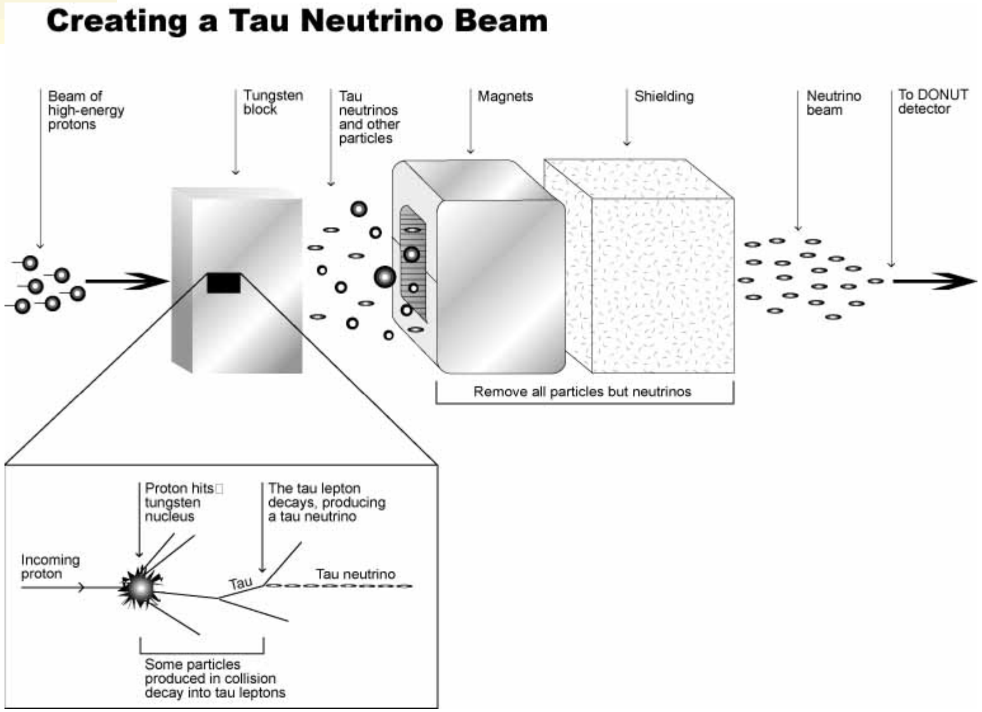
Creating a Tau Neutrino Beam
Beam of high-energy protons
Tungsten block
Tau neutrinos and other particles
Magnets
Shielding
Neutrino beam
To DONUT detector
Remove all particles but neutrinos
Proton hits tungsten nucleus
The tau lepton decays, producing a tau neutrino
Incoming proton
Tau
Tau neutrino
Some particles produced in collision decay into tau leptons

DONUT

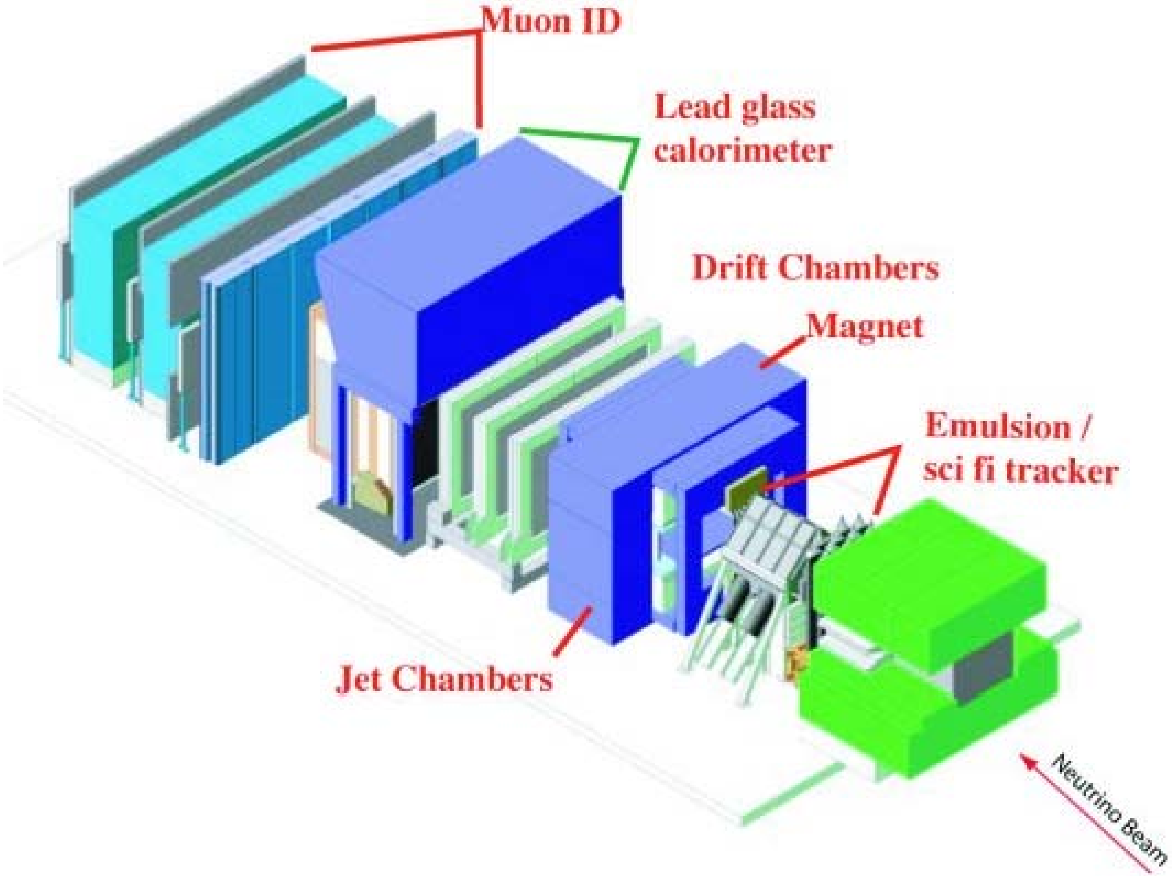
Muon ID
Lead glass
calorimeter
Drift Chambers
Magnet
Emulsion /
sci fi tracker
Jet Chambers
Neutrino Beam

DONUT

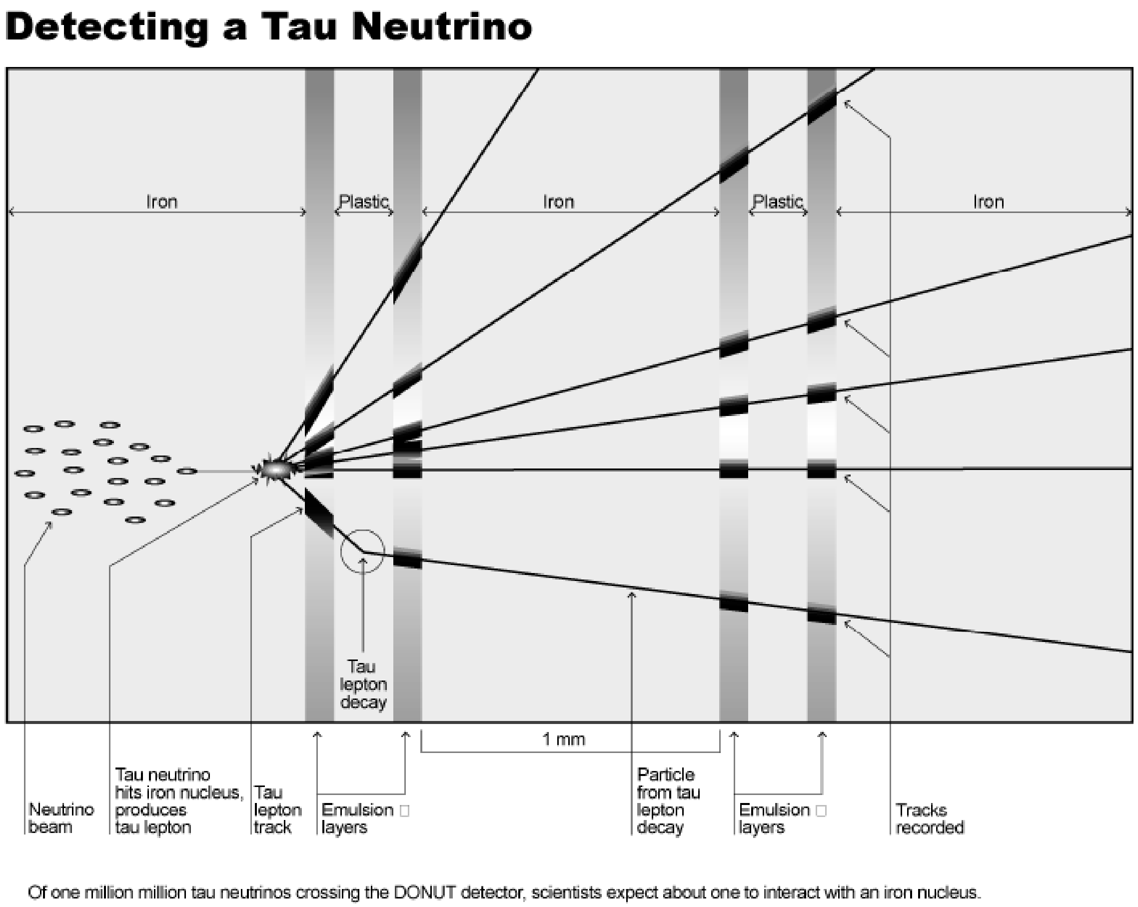

Tau lepton has very short lifetime and is therefore identified by the characteristic 'kink' on the decay point.

DONUT

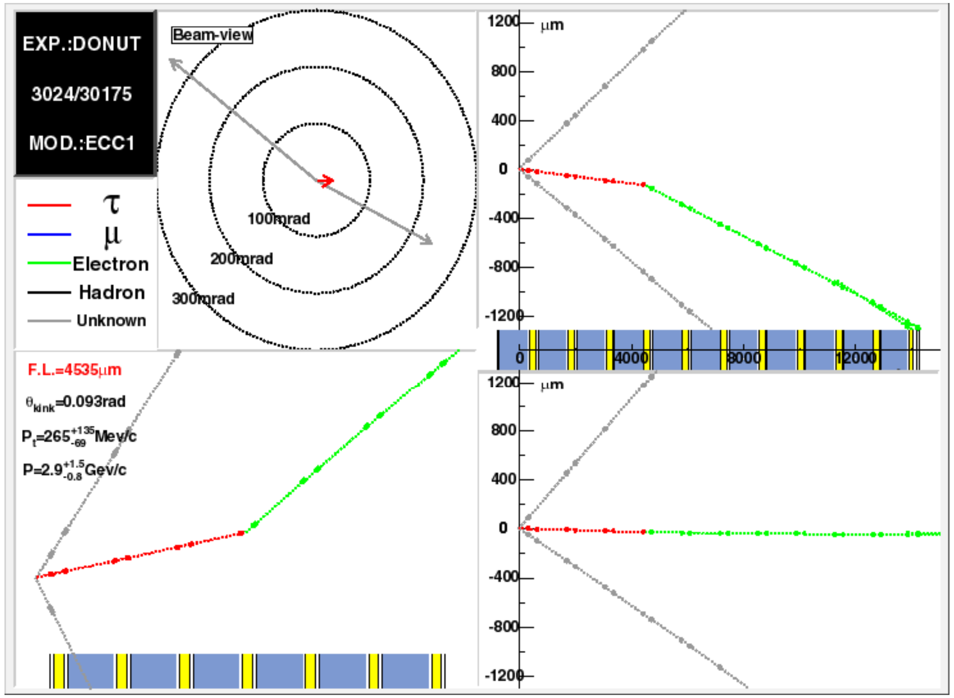

One of the 4 tau candidates.

Emulsion resolution 0.5um !

CERN Neutrino Gran Sasso

(CNGS)

Thanks to Edda Gschwendtner

CNGS

If neutrinos have mass:

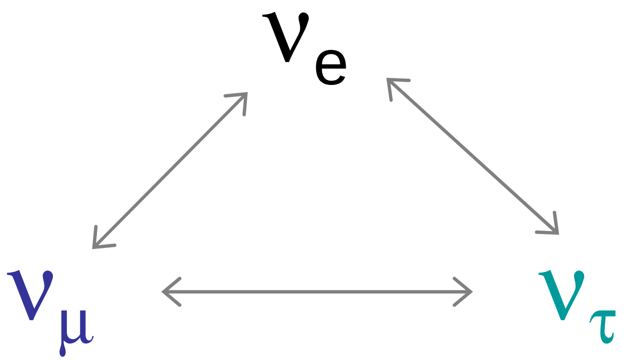

Muon neutrinos produced at CERN.
See if tau neutrinos arrive in Italy.

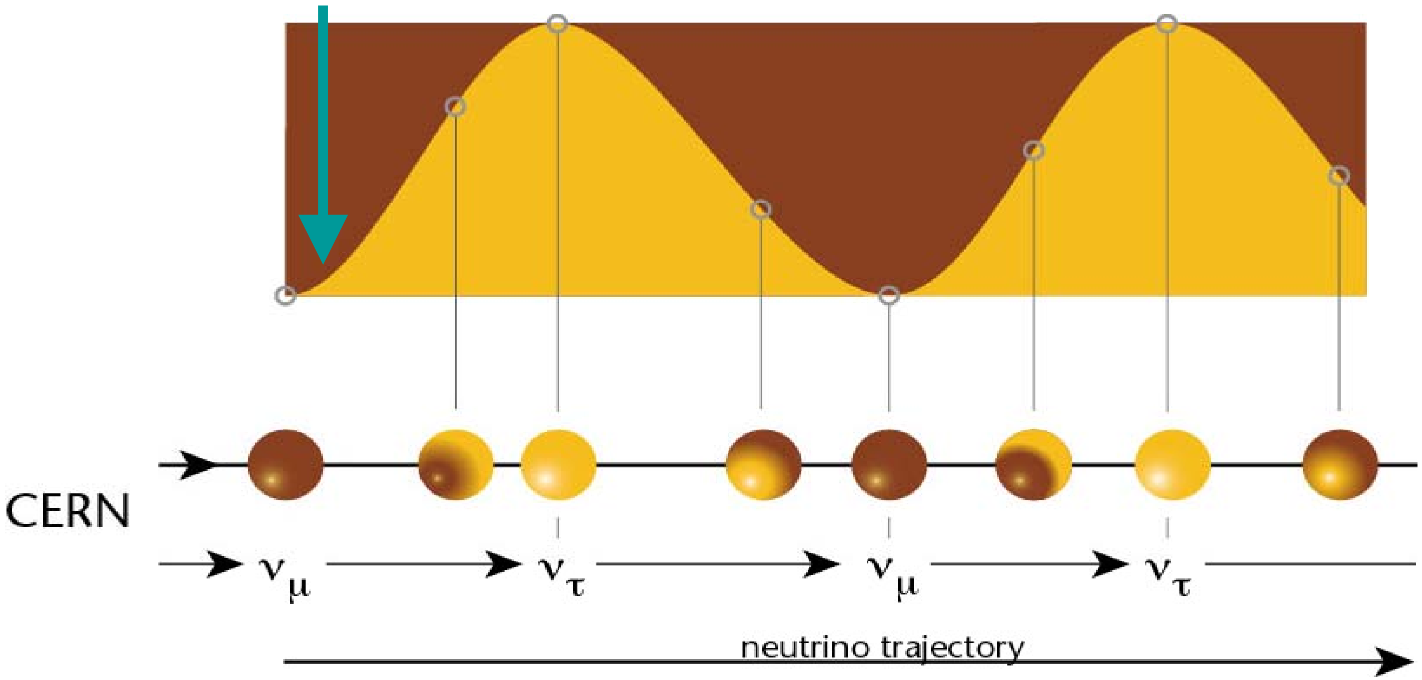

CNGS Project

CNGS (CERN Neutrino Gran Sasso)

- A long base-line neutrino beam facility (732km)
- send ν_μ beam produced at CERN
- detect ν_τ appearance in OPERA experiment at Gran Sasso

➔ direct proof of ν_μ - ν_τ oscillation (appearance experiment)

CNGS

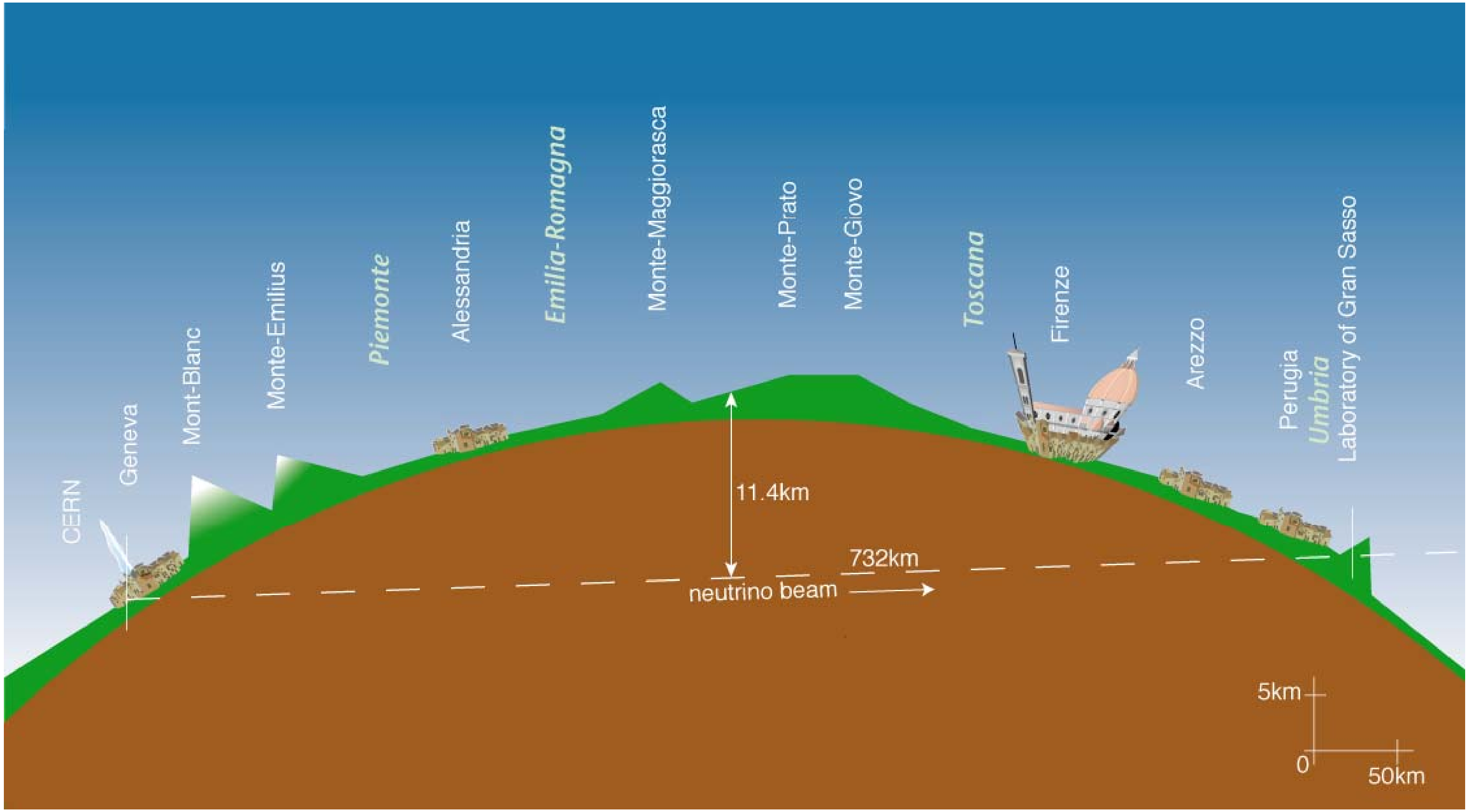
CERN
Geneva
Mont-Blanc
Monte-Emilius
Piemonte
Alessandria
Emilia-Romagna
Monte-Maggiorasca
Monte-Prato
Monte-Giovo
Toscana
Firenze
Arezzo
Perugia
Umbria
Laboratory of Gran Sasso
11.4km
732km
neutrino beam
5km
0
50km

Neutrinos at CNGS: Some Numbers

For 1 day of CNGS operation, we expect:

protons on target	**2×10^{17}**
pions / kaons at entrance to decay tunnel	**3×10^{17}**
ν_μ **in direction of Gran Sasso**	**10^{17}**
ν_μ **in 100 m^2 at Gran Sasso**	**3×10^{12}**

ν_μ events per day in OPERA	$\approx$ 25 per day
ν_τ events (from oscillation)	$\approx$ 2 per year

CNGS Layout

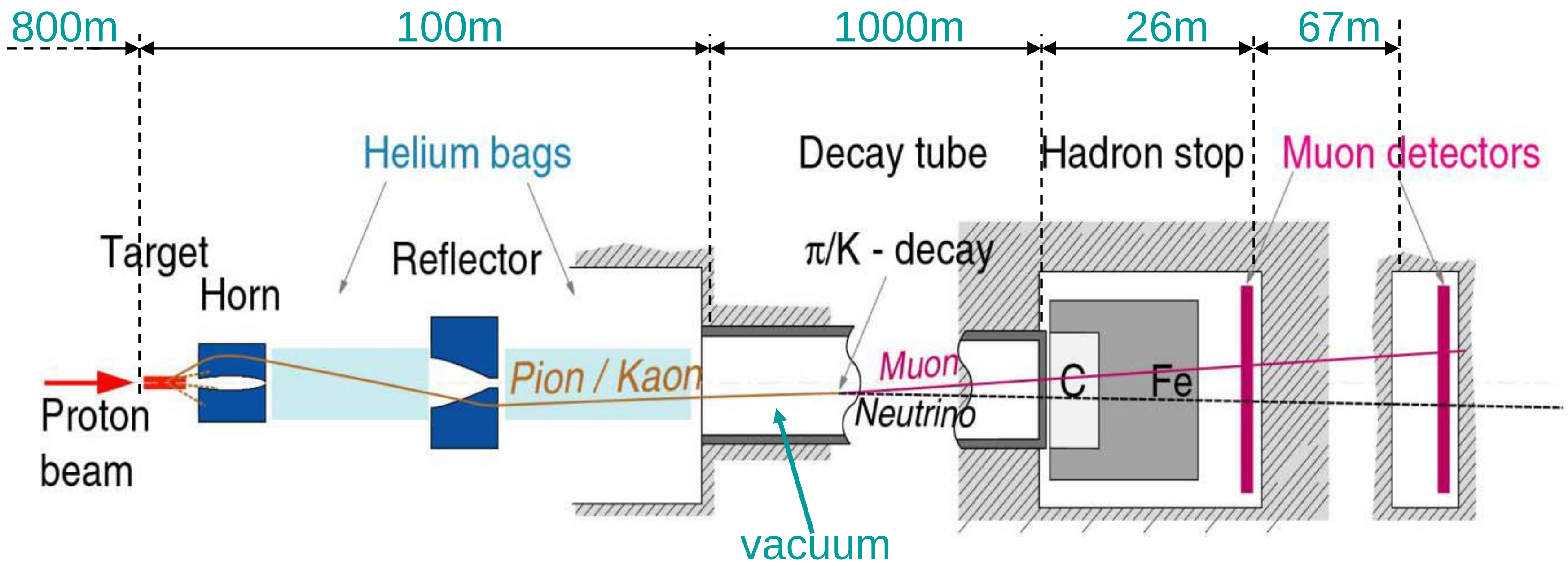

$p + C \rightarrow$ (interactions) $\rightarrow \pi^+, \; K^+ \rightarrow$ (decay in flight) $\rightarrow \mu^+ + \nu_\mu$

CNGS

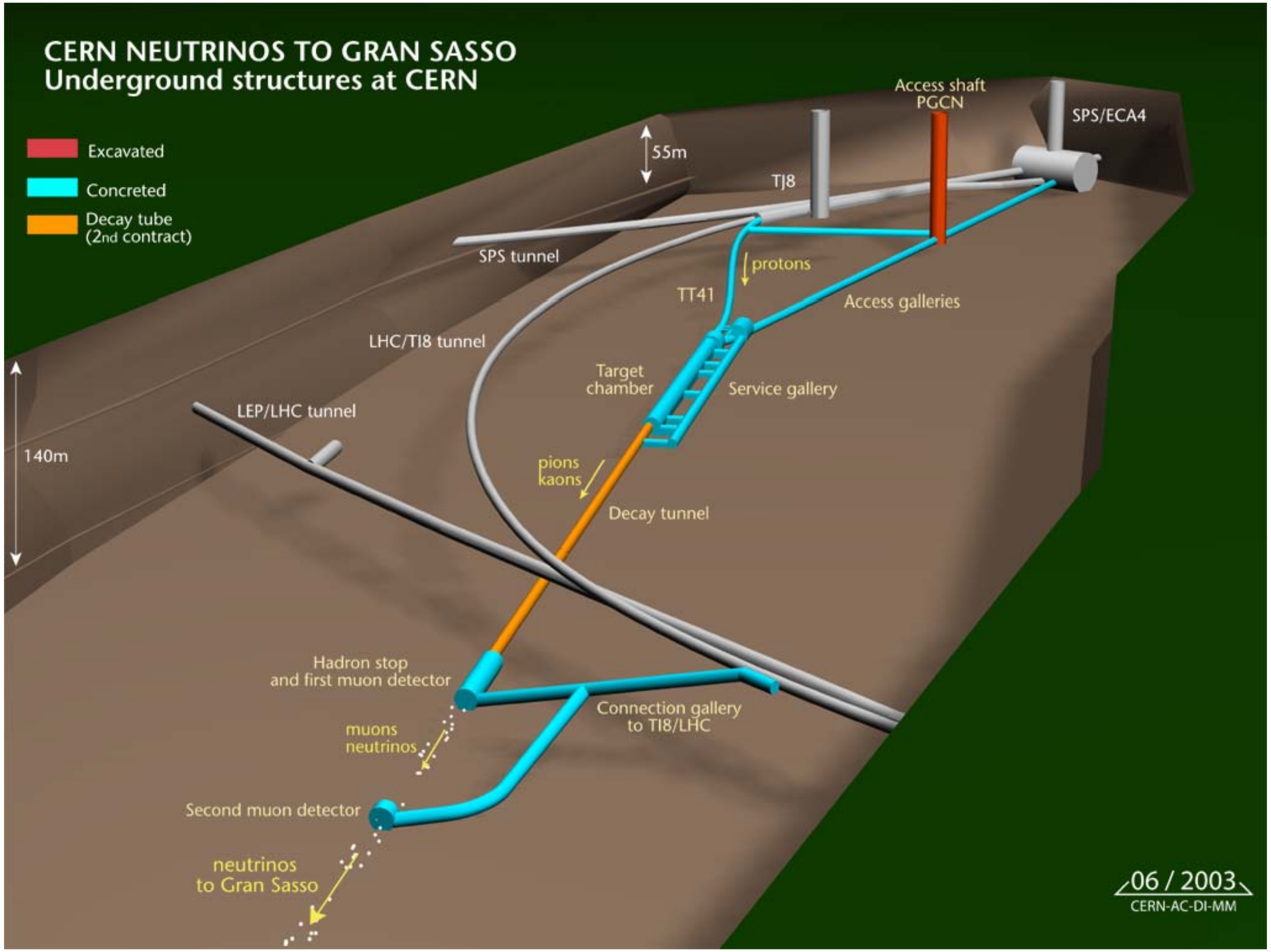

CERN NEUTRINOS TO GRAN SASSO
Underground structures at CERN
Excavated
Concreted
Decay tube
(2nd contract)
Access shaft
PGCN
SPS/ECA4
55m
TJ8
SPS tunnel
protons
TT41
Access galleries
LHC/TI8 tunnel
Target
chamber
Service gallery
LEP/LHC tunnel
140m
pions
kaons
Decay tunnel
Hadron stop
and first muon detector
Connection gallery
to TI8/LHC
muons
neutrinos
Second muon detector
neutrinos
to Gran Sasso
06 / 2003
CERN-AC-DI-MM

CNGS

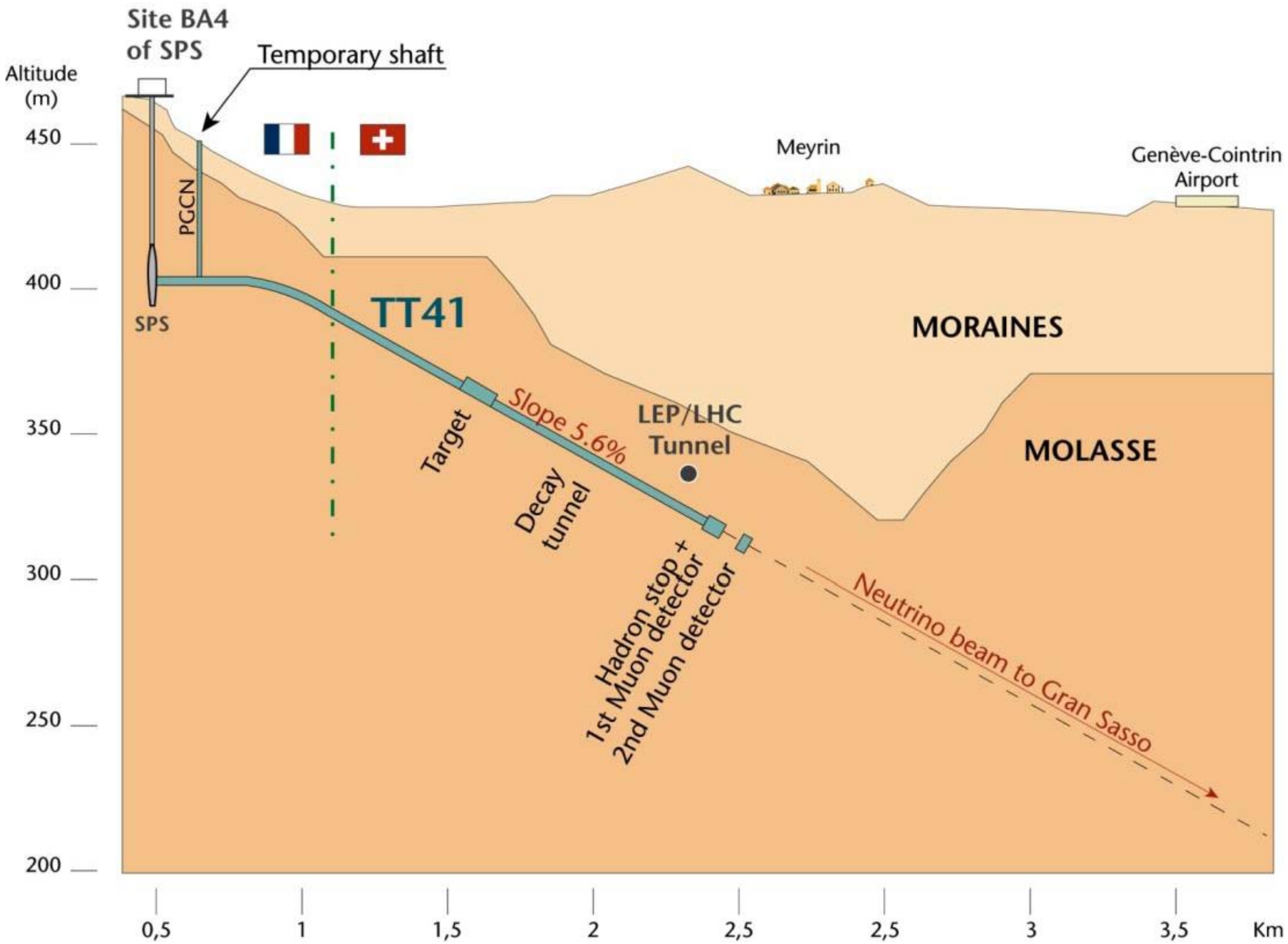

Site BA4
of SPS
Temporary shaft
Altitude
(m)
450
400
350
300
250
200
PGCN
SPS
TT41
Meyrin
Genève-Cointrin
Airport
MORAINES
MOLASSE
Target
Slope 5.6%
LEP/LHC
Tunnel
Decay
tunnel
Hadron stop +
1st Muon detector
2nd Muon detector
Neutrino beam to Gran Sasso
0,5
1
1,5
2
2,5
2,5
3
3,5
Km

Radial Distribution of the ν_μ-Beam at GS

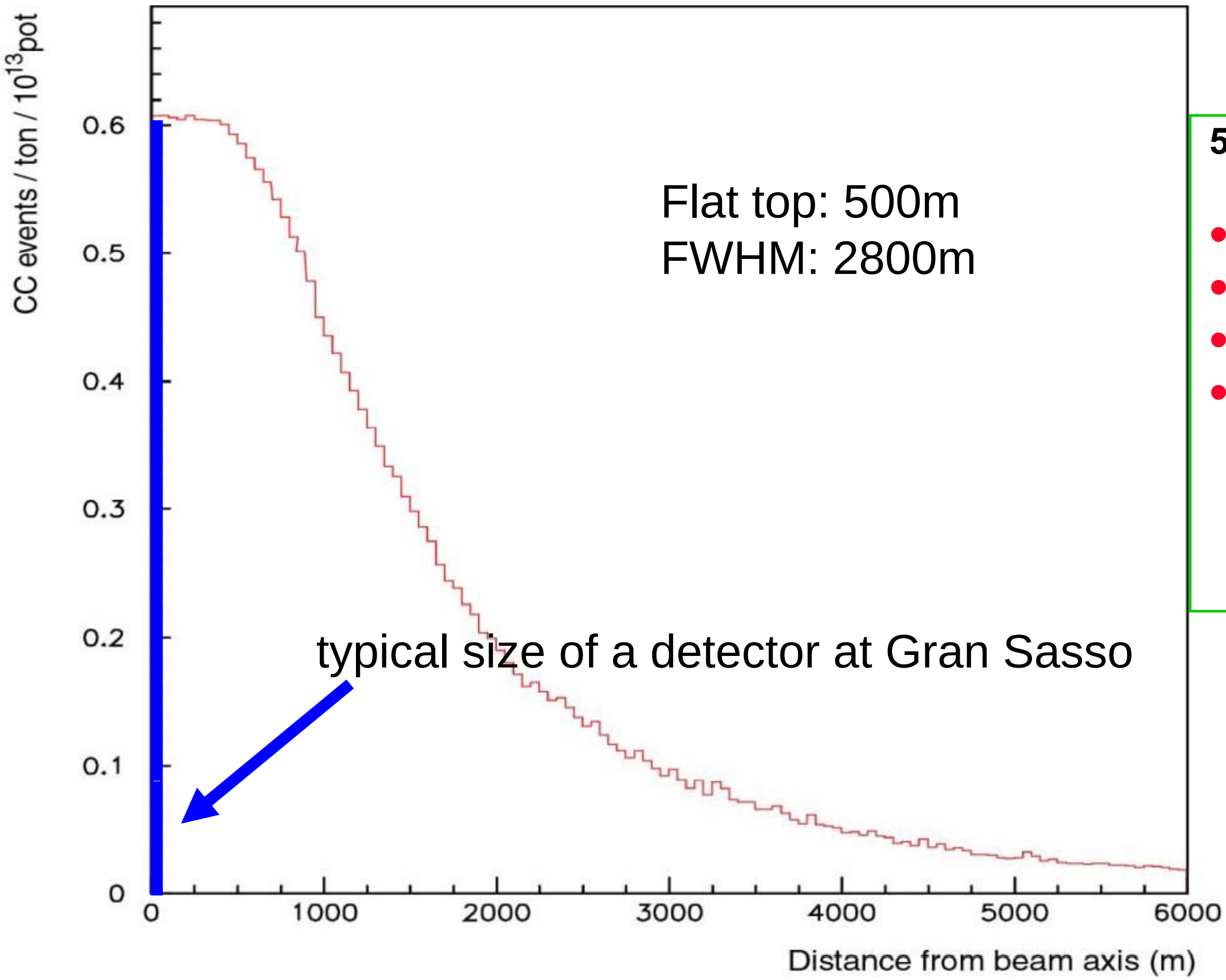

5 years CNGS operation, 1800 tons target:

- 30000 neutrino interactions
- ~150 ν_τ interactions
- ~15 ν_τ identified
- < 1 event of background

Opera Experiment at Gran Sasso

Basic unit: brick

56 Pb sheets + 56 photographic films (emulsion sheets)

Lead plates: massive target
Emulsions: micrometric precision

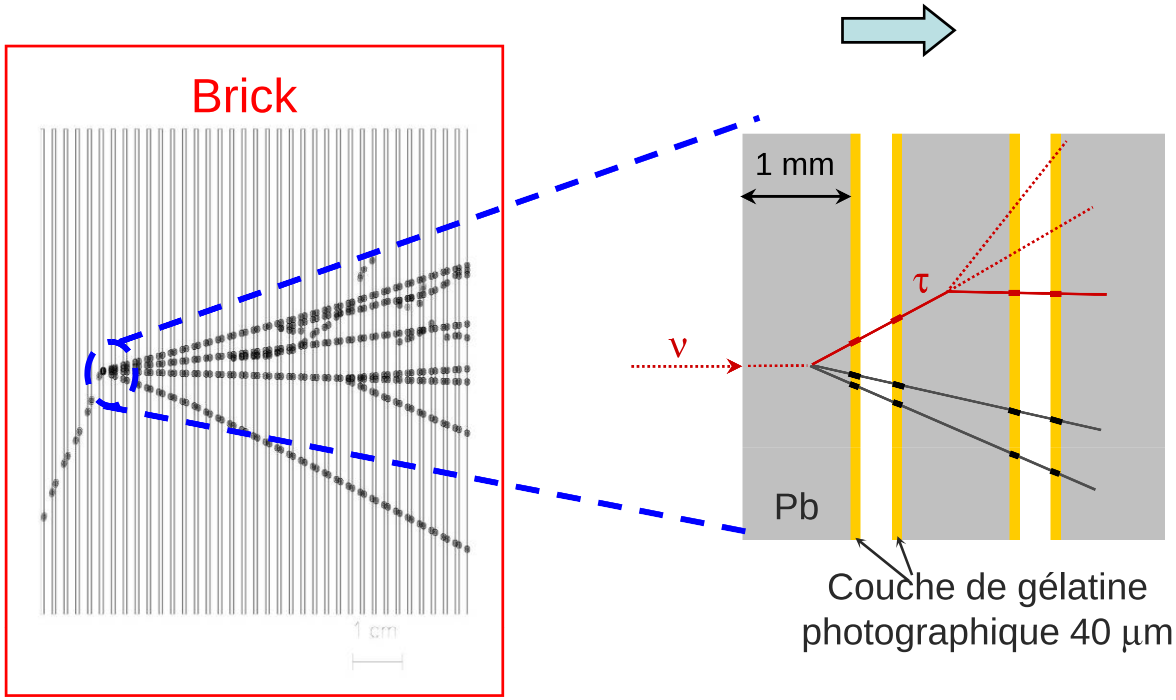

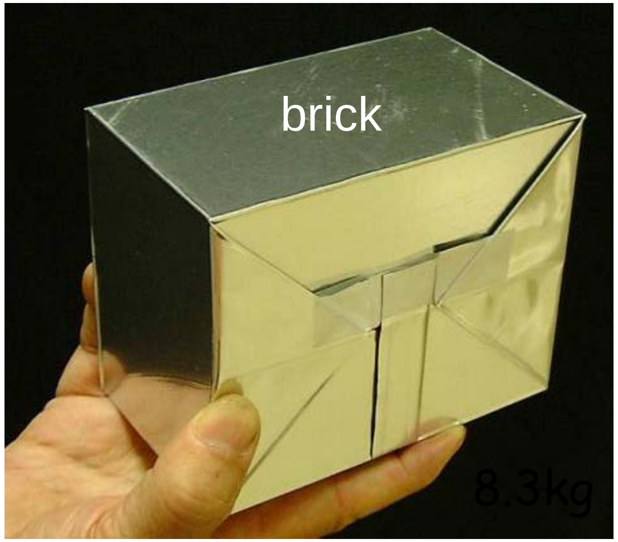

10.2 x 12.7 x 7.5 cm^3

Opera Experiment at Gran Sasso

In total: 206336 bricks, 1766 tons

31 target planes / supermodule

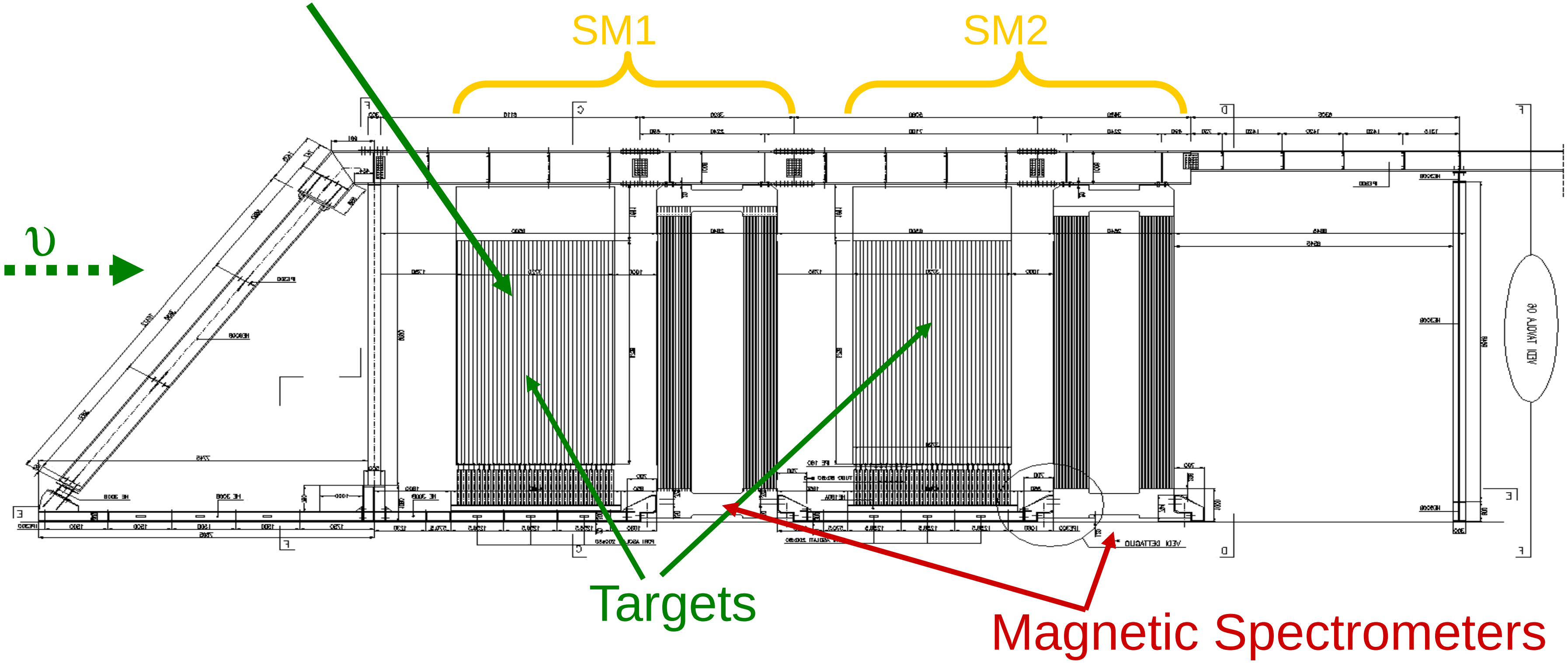

First observation of CNGS beam neutrinos : August 18th, 2006

Opera Experiment at Gran Sasso

Second Super-module

Scintillator planes 5900 m^2
8064 7m long drift tubes

Details of the first spectrometer

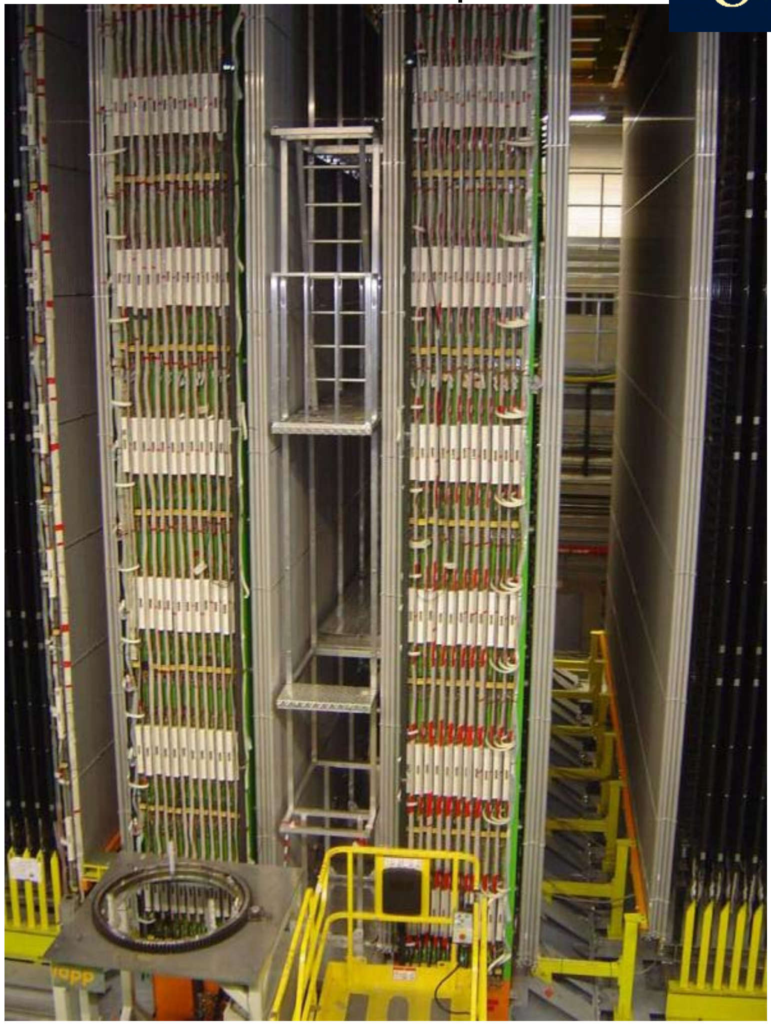

3050 m^2 Resistive Plate Counters
2000 tons of iron for the two magnets

Opera Experiment at Gran Sasso

The Brick Manipulator System (BMS) prototype:
a lot of fun for children and adults !

Tests with the prototype wall

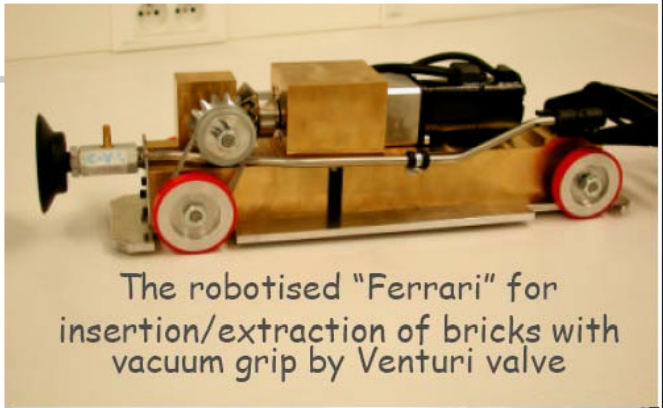

The robotised "Ferrari" for insertion/extraction of bricks with vacuum grip by Venturi valve

"Carousel" brick dispensing and storage system

AMS

Alpha **M**agnetic **S**pectrometer

Try to find Antimatter in the primary cosmic rays.
Study cosmic ray composition etc. etc.

AMS

Will be installed on the space station.

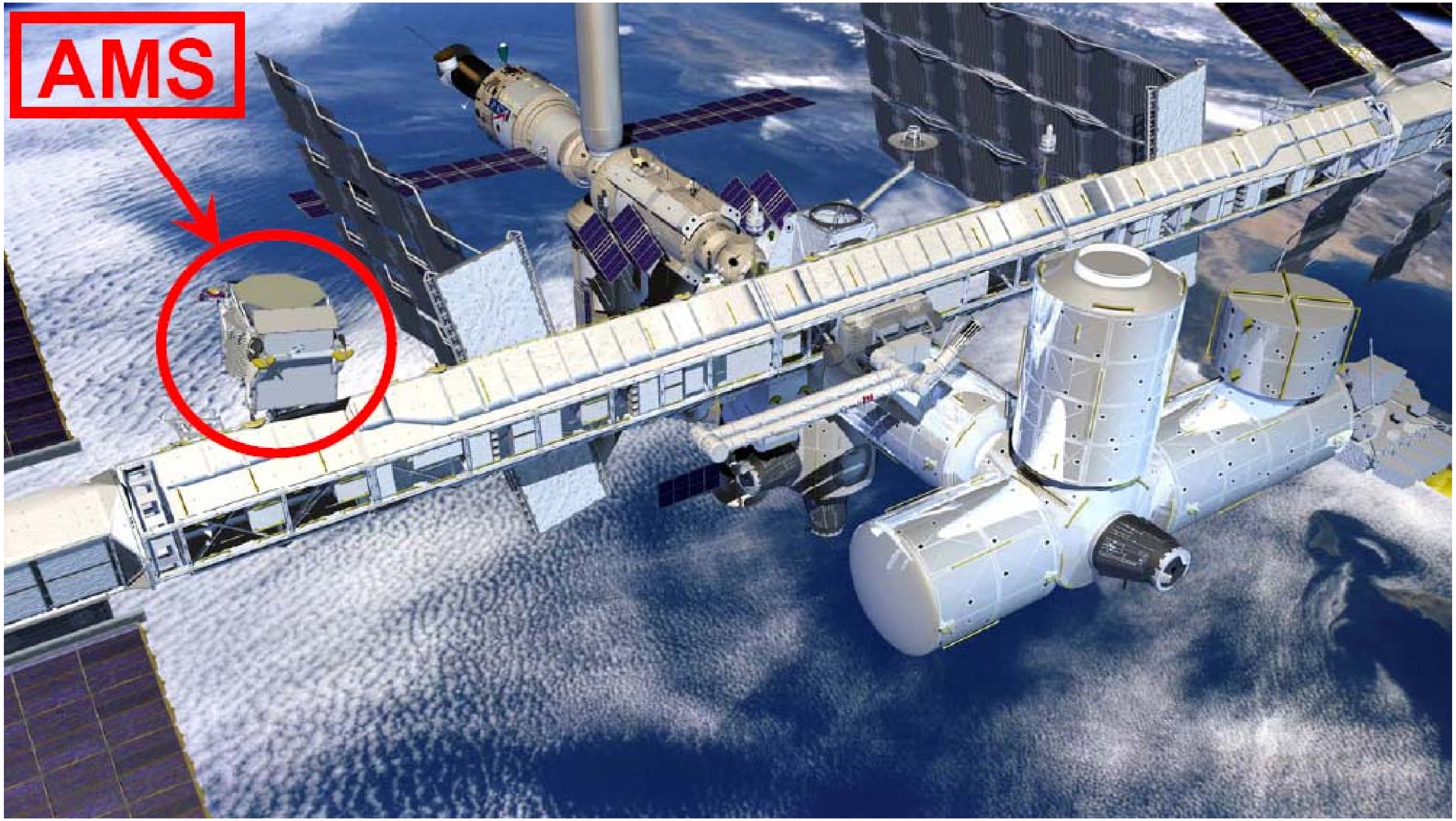

AMS

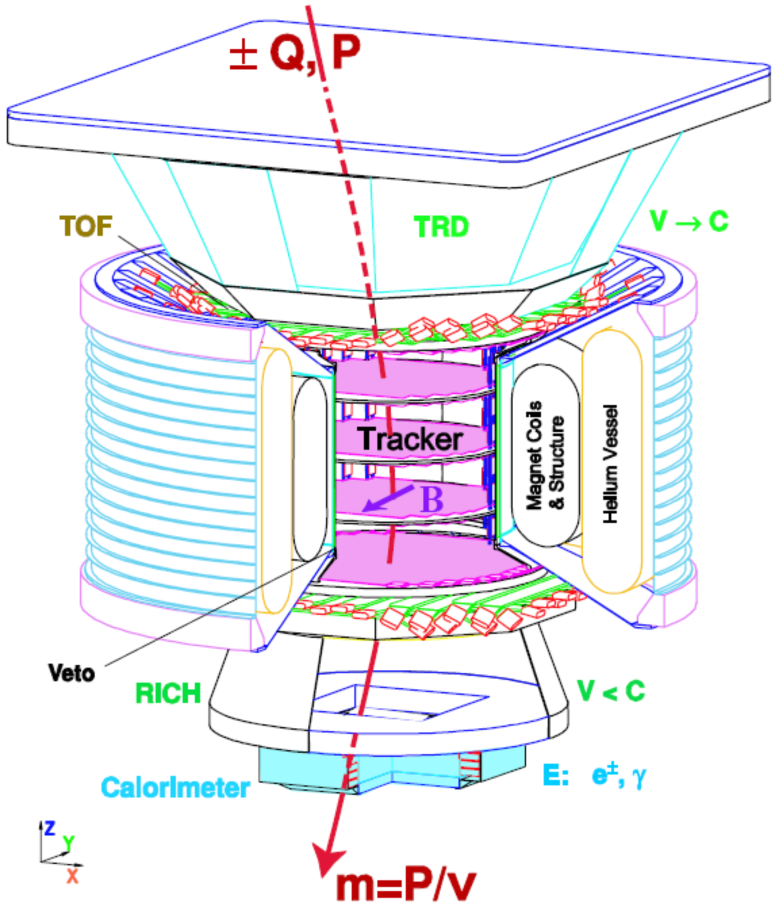

± Q, P
TOF
TRD
V → C
Tracker
B
Magnet Coils & Structure
Helium Vessel
Veto
RICH
V < C
Calorimeter
E: e±, γ
Z
Y
X
m=P/v

AMS

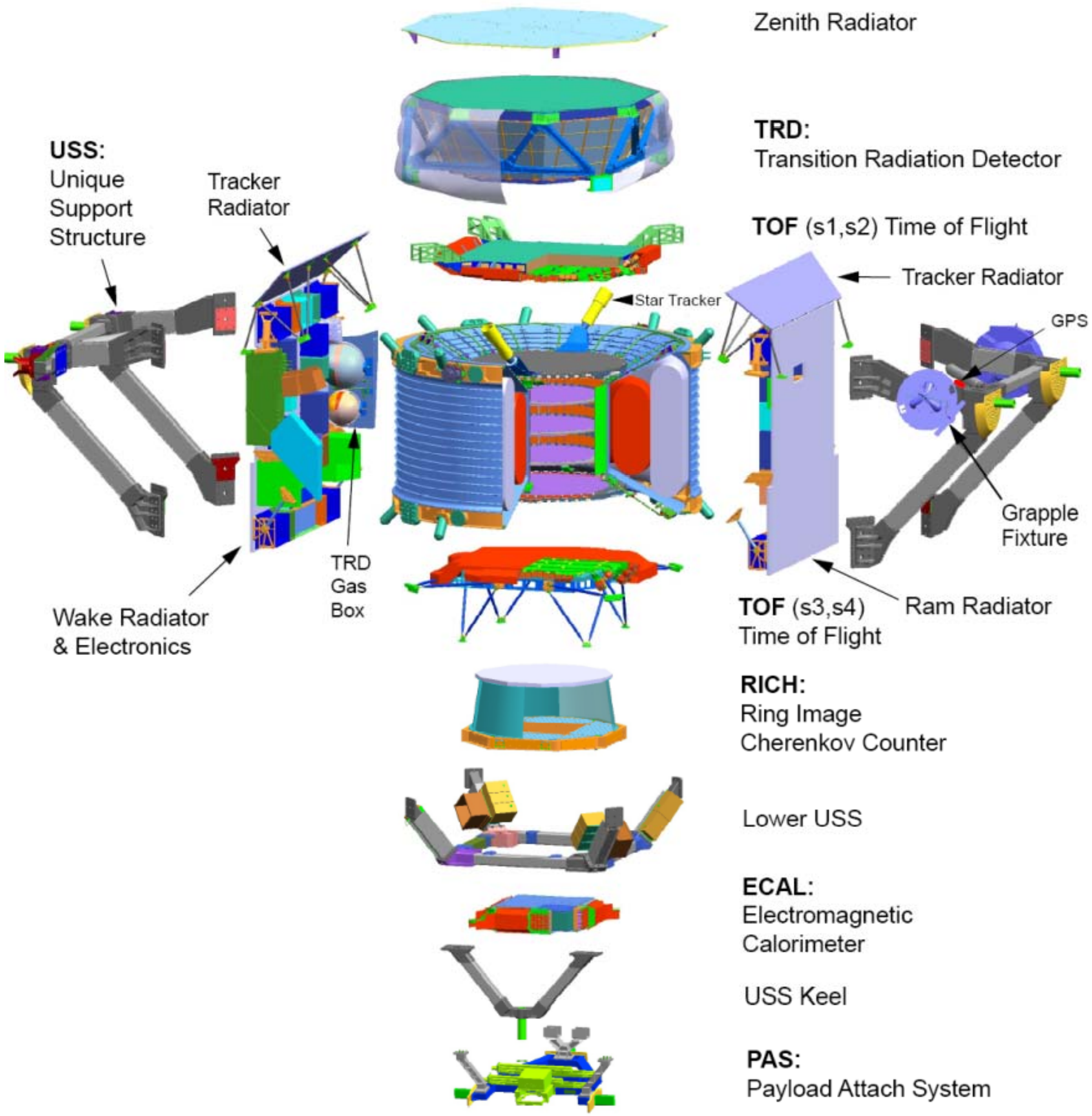

Zenith Radiator
TRD:
Transition Radiation Detector
USS:
Unique
Support
Structure
Tracker
Radiator
TOF (s1,s2) Time of Flight
Tracker Radiator
Star Tracker
GPS
Grapple
Fixture
TRD
Gas
Box
Wake Radiator
& Electronics
TOF (s3,s4)
Time of Flight
Ram Radiator
RICH:
Ring Image
Cherenkov Counter
Lower USS
ECAL:
Electromagnetic
Calorimeter
USS Keel
PAS:
Payload Attach System

Pierre Auger Cosmic Ray Obeservatory

Pierre Auger Cosmic Ray Observatory

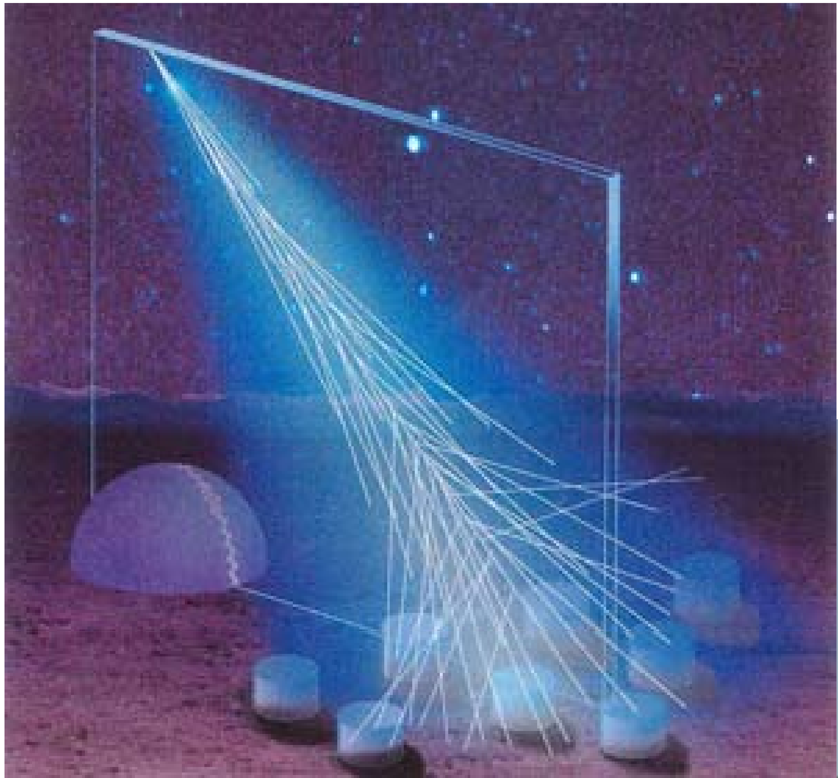

Use earth's atmosphere as a calorimeter. 1600 water Cherenkov detectors with 1.5km distance.

Placed in the Pampa Amarilla in western Argentina.

Pierre Auger Cosmic Ray Obeservatory

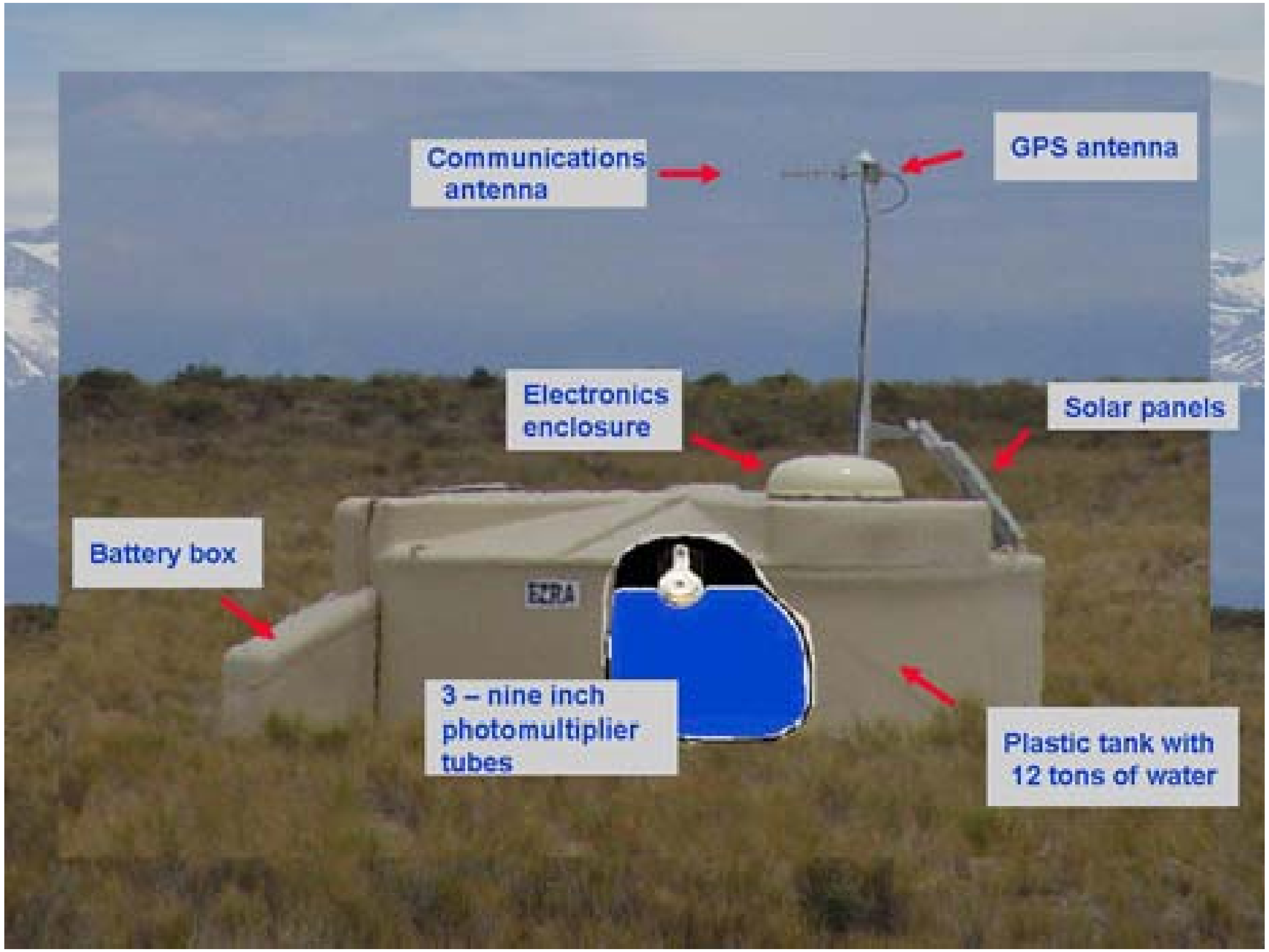

Pierre Auger Cosmic Ray Obeservatory

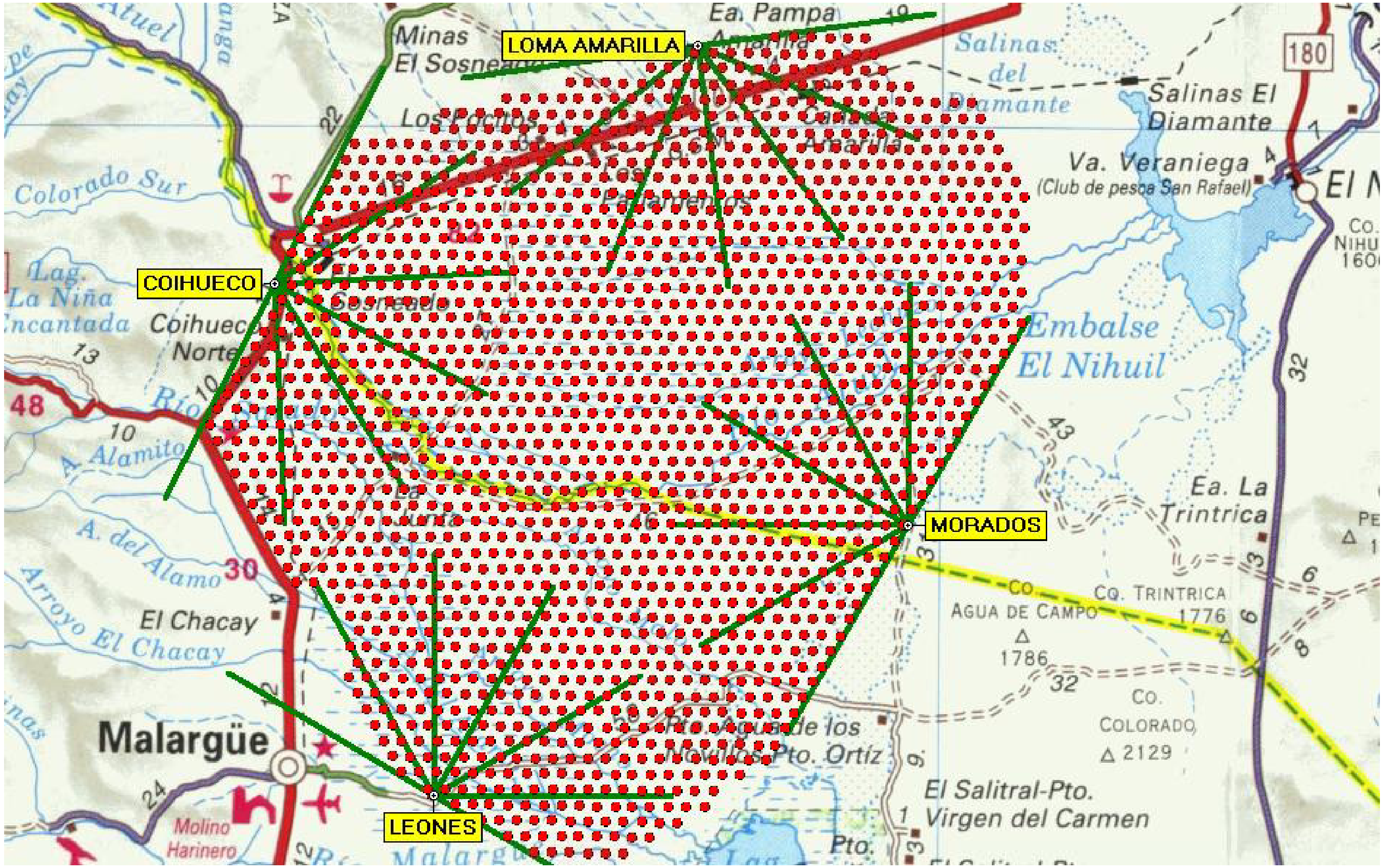

Pierre Auger Cosmic Ray Obeservatory

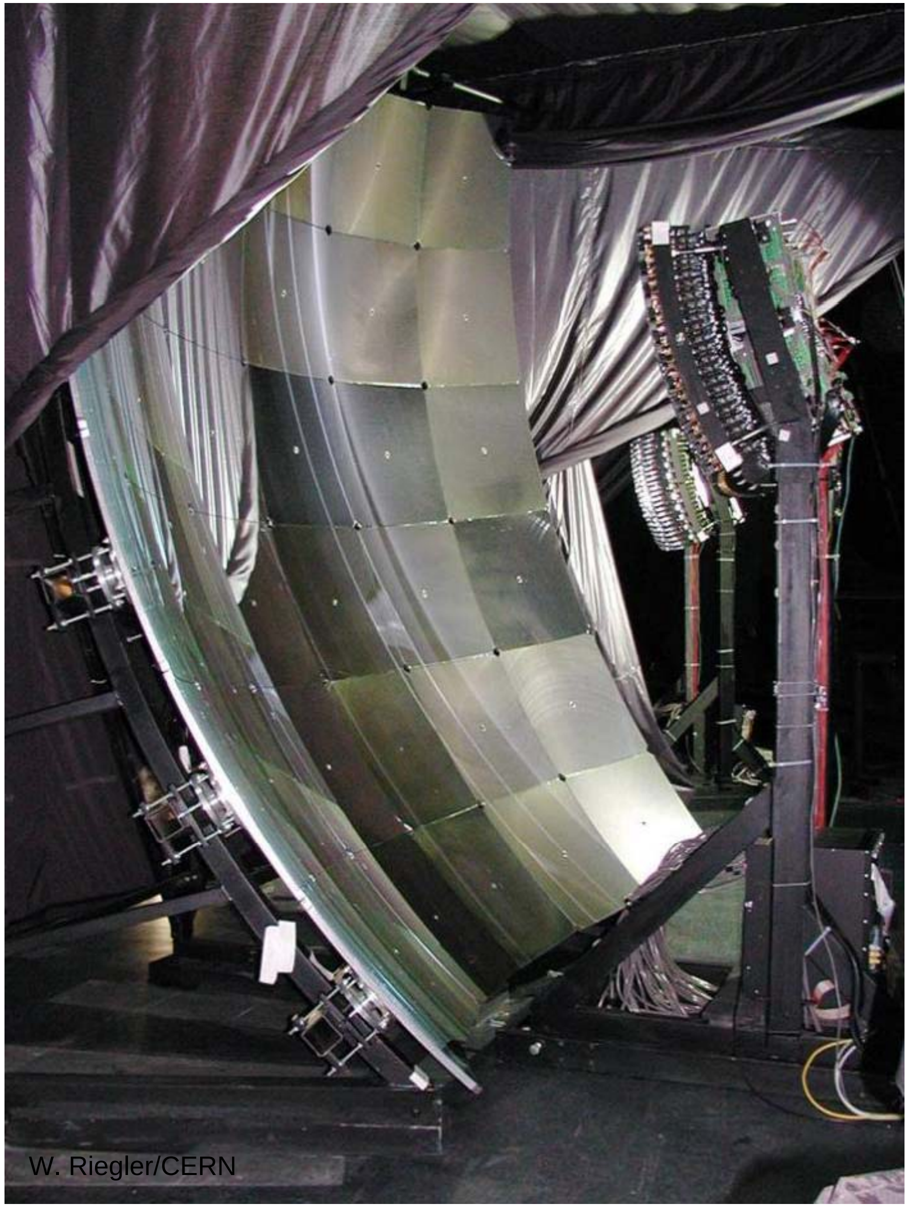

In addition: Fluorescence detectors around the array of water tanks.

Event 1234800

See CR incoming direction | See individual station data

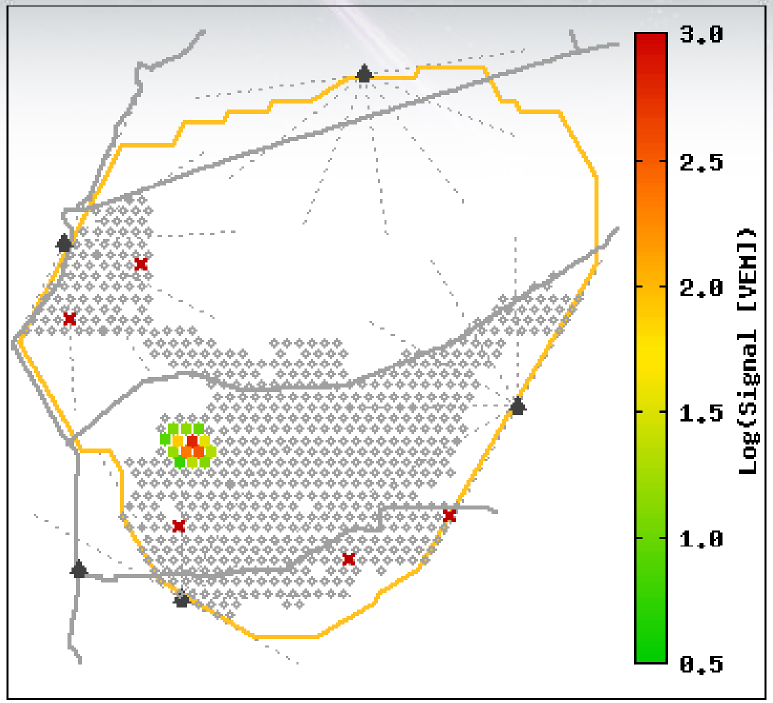

37 EeV = Exa Electron Volt = 37 x 10^{18} eV

Generic Information	
Id	1234800
Date	Sat Mar 5 15:54:48 2005
Nb Station	14
Energy	37.4 ± 1.2 EeV
Theta	43.4 ± 0.1 deg
Phi	-27.3 ± 0.2 deg
Curvature	15.8 ± 0.8 km
Core Easting	460206 ± 20 m
Core Northing	6089924 ± 11 m
Reduced Chi^2	2.30

Event 1234800

See event reconstruction data | See CR incoming direction

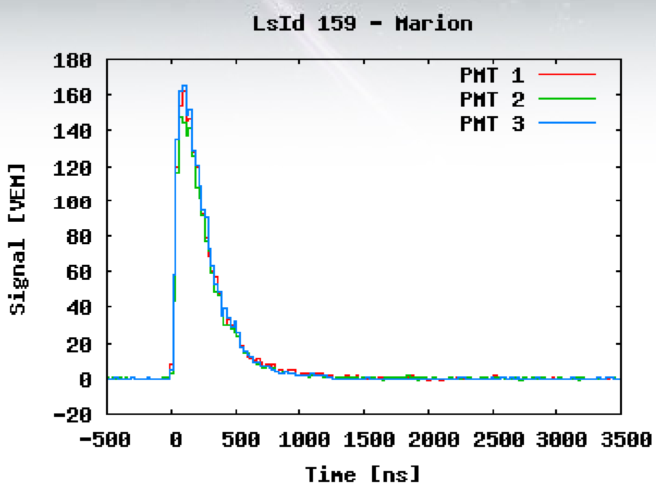

Signal in VEM for the 3 PMTs of station 159 (Marion) as a function of time

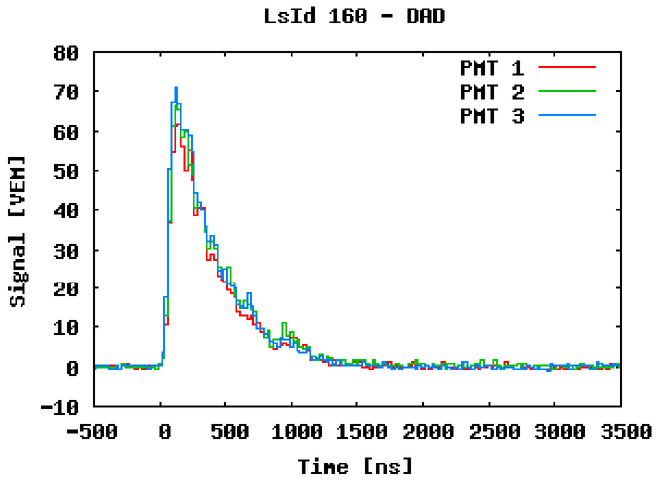

Signal in VEM for the 3 PMTs of station 160 (DAD) as a function of time

A few Reasons why you want to become an Experimental Particle Physicist

The Standard Model of Particles Physics, a theory that was established in the early 1970ies, is in excellent agreement with experiments. Especially the LEP experiments verified the theory to impressive precision.

The Higgs Particle, a necessary element of the standard model, is being hunted at LHC.

Although the standard model is perfectly fitting the experiment, we know/think that it cannot be the final answer:

CP violation and the other CKM matrix elements are put into the model explicitly and they are not derived from a theory.

The masses of the particles are also unexplained.

The Matter- Antimatter asymmetry in the Universe cannot be explained by the level of standard model CP violation.

The cosmological constant predicted by the standard model differs by 120 orders of magnitude from the observed one.

The Higgs mass renormalization requires fine tuning operations etc. etc.

A few Reasons why you want to become an Experimental Particle Physicist

Incredible efforts by the smartest theorists did not really advance on these questions and did not touch base with experiment.

It is very difficult to find out what is wrong with the theory if all experimental results are fitting the theory.

If we would find the standard model Higgs at LHC it would be an very impressive confirmation of the Standard Model, but we would not at all advance on the questions quoted earlier.

Hopefully we find something in contradiction with the Standard Model !!!

The next step in advancing our knowledge will come from Experiment. Either LHC or some other future machine.

We have to invent new technologies for future accelerators and experiments !

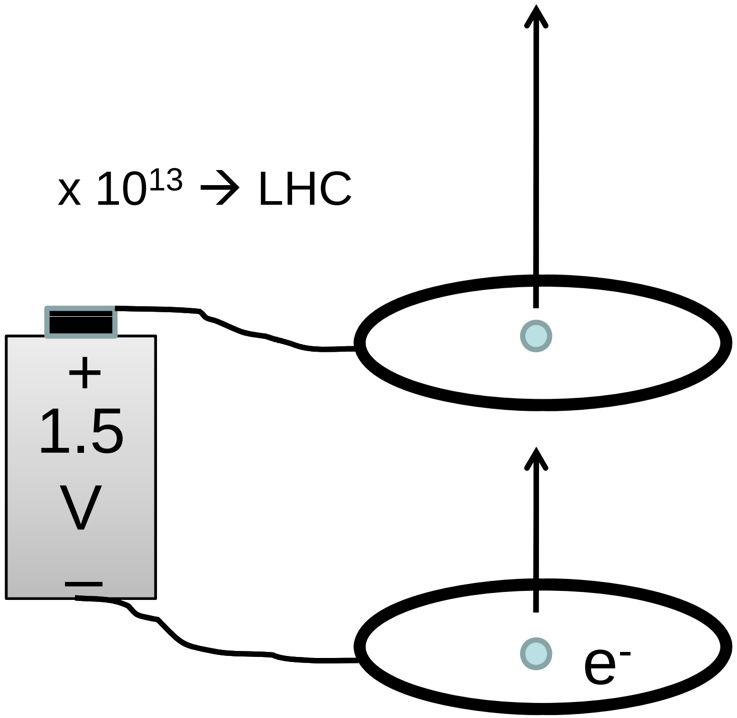

Physicist 1: How can we build an accelerator with 10 times more energy ?

Physicist 2: Hmm – I have an idea !! We build a 10 times larger accelerator !

You

have to develop the tricks and techniques to advance on these most fundamental questions !

dE/dx

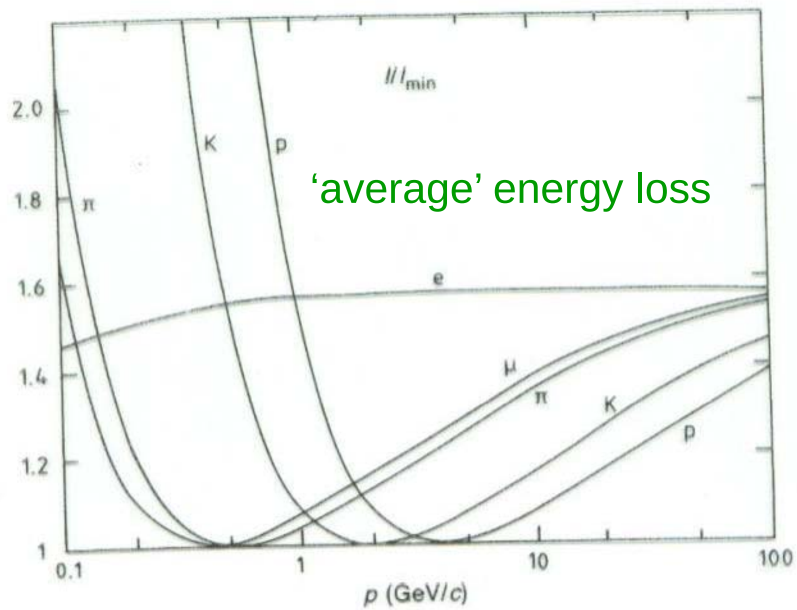

Measured energy loss

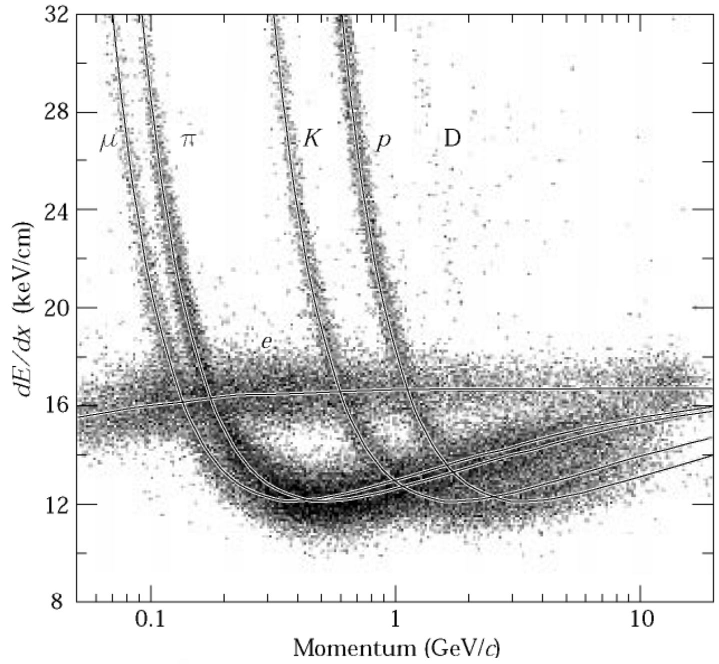

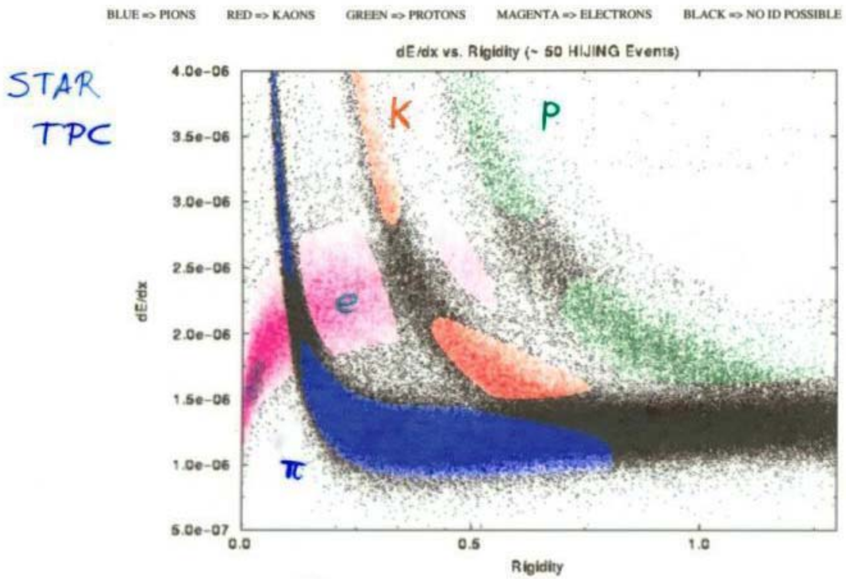

In certain momentum ranges, particles can be identified by measuring the energy loss.

Time of Flight (TOF)

E.g: $D = 2\,m$, $\sigma_t = 100\,ps$ $(10^{-10}\,s)$

3σ Significance $\rightarrow$ $T = t_2 - t_1 > 300\,ps$

$p = m v \gamma \rightarrow v = \frac{c}{\sqrt{1+\frac{m^2c^2}{p^2}}}$, $T = \frac{D}{v}$

$$T = \frac{D}{c}\sqrt{1+\frac{m^2c^2}{p^2}}$$

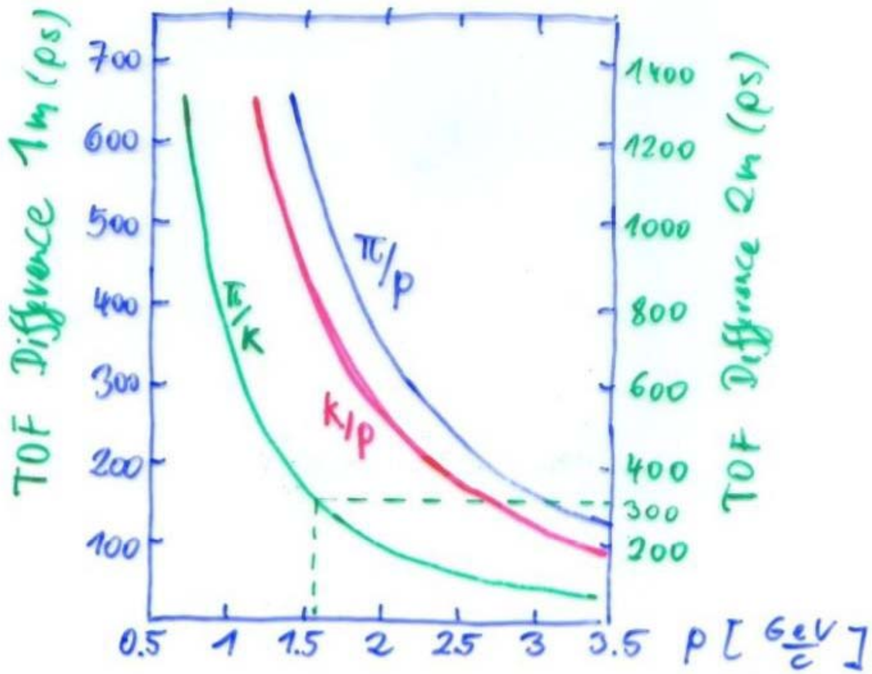

1.5 GeV/c

NA49 combined particle ID: TOF + dE/dx (TPC)

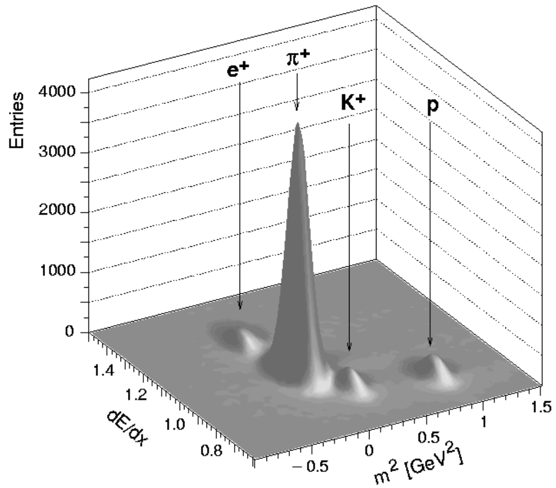

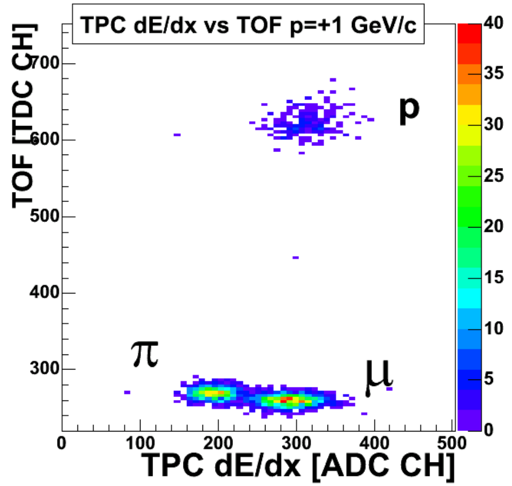

Cherenkov Radiation

If the velocity of a charged particle is larger than the velocity of light in the medium $v > \frac{c}{n}$ (n... Refractive Index of material) it emits 'Cherenkov' radiation at a characteristic angle of $\cos\theta_c = \frac{1}{n\beta}$ $(\beta = \frac{v}{c})$

$$\frac{dN}{dx} \approx 2\pi\alpha Z_1^2 \left(1 - \frac{1}{\beta^2 n^2}\right) \frac{\lambda_2 - \lambda_1}{\lambda_2 \cdot \lambda_1}$$

= Number of emitted Photons / length with λ between λ_1 and λ_2

With $\lambda_1 = 400\,nm$ $\lambda_2 = 700\,nm$

$$\frac{dN}{dx} = 490 \left(1 - \frac{1}{\beta^2 n^2}\right) \left[\frac{1}{cm}\right]$$

Material	n-1	β threshold	γ threshold
solid Sodium	3.22	0.24	1.029
lead glass	0.67	0.60	1.25
water	0.33	0.75	1.52
silica aerogel	0.025-0.075	0.93-0.976	2.7 - 4.6
air	$2.93 \cdot 10^{-4}$	0.9997	41.2
He	$3.3 \cdot 10^{-5}$	0.99997	123

Ring Imaging Cherenkov Detector

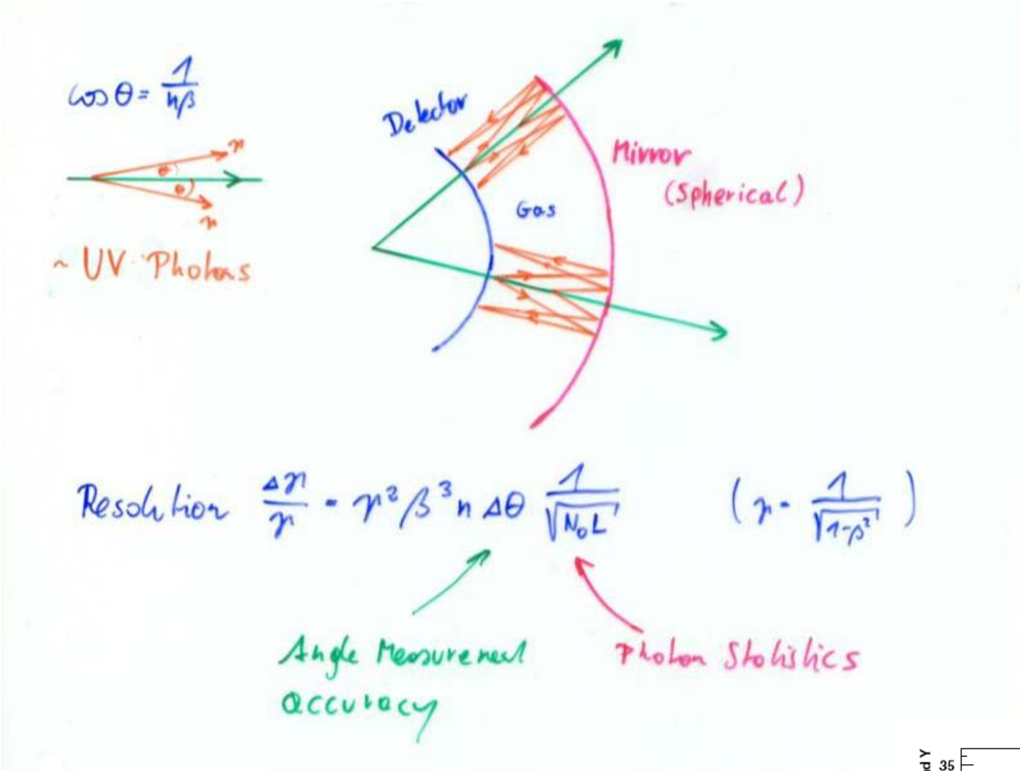

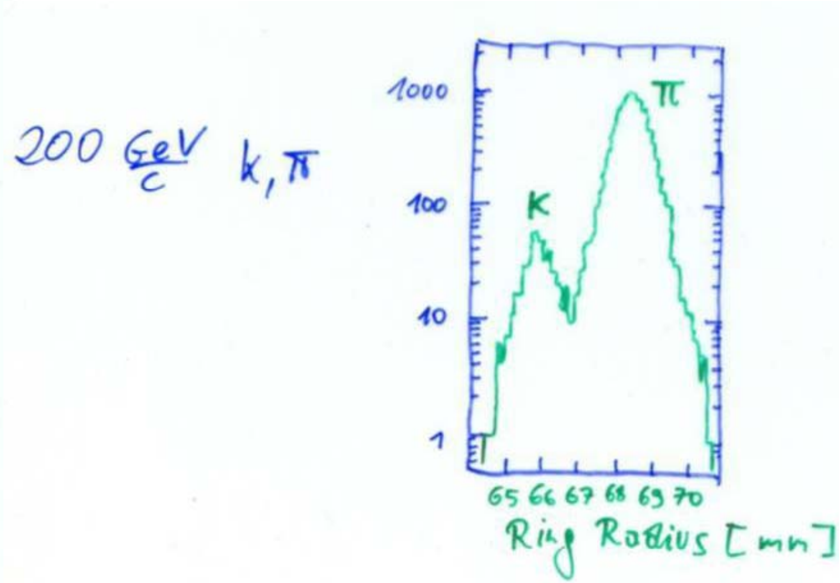

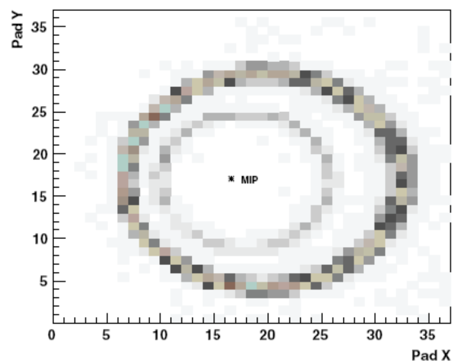

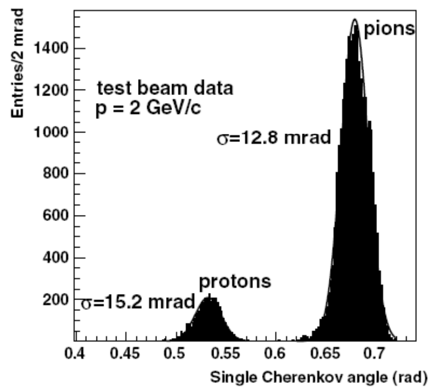

Transition Radiation

Radiation (~ keV) emitted by ultra-relativistic Particles when they traverse the boarder of 2 Materials of different Dielectric Permittivity ($\varepsilon_1, \varepsilon_2$)

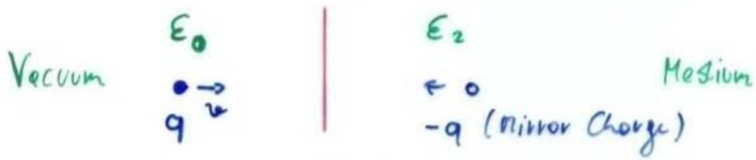

Classical Picture

$q = Z_1 e$

$$I = \frac{1}{3} \alpha Z_1^2 (\hbar\omega_p) \gamma$$ ... Radiated Energy per Transition

$\hbar\omega_p$ .... plasma Frequency of the Medium

.... ~20 eV for Styrene

About half the Energy is radiated between

$$0.1\, \hbar\omega_p \gamma < \hbar\omega < \hbar\omega_p \gamma$$

E.g. $\gamma = 1000$ 2-20 keV X-Rays

$$N_\gamma \sim \frac{2}{3} \alpha Z_1^2 \sim 5 \cdot 10^{-3} \cdot Z_1^2$$

γ - Dependence from hardening rather than N_γ

Emission Angle ~ $\frac{1}{\gamma}$

The Number of Photons can be increased by placing many foils of Material.

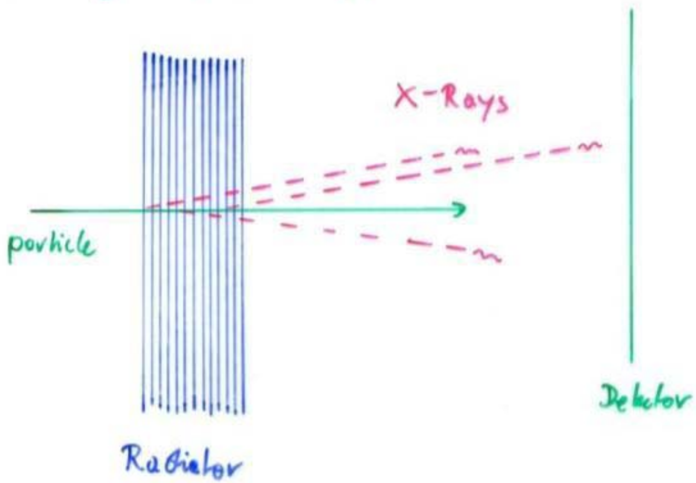

AMANDA

Antarctic **M**uon **A**nd **N**eutrino **D**etector **A**rray

AMANDA

South Pole

AMANDA

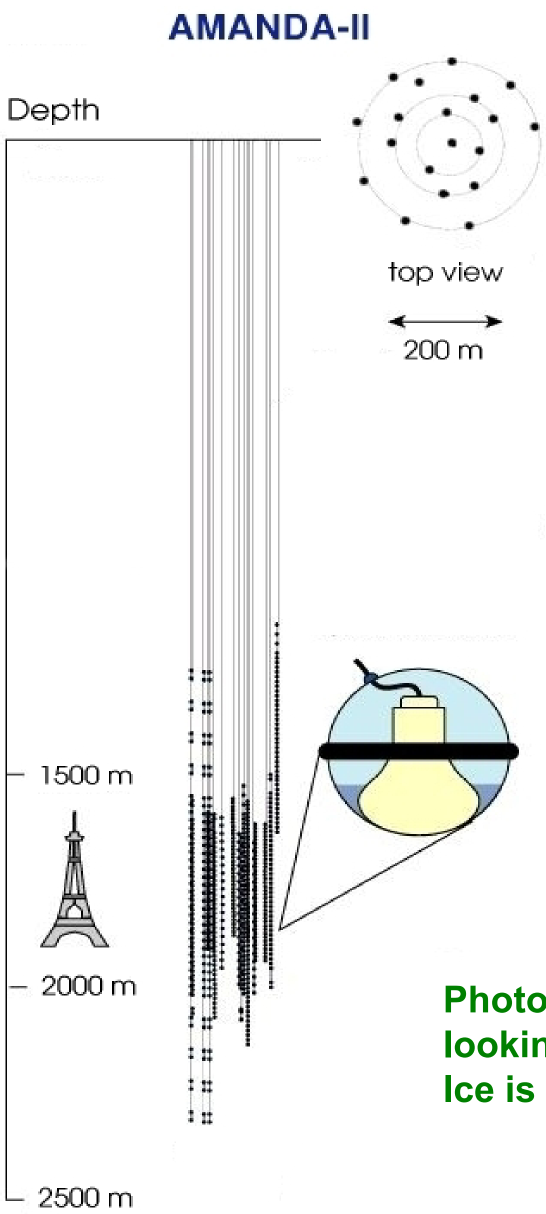

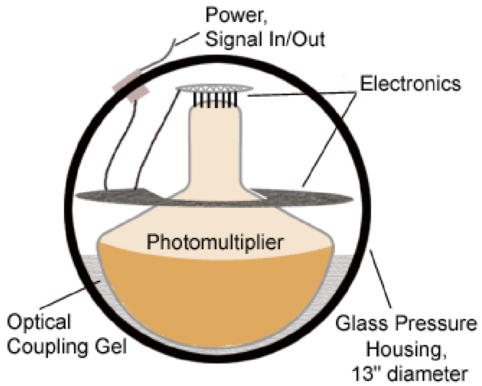

Photomultipliers in the Ice,
looking downwards.
Ice is the detecting medium.

AMANDA

Look for upwards going Muons from Neutrino Interactions.
Cherekov light propagating through the ice.

→ Find neutrino point sources in the universe !

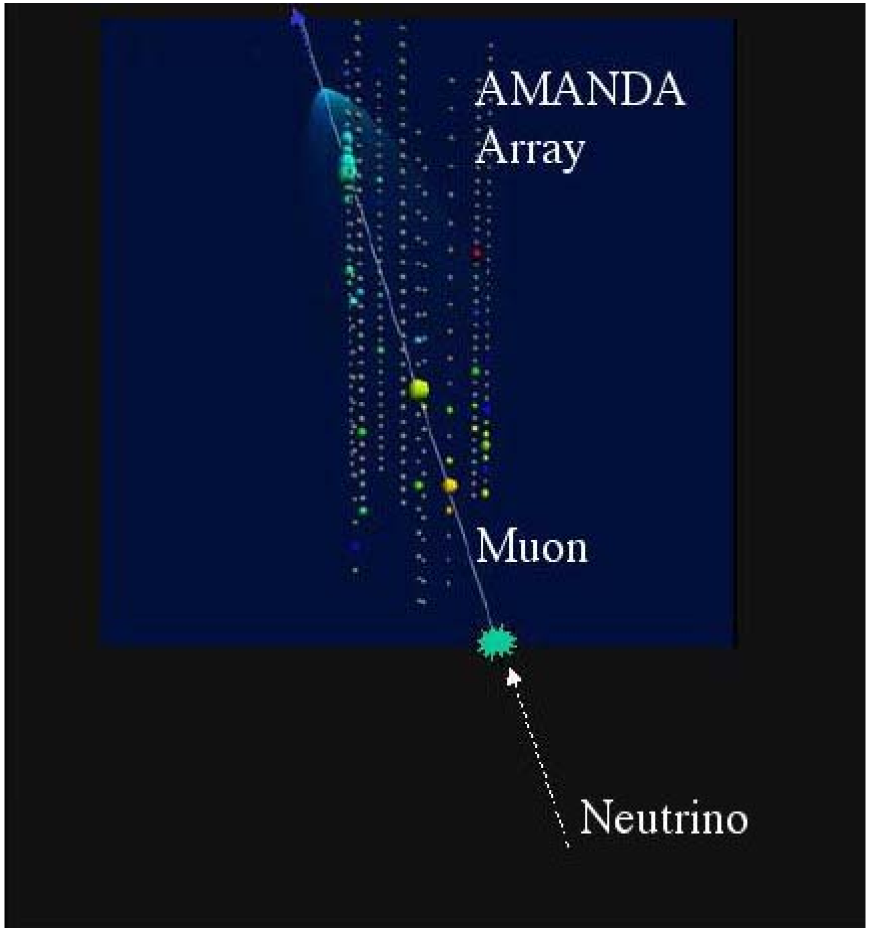

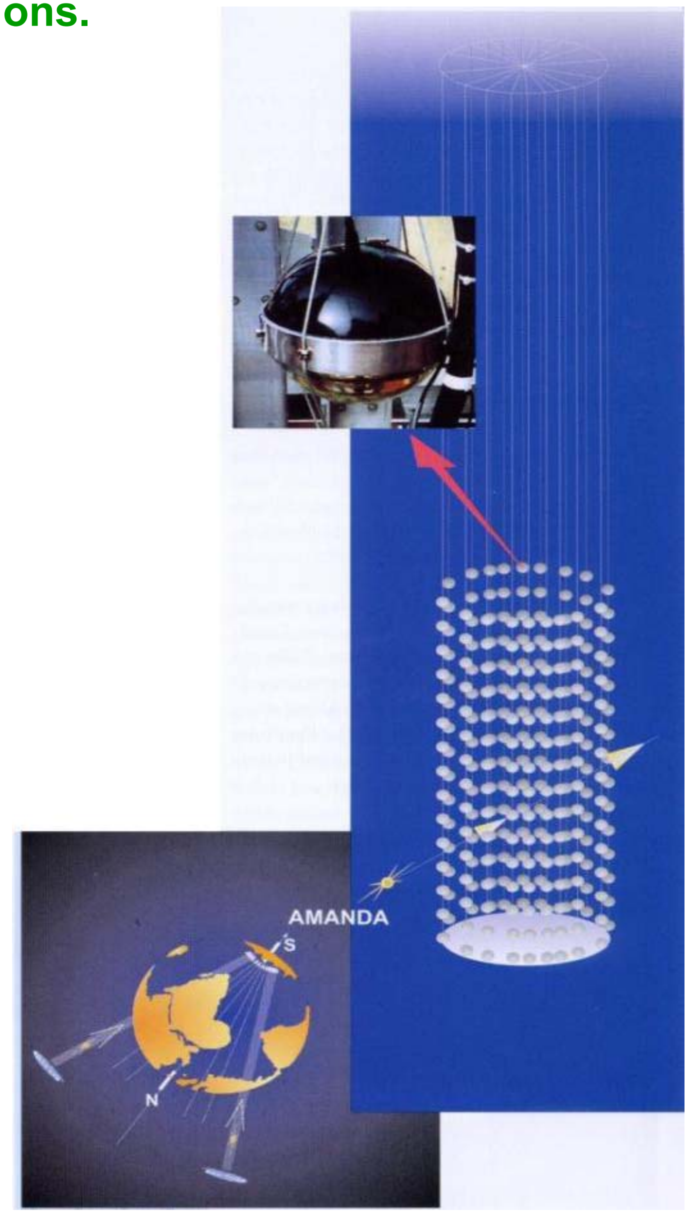

AMANDA

Event Display

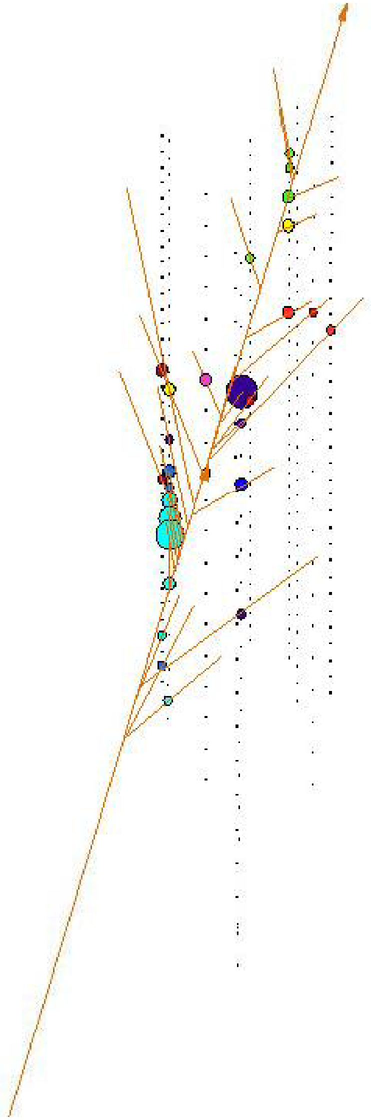

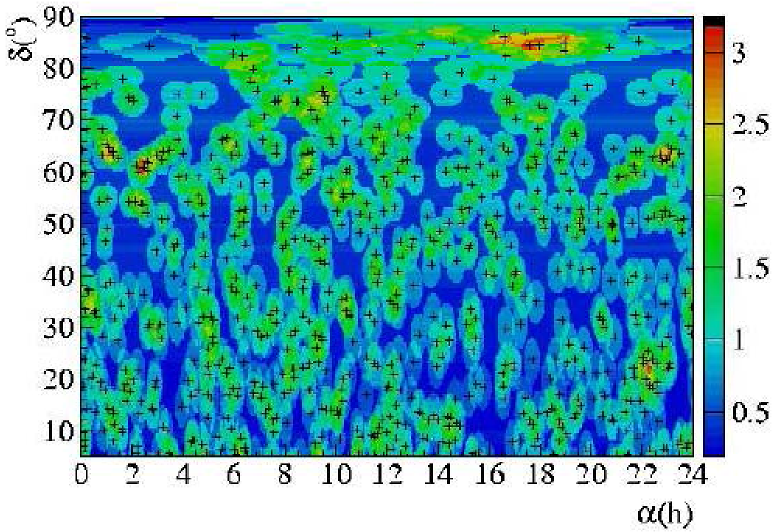

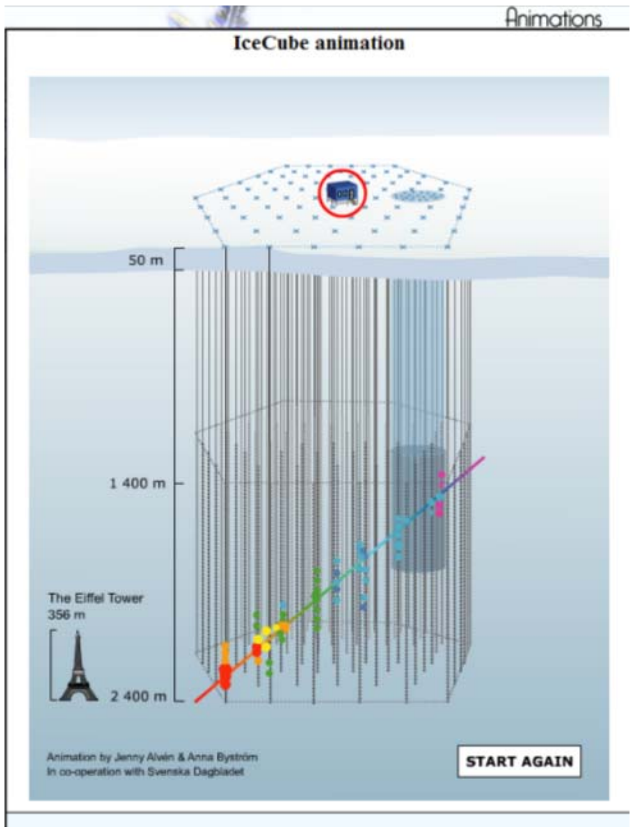

Up to now: No significant point sources but just neutrinos from cosmic ray interactions in the atmosphere were found .

→ Ice Cube for more statistics !

Pierre Auger Cosmic Ray Observatory

Pierre Auger Cosmic Ray Observatory

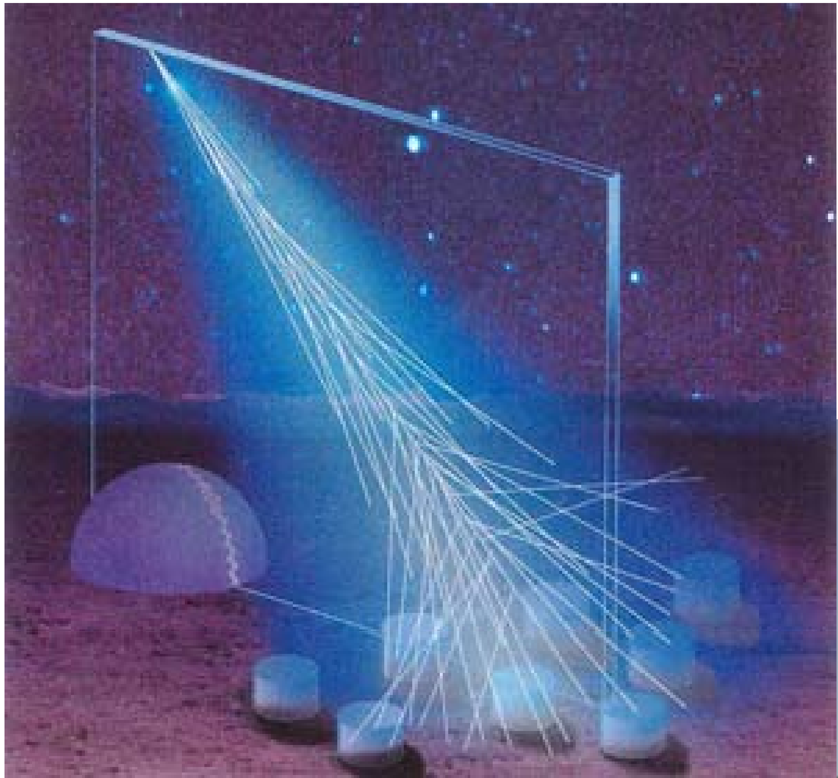

Use earth's atmosphere as a calorimeter. 1600 water Cherenkov detectors with 1.5km distance.

Placed in the Pampa Amarilla in western Argentina.

Pierre Auger Cosmic Ray Observatory

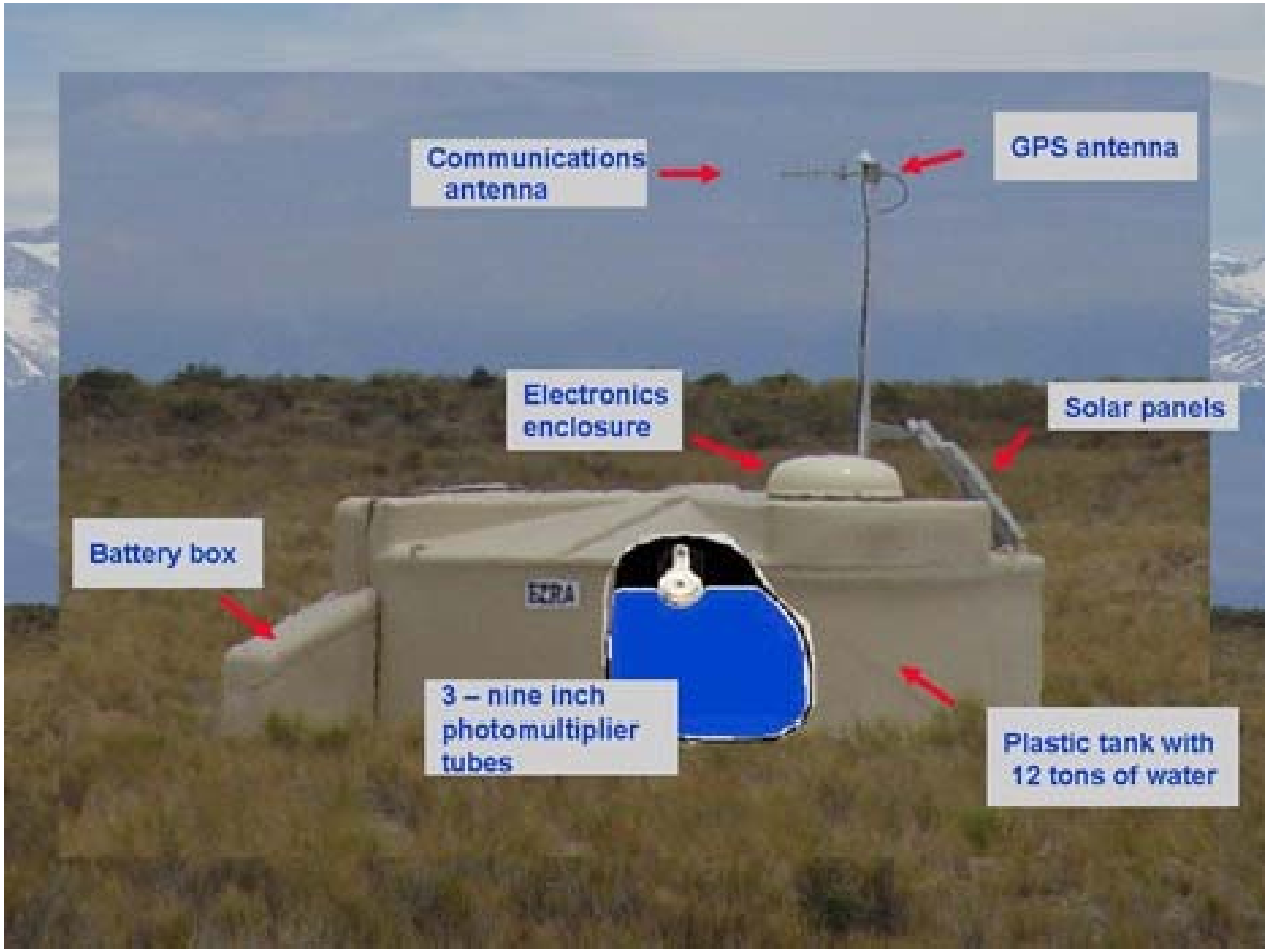

Pierre Auger Cosmic Ray Observatory

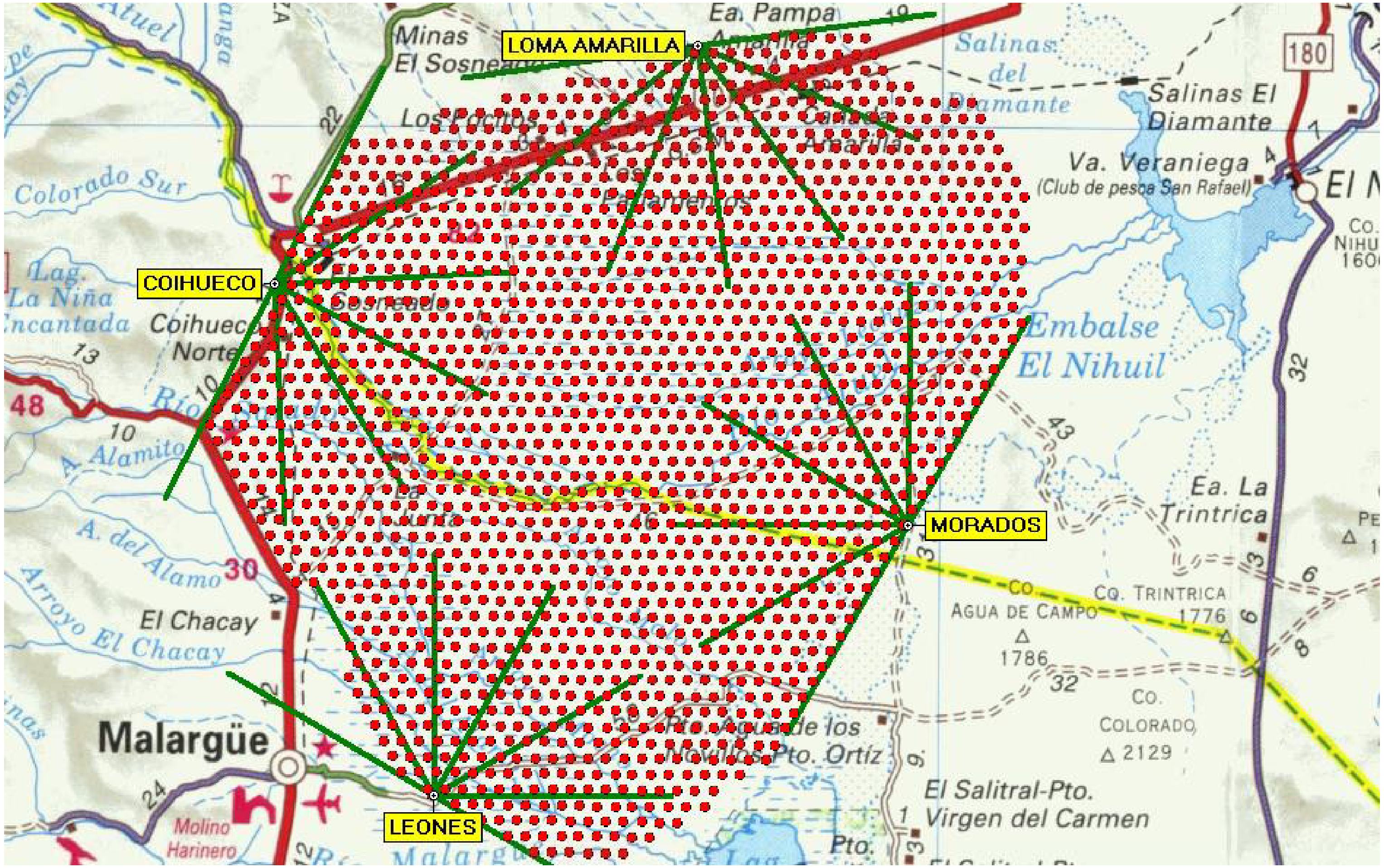

Pierre Auger Cosmic Ray Observatory

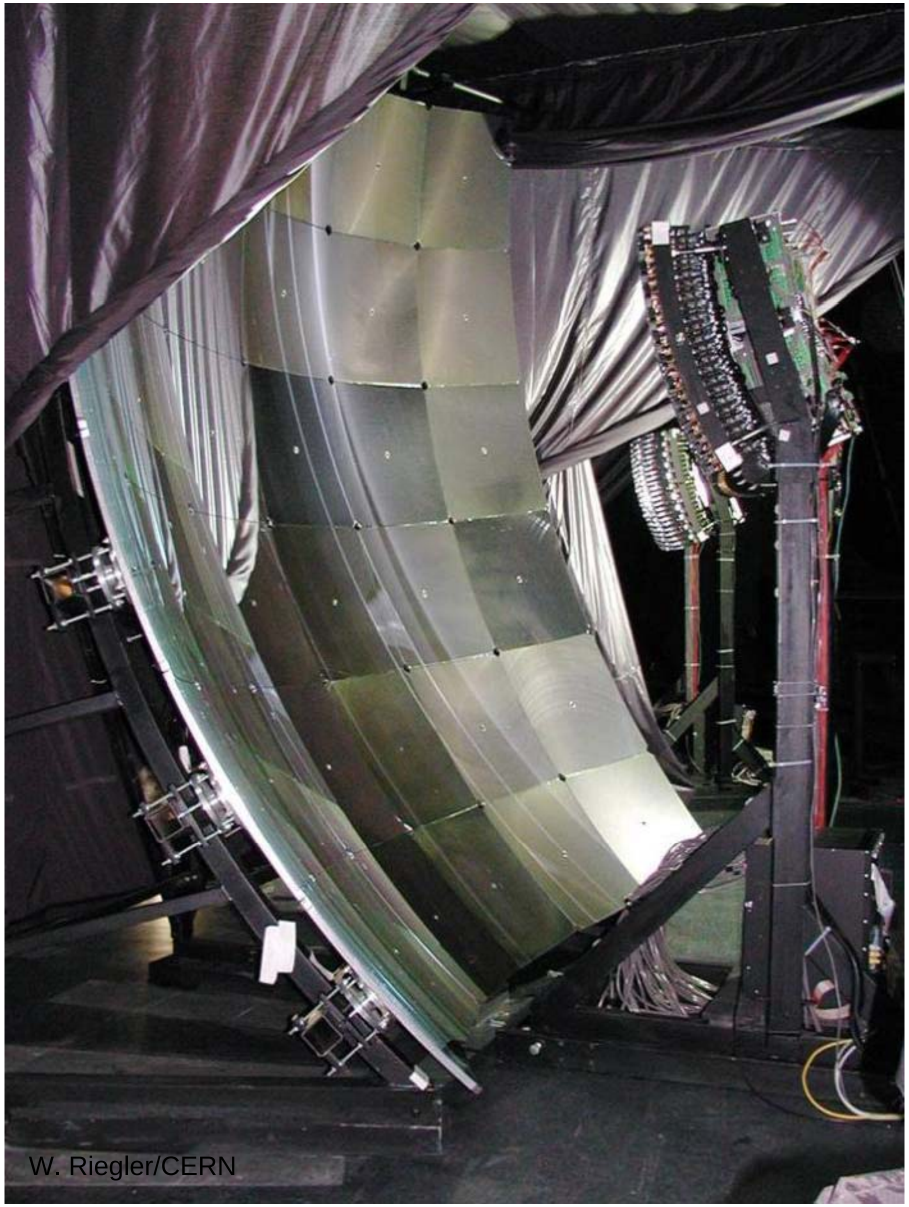

In addition: Fluorescence detectors around the array of water tanks.

Event 1234800

See CR incoming direction | See individual station data

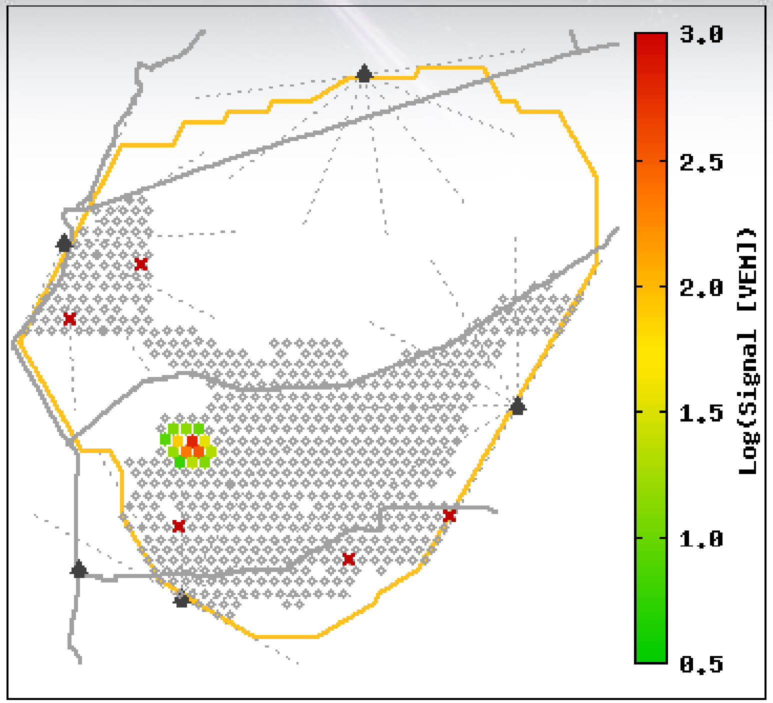

37 EeV = Exa Electron Volt = 37 x 10^{18} eV

Generic Information	
Id	1234800
Date	Sat Mar 5 15:54:48 2005
Nb Station	14
Energy	37.4 ± 1.2 EeV
Theta	43.4 ± 0.1 deg
Phi	-27.3 ± 0.2 deg
Curvature	15.8 ± 0.8 km
Core Easting	460206 ± 20 m
Core Northing	6089924 ± 11 m
Reduced Chi^2	2.30

Event 1234800

See event reconstruction data | See CR incoming direction

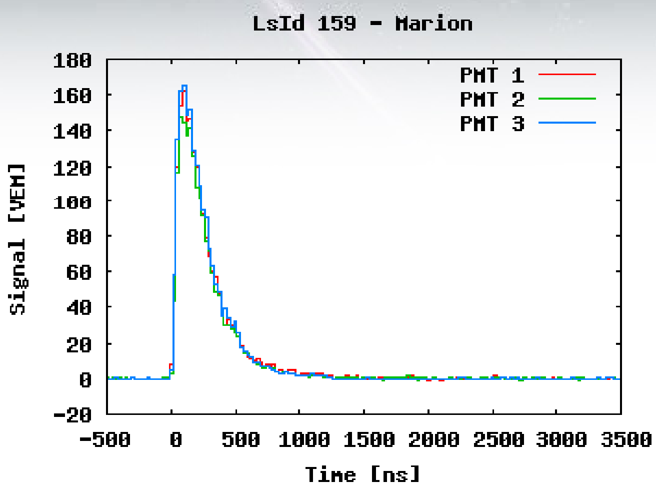

Signal in VEM for the 3 PMTs of station 159 (Marion) as a function of time

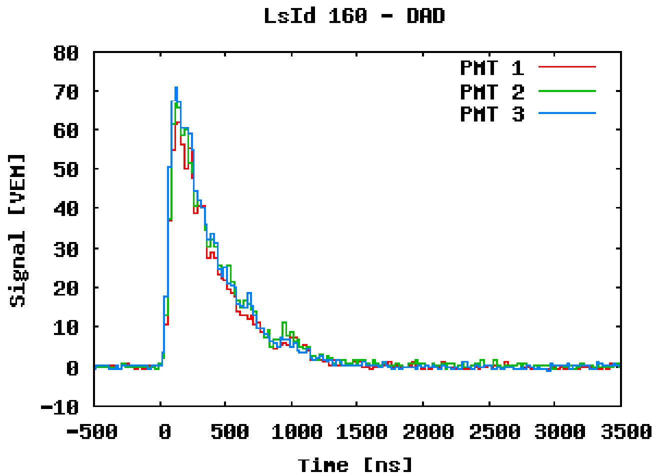

Signal in VEM for the 3 PMTs of station 160 (DAD) as a function of time

The Charge Signal

extra slide not shown

Collected Charge for a Minimum Ionizing Particle (MIP)

- **Mean energy loss**
  dE/dx (Si) = 3.88 MeV/cm
  $\Rightarrow$ 116 keV for 300μm thickness

- **Most probable energy loss**
  $\approx$ 0.7 $\times$mean
  $\Rightarrow$ 81 keV

- **3.6 eV to create an e-h pair**
  $\Rightarrow$ 72 e-h / μm (mean)
  $\Rightarrow$ 108 e-h / μm (most probable)

- **Most probable charge** (300 μm)

  $\approx$ 22500 e $\approx$ 3.6 fC

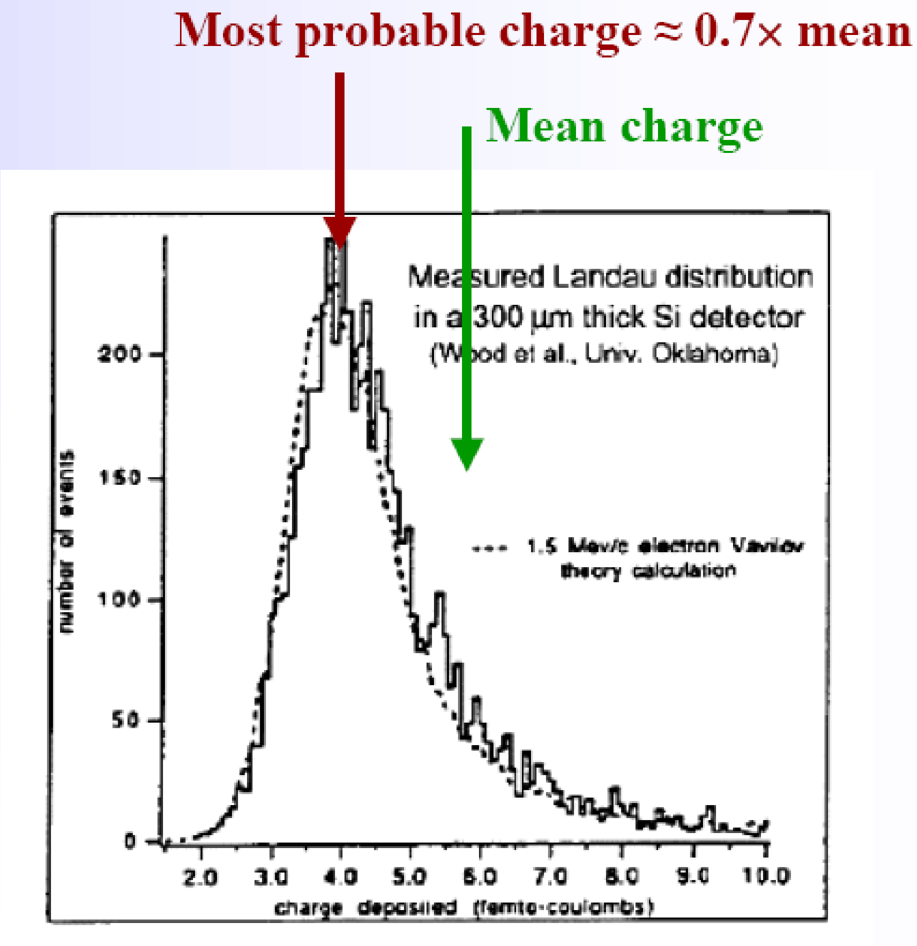

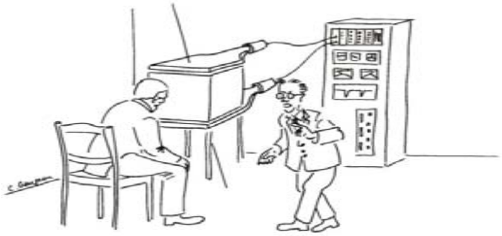

e^+e^- collider. P_{tot}=0,
If the Σ p_i of all collision products is ≠0 → neutrino escaped

Question: Is the transverse momentum at the IP really zero (Betatron Oscillations) ?

Helmut Burkhard/CERN

At 100 GeV, the beams at the IP have the following rms transverse momenta :
in x : 100 GeV * 160e-6 = 16 MeV
in y : 100 GeV * 62.03e-6 = 6.2 MeV
Longitudinal, energy spread rms 155.707 MeV

These are relatively small numbers and only of importance as small corrections for precision measurements, like the Z-lineshape measurements.

Much larger first order effects are radiative corrections like "beam- beam Bremsstrahlung" - or initial state radiation.

Solid State Detectors

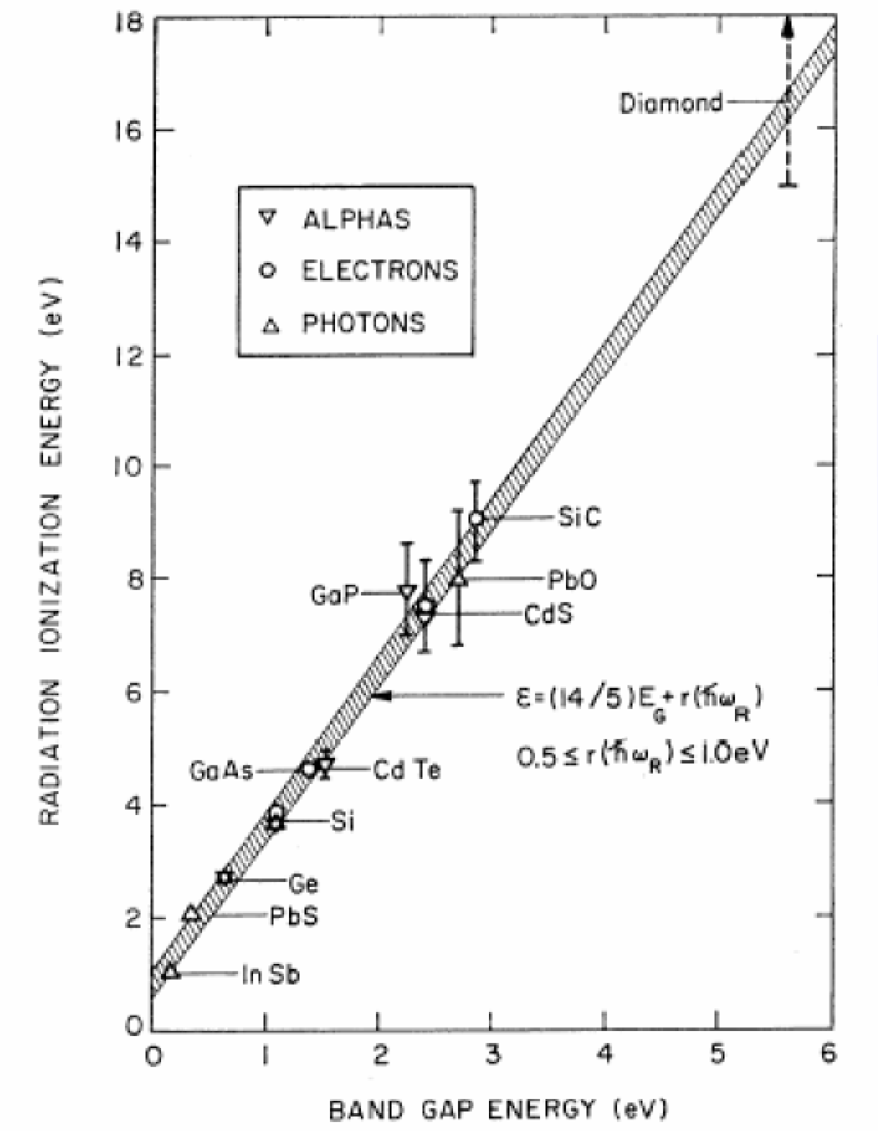

	Diamond	SiC (4H)	GaAs	Si	Ge
Atomic number Z	6	14/6	31/33	14	32
Bandgap E_g [eV]	5.5	3.3	1.42	1.12	0.66
E(e-h pair) [eV]	13	7.6-8.4	4.3	3.6	2.9
density [g/cm^3]	3.515	3.22	5.32	2.33	5.32
e-mobility μ_e [cm^2/Vs]	1800	800	8500	1450	3900
h-mobility μ_h [cm^2/Vs]	1200	115	400	450	1900

Depletion Voltage

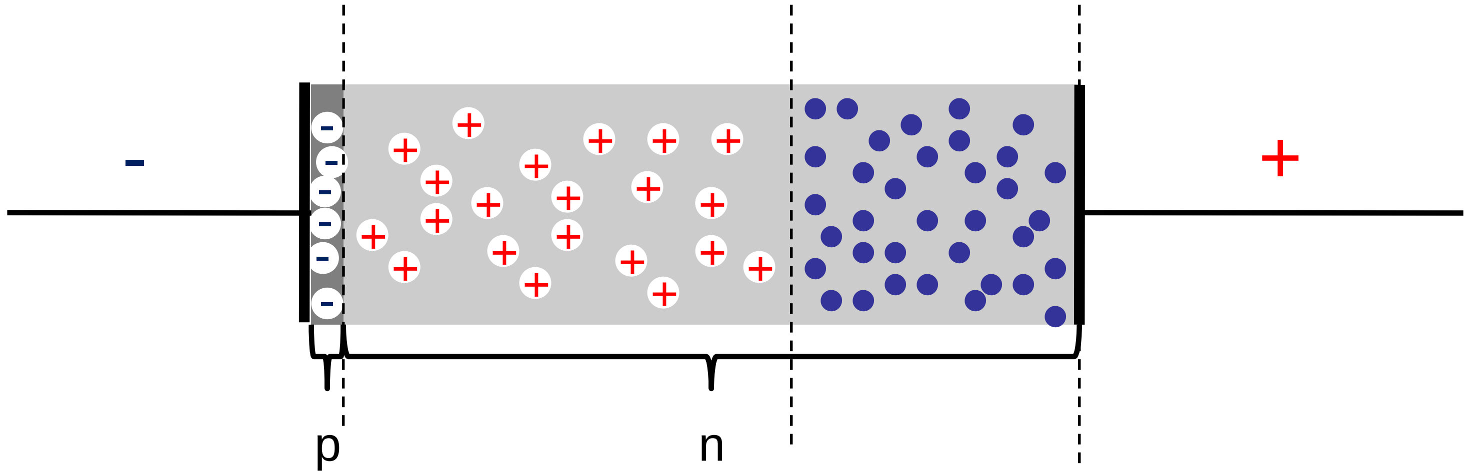

The capacitance of the detector decreases as the depletion zone increases.

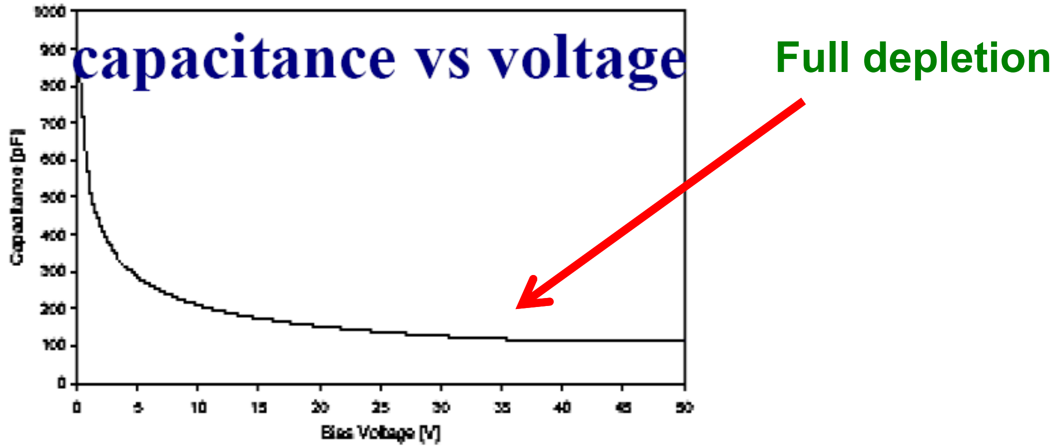

Simulated EM Shower Profiles in $PbWO_4$

Simulation of longitudinal shower profile **Simulation of transverse shower profile**

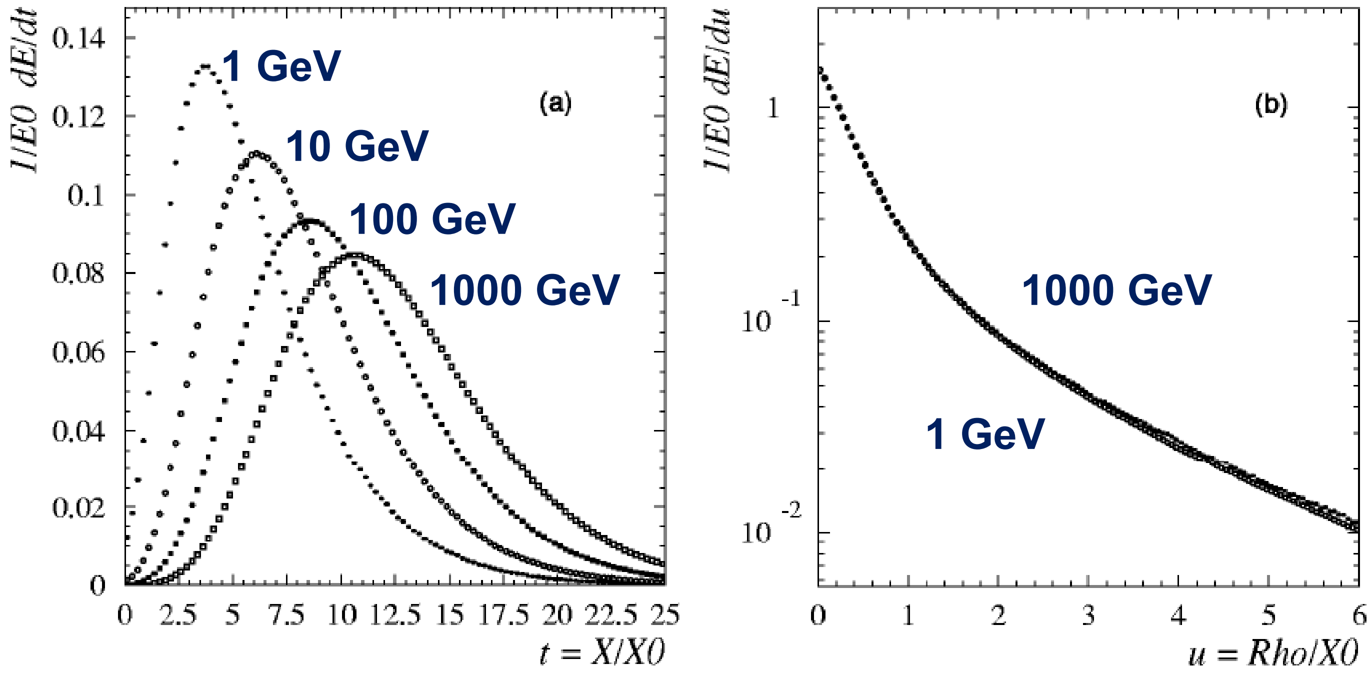

FIG. 2. (a) Simulated shower longitudinal profiles in $PbWO_4$, as a function of the material thickness (expressed in radiation lengths), for incident electrons of energy (from left to right) 1 GeV, 10 GeV, 100 GeV, 1 TeV. (b) Simulated radial shower profiles in $PbWO_4$, as a function of the radial distance from the shower axis (expressed in radiation lengths), for 1 GeV (closed circles) and 1 TeV (open circles) incident electrons. From Maire (2001).

In calorimeters with thickness ~ 25 X_0, the shower leakage beyond the end of the active detector is much less than 1% up to incident electron energies of ~ 300 GeV (LHC energies).

Energy Resolution of Calorimeters

Stochastic term:
Fluctuations related to the physics development of the shower.

Noise term:
From electronics noise of the readout chain.
For constant electronics noise → double signal = double S/N

Constant term:
Instrumental effects that cause variations of the calorimeter response with the particle impact point.

$$\frac{\sigma}{E} = \frac{a}{\sqrt{E}} \oplus \frac{b}{E} \oplus c$$

Add in squares

For homogeneous calorimeters the noise term and constant term become dominant.

For sampling calorimeters the stochastic term, then called 'sampling' term becomes dominant.

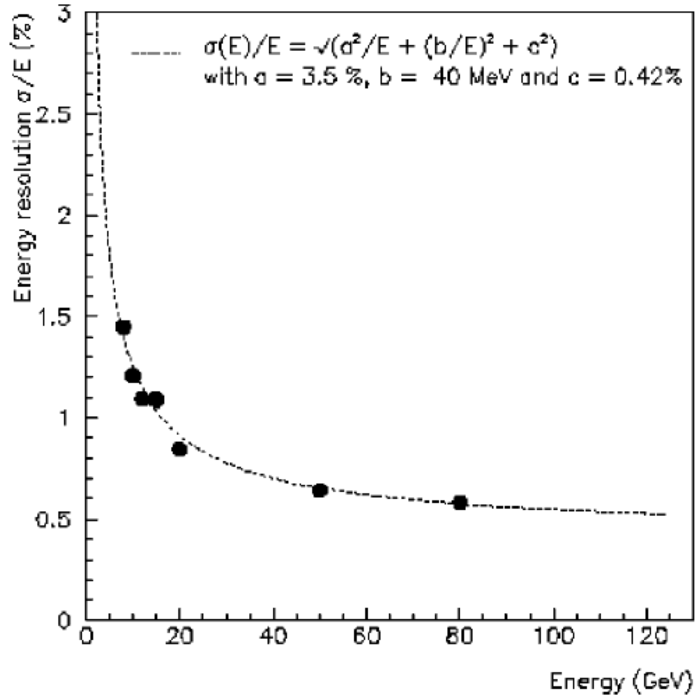

FIG. 3. Fractional electron energy resolution as a function of energy measured with a prototype of the NA48 liquid krypton electromagnetic calorimeter (NA48 Collaboration, 1995). The line is a fit to the experimental points with the form and the parameters indicated in the figure.

Scintillator Sampling Calorimeters

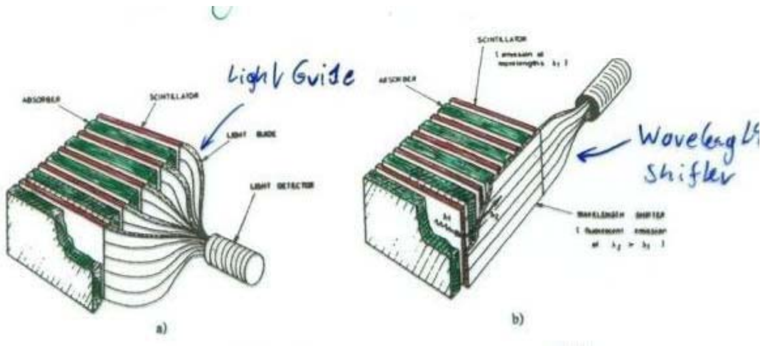

Wavelength shifters absorb photons from the scintillators and emit light at a longer wavelength which does not go back into the scintillator but is internally reflected along the readout plate to the photon detector → compact design.

A large number of sampling calorimeters use organic scintillators arranged in fibers or plates.

The drawbacks are that the optical readout suffers from radiation damage and non-uniformities at various stages are often the source of a large constant term.

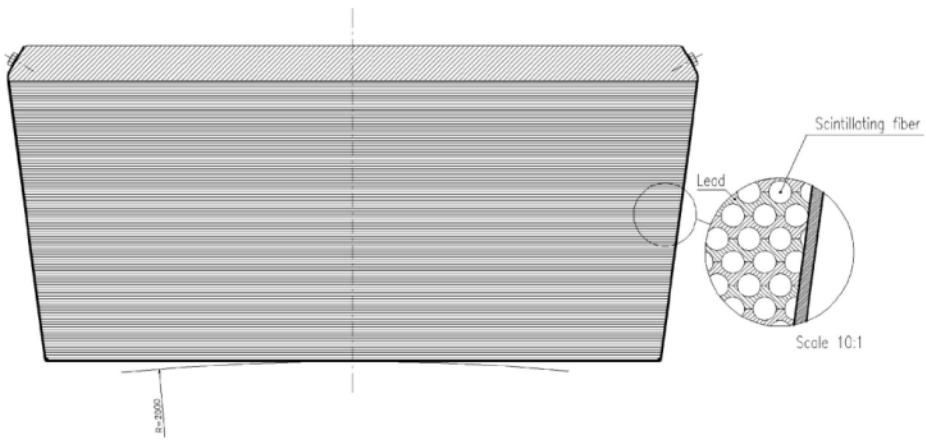

FIG. 13. Schematic layout of the barrel part of the KLOE electromagnetic calorimeter (Antonelli *et al.*, 1995).

Kloe EM calorimeter:

5%/Sqrt[E(GeV)] !

Gas and Solid State Sampling Calorimeters

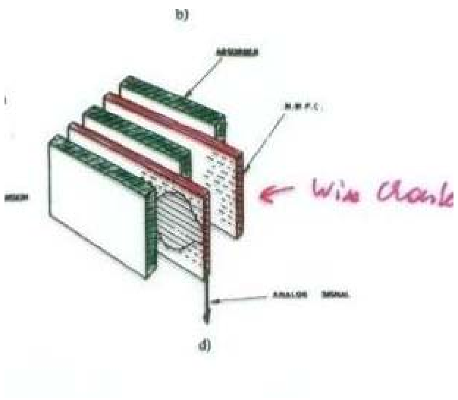

Gas sampling calorimeters have been widely employed until recently (LEP) because of their low cost and segmentation flexibility.

They are not well suited to present and future machines because of their modest EM energy resolution ~ 20%/Sqrt[E(GeV)].

Solid state detectors as active readout medium use mostly silicon. The advantage is very high signal to noise ratio (large signals). Often used on a small scale as luminosity monitors.

The disadvantage is the high cost, preventing large calorimeters, and poor radiation resistance.

Liquid Sampling Calorimeters

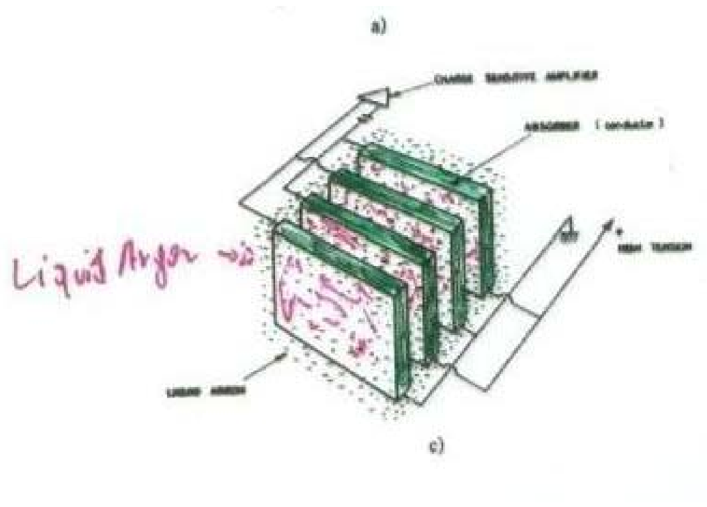

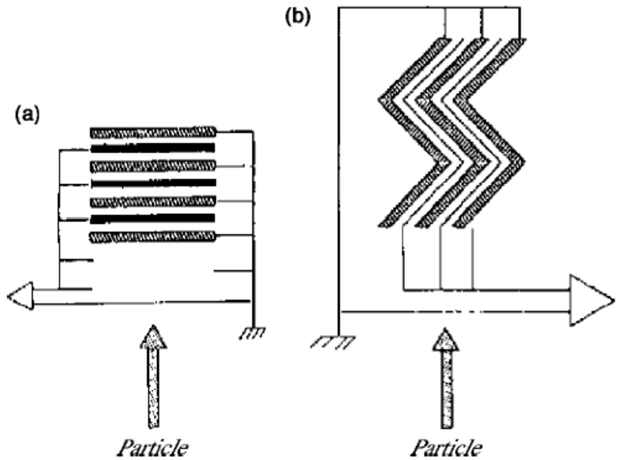

FIG. 15. Schematic view of a traditional sampling calorimeter geometry (a) and of the accordion calorimeter geometry (b).

These offer good application perspectives for future experiments.

Warm liquids work at room temperature, avoiding cryogenics but they are characterized by poor radiation resistance and suffer from purity problems

→Noble liquids at cryogenic temperatures.

The advantages are operation in 'ion chamber mode', i.e. deposited charge is large and doesn't need multiplication, which ensures better uniformity compared to gas calorimeters that need amplification.

They are relatively uniform and easy to calibrate because the active medium is homogeneously distributed inside the volume. They provide good energy resolution (e.g. ATLAS 10%/Sqrt[E(GeV)])
And stable operation with time.

They are radiation hard.

With the standard liquid argon sampling calorimeters the alternating absorber and active layers are disposed perpendicular to the direction of the incident particle.
→ Long cables are needed to gang together the readout electrodes, causing signal degradation, dead spaces between the calorimeter towers and therefore reduced hermeticity.

Sampling Calorimeters

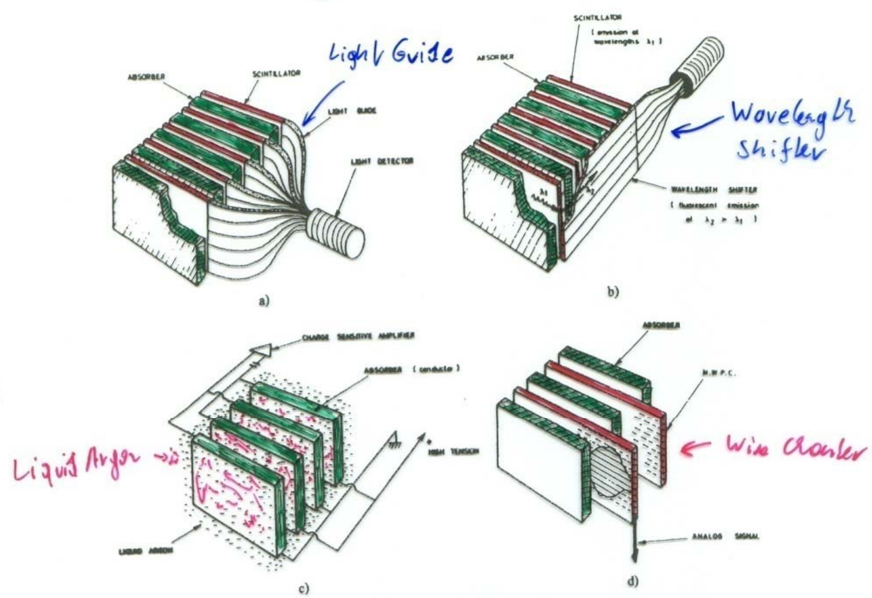

Alternation of "passive" absorber plates and "active" readout sections

Advantage:
- optimum choice of Absorber Material
- optimum choice of Signal Readout
- Compact and cheap Construction

"passive": Pb, Fe ....

"active": Scintillator (Signal -> Photons)
Noble Liquid, e.g. Ar (Signal -> e^-, I^+)
Wire Chambers (Signal -> e^-, I^+)

Liquid Argon Sampling Calorimeters

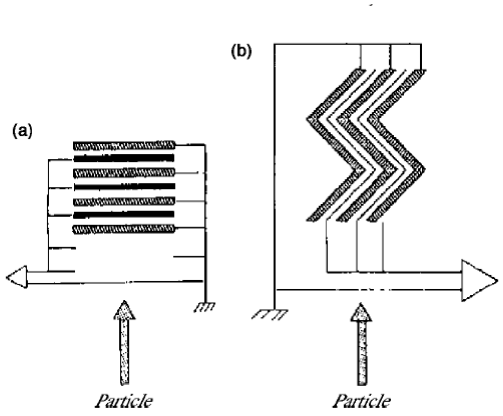

FIG. 15. Schematic view of a traditional sampling calorimeter geometry (a) and of the accordion calorimeter geometry (b).

For the ATLAS LAr Calorimeter this was solved by placing the absorbers in an accordeon geometry parallel to the particle direction and the electrodes can easily be read out from the 'back side'.

ATLAS: Lead layers of 1.1-2.2mm, depending on the rapidity region, are separated by 4mm liquid Argon gaps.

Test beam results show
10%/Sqrt[E(GeV)]   x 0.25/E(GeV)   x 0.3%

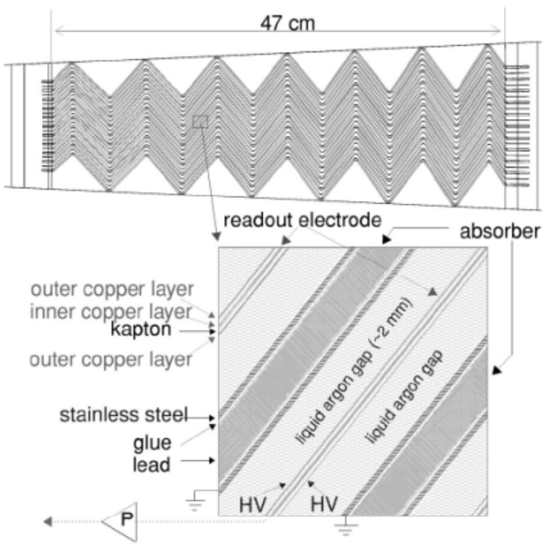

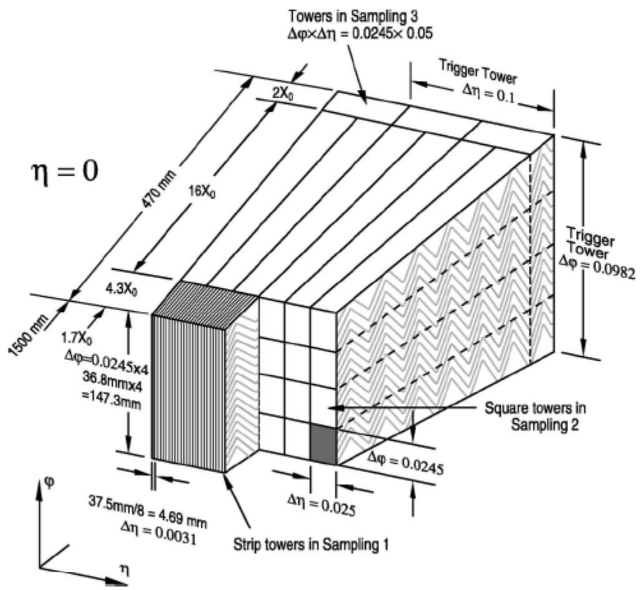

FIG. 17. Schematic view of the segmentation of the ATLAS electromagnetic calorimeter.

Hadron Calorimeters

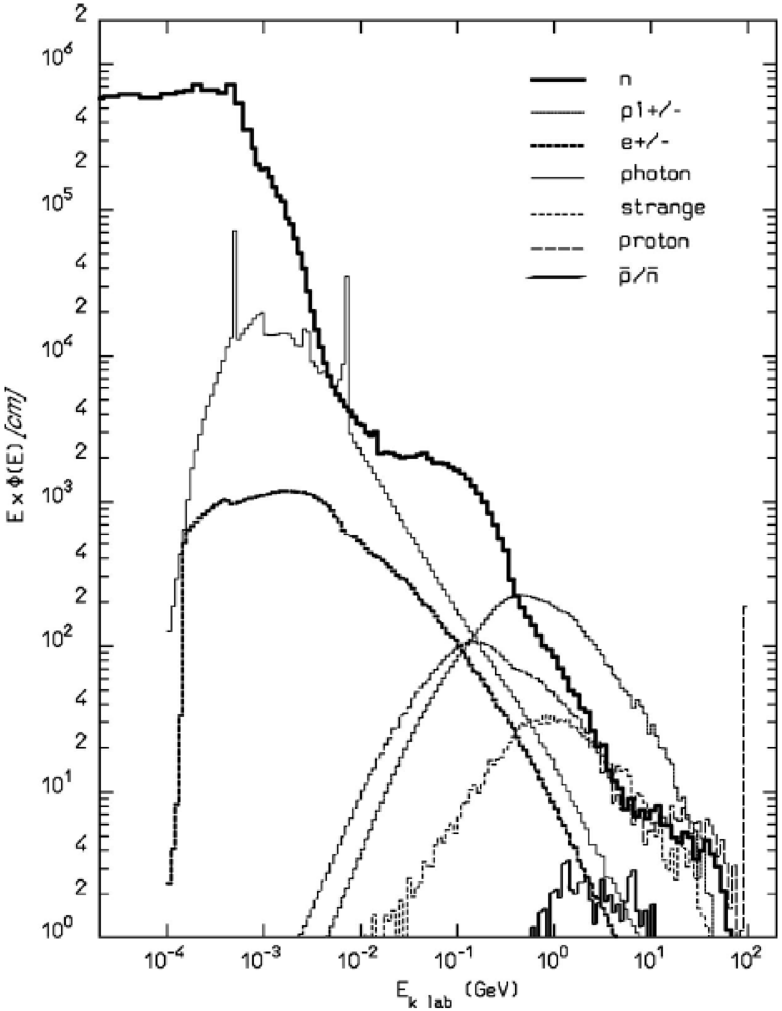

‘Deciphering this message becomes the story of hadronic calorimetry’

C.W. Fabjan and F. Gianotti, Rev. Mod. Phys., Vol. 75, N0. 4, October 2003

FIG. 19. Particle spectra produced in the hadronic cascade initiated by 100-GeV protons absorbed in lead. The energetic component is dominated by pions, whereas the soft spectrum is composed of photons and neutrons. The ordinate is in “lethargic” units and represents the particle track length, differential in $\log E$. The integral of each curve gives the relative fluence of the particle. Fluka calculations (Ferrari, 2001).

Hadron Calorimeters

The signals from an electron or photon entering a hadronic calorimeter is typically larger than the signal from a hadron cascade because the hadroic interactions produce a fair fraction of invisible effects (excitations, neutrons …).

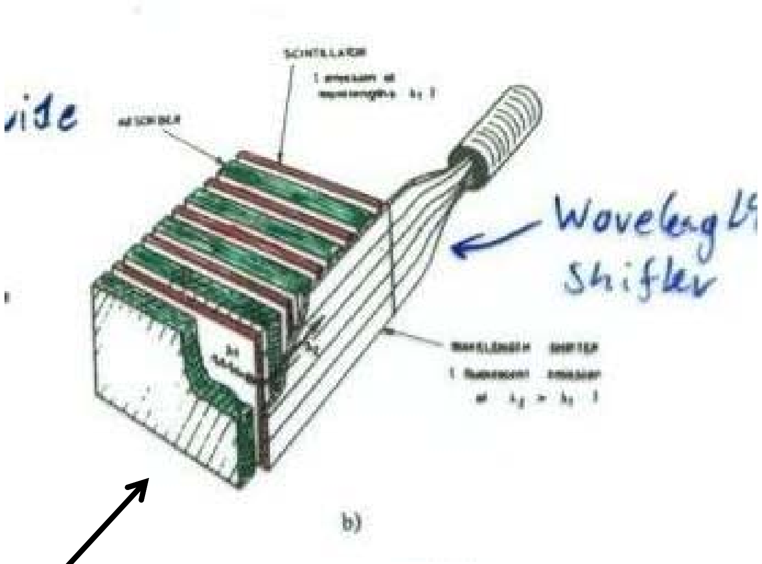

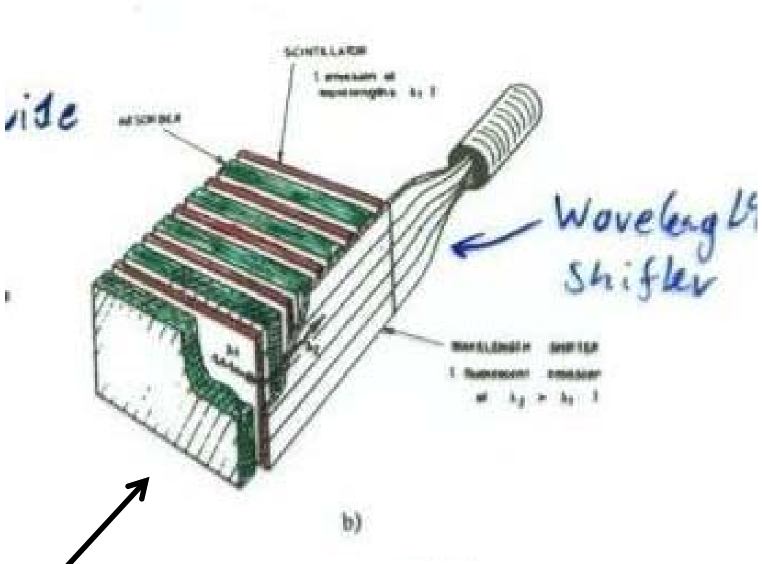

Pion 10GeV

Electron 10GeV

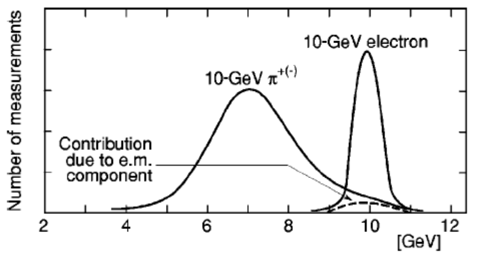

Hadron Calorimeters

Because a fair fraction of shower particles consists of $\square_0$ which instantly decay into two photons, part of the hadronic cascade becomes an EM cascade – 'and never comes back'.

Because the EM cascade had a larger response than the Hardon cascade, the event/event fluctuation of produced $\square_0$ particles causes a strong degradation of the resolution.

Is it possible to build a calorimeter that has the same response (signal) for a 10GeV electron and 10GeV hadron ? → compensating calorimeters.

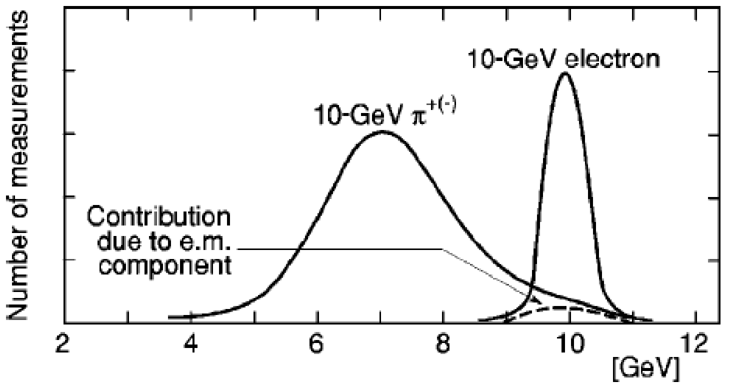

Signal (in energy units) obtained for a 10 GeV energy deposit

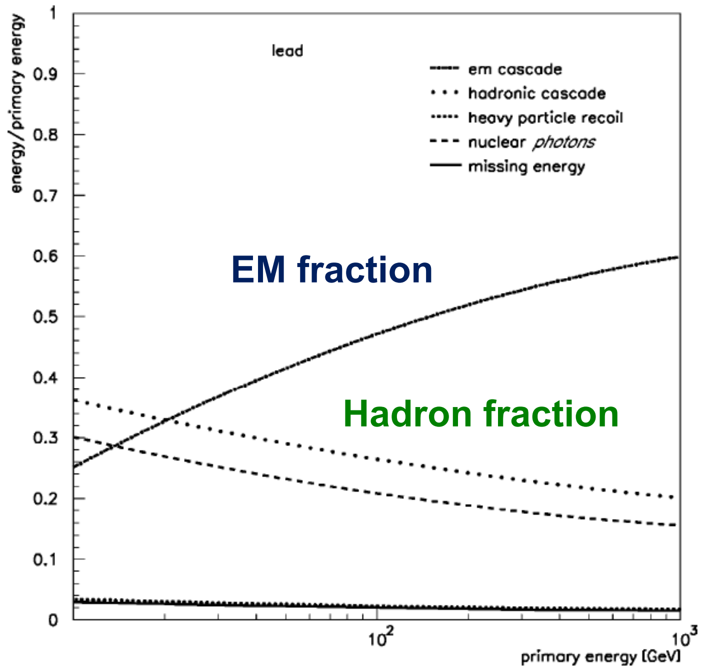

FIG. 21. Characteristic components of proton-initiated cascades in lead. With increasing primary energy the π^0 component increases (Ferrari, 2001).

Compensating Hadron Calorimeters

In a homogeneous calorimeter it is clearly not possible to have the same response for electrons and hadrons.

For sampling calorimeters the sampling frequency and thickness of active and possibe layers can be tunes such that the signal for electrons and hadrons is indeed equal !

Using Uranium or Lead with scintillators, hadron calorimters with excellen energy resolution and linearity have been built.

Energy resolution

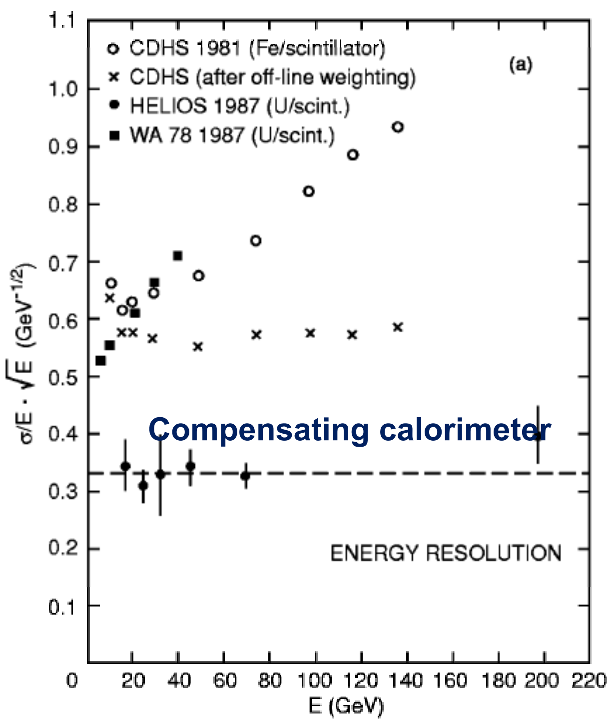

Linearity

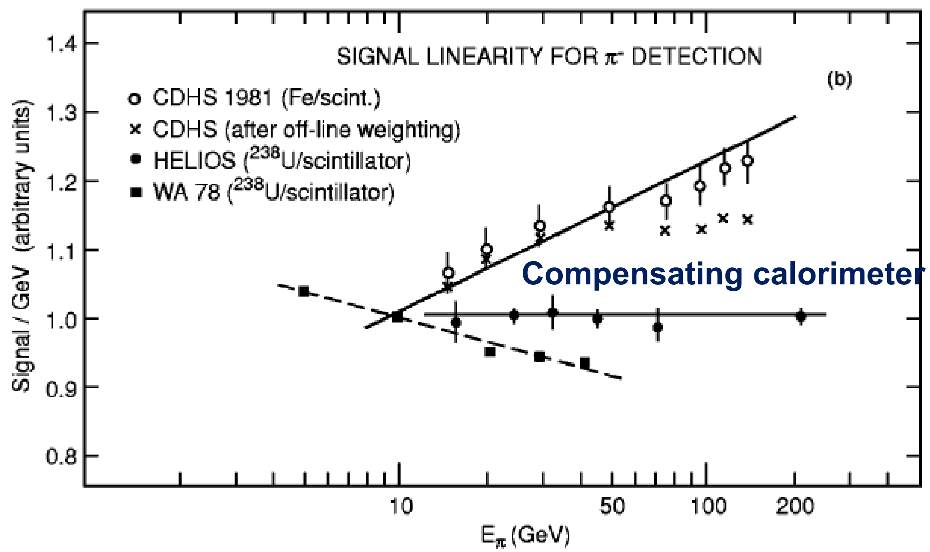

Compensating Hadron Calorimeters

Resolution and linearity of a hadron calorimeter is best if e/h=1. For all other values e/h<>1 the resolution in linearity is worse.

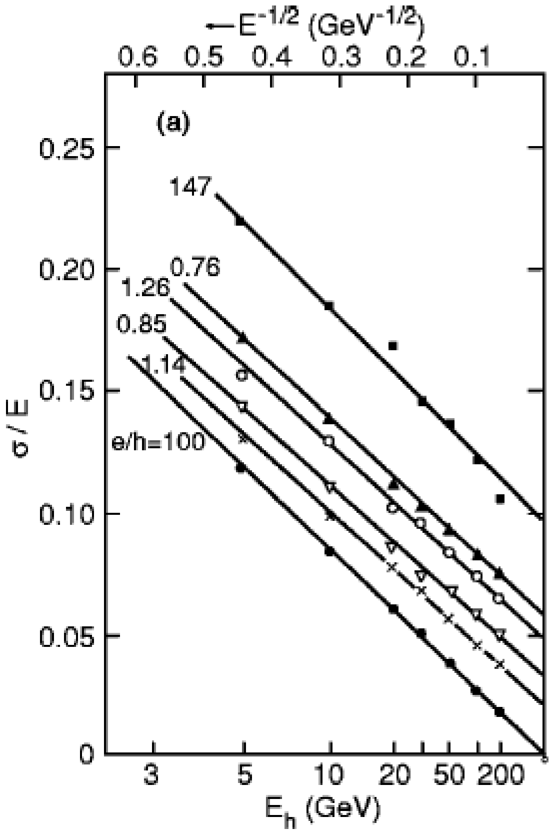

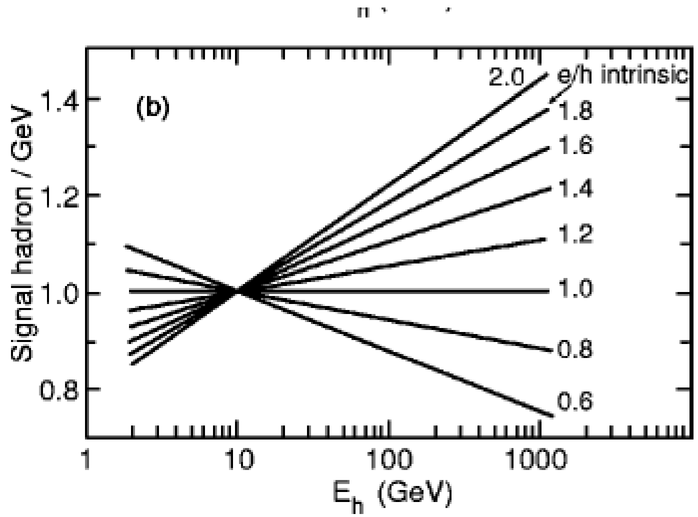

FIG. 24. Monte Carlo simulation of the effects of $e/\pi \neq 1$ on energy resolution (a) and response linearity (b) of hadron calorimeters with various values for e/h (intrinsic), where h (intrinsic) denotes the response to the purely hadronic component of the shower (Wigmans, 1988).

Conclusion

The story of modern calorimetry is a textbook example of physics research driving the development of an experimental method.

The long quest for precision electron and photon spectroscopy explains the remarkable progress in new instrumentation techniques, for both sampling and homogeneous calorimeters.

The study of jets of particles as the macroscopic manifestation of quarks has driven the work on hadronic calorimeters.

C.W. Fabjan and F. Gianotti, Rev. Mod. Phys., Vol. 75, N0. 4, October 2003

Particle Identification

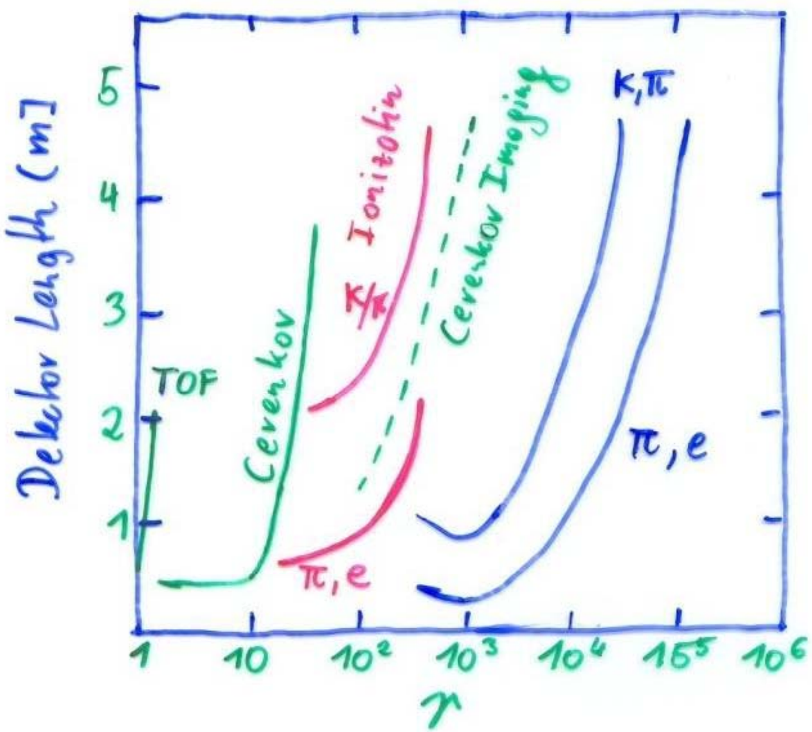

1) • For low Energies the Time of Flight (TOF) measures the velocity $p, v \rightarrow m$

2) • For larger Energies the Cerenkov Threshold $v > \frac{c}{n}$ discriminates between Particles

3) • For $\gamma \sim 100$ the multiple $\frac{dE}{dx}$ measurements provide Identification

4) • Cerenkov Angle Measurements $\cos\theta = \frac{1}{n\beta}$ provide Particle ID

5) • At very high γ the Transition Radiation allows Identification